

THE GROUP OF DISJOINT 2–SPHERES IN 4–SPACE

ROB SCHNEIDERMAN AND PETER TEICHNER

ABSTRACT. We compute the group $LM_{2,2}^4$ of link homotopy classes of link maps of two 2–spheres into S^4 . By definition, a *link map* is required to keep the two components disjoint and a *link homotopy* is a homotopy through link maps. $LM_{2,2}^4$ turns out to be a countably generated free abelian group, detected by two basic self-intersection invariants. As a consequence, we show that any link map with one topologically embedded component is link homotopic to the unlink!

Our proof introduces a new basic link homotopy, which we call a *Whitney homotopy*, that shrinks an embedded *Whitney sphere* constructed from four copies of a Whitney disk. Freedman’s disk embedding theorem is applied to get the necessary embedded Whitney disks, after constructing sufficiently many *accessory spheres* as algebraic duals for immersed Whitney disks. To construct these accessory spheres and immersed Whitney disks we use the algebra of metabolic forms over $\mathbb{Z}[\mathbb{Z}]$, and introduce a number of new geometric constructions, including maneuvers involving the boundary arcs of Whitney disks.

1. INTRODUCTION

In 1925, Emil Artin [2] constructed knotted 2–spheres in 4–space by spinning a knotted arc K , with ends on a 2–plane in \mathbb{R}^3 , by 360 degrees. During this rotation of \mathbb{R}^4 which keeps the plane fixed, the rotated arcs sweep out a 2–sphere. Artin showed that the fundamental group of the complement of this *spun 2–knot* $S_K \subset \mathbb{R}^4$ is that of the original arc and hence that 2–knot theory is at least as complicated as classical knot theory.

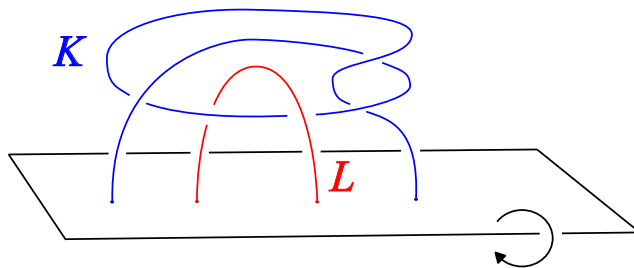


FIGURE 1. Artin’s spun 2–knot S_K with an Andrews–Curtis 2–sphere S_L in its complement.

Andrews–Curtis showed in [1] that the second homotopy group $\pi_2(\mathbb{R}^4 \setminus S_K)$ can be non-trivial. In fact, they proved that spinning the arc L in Figure 1 gives an embedded 2–sphere S_L in the complement of S_K which is not null homotopic. Note that since the

arc L is unknotted, the spun 2-knot S_L is unknotted as well and hence $\pi_2(\mathbb{R}^4 \setminus S_L) = 0$. In particular, S_K shrinks in the complement of S_L . By symmetry, this null homotopy can be excluded by introducing a trefoil knot T into L (changing L by a homotopy in the complement of K), leading to a new two-component 2-link $(S_K, S_T) : S^2 \amalg S^2 \hookrightarrow \mathbb{R}^4$ such that neither component is null homotopic in the complement of the other.

By construction, there is a homotopy of S_T in the complement of S_K (leading from the trefoil arc T back to the arc L in Figure 1) and then a null homotopy of S_K in the complement of S_L . So the 2-link (S_K, S_T) is still not as robust as we might expect it to be! More precisely, it is *link homotopic* to the unlink using the following notion:

Definition 1. A *link map* is a continuous map such that connected components of the source are mapped *disjointly* into the target. A *link homotopy* is just a homotopy *through* link maps. So even if the components start off as embeddings, they are allowed to self-intersect during a link homotopy.

A nice consequence of our main result, Theorem 3, shows that the above link homotopies in the Andrews–Curtis examples are not a coincidence:

Corollary 2. *Let $(f_1, f_2) : S^2 \amalg S^2 \rightarrow S^4$ be a link map such that f_1 is an embedding (a homeomorphism onto its image). Then (f_1, f_2) is link homotopic to the trivial link.*

We are not aware of other theorems about wild 2-knots in S^4 , but in [6] infinitely many wild 2-knots were constructed as limit sets of (geometrically finite) Kleinian groups.

Remark. We will see shortly how this unlinking follows logically from Theorem 3. It is important to point out, however, that one does not really need the full power of that theorem (which uses the tricky and long arguments in the proof of Proposition 22). We will explain in Section 6 how Corollary 2 is really a corollary to our easier “Metabolic Unlinking Theorem”, Theorem 20.

The main problem that arises in the proof of Corollary 2 is that $\pi_2(S^4 \setminus f_1)$ can be nontrivial even if f_1 is a smooth embedding, as in the Andrews–Curtis example (S_K, S_T) above. One is therefore forced to introduce self-intersections into f_1 during the link homotopy and it is thus natural to consider link maps from the beginning.

The question whether an *embedding* of two 2-spheres in S^4 is link homotopically trivial was first posed by Massey and Rolfsen in 1982, see the problem list [12, p.258]. Arthur Bartels and the second author answered this question by proving in [5] that an embedded link of 2-spheres in S^4 *with arbitrarily many components* is indeed link homotopically trivial. In [3], this result was used to completely classify link homotopy classes of string 2-links, i.e. embeddings of annuli in $S^3 \times I$ (with unlinks on the boundary) by certain Milnor invariants. The argument in [5] was generalized in [4] and [27] to show that embedded codimension 2 links are link homotopically trivial in all dimensions $n \geq 4$.

Returning to the 4-dimensional, two component case, Fenn and Rolfsen had given the first example of a link map $S^2 \amalg S^2 \rightarrow S^4$, necessarily with both components non-embedded, which is not link homotopically trivial [13]. They used a version of the Arf

invariant to detect the linking. In fact, there exist more robust link homotopy invariants which can be described as follows. We first turn any link map $(f_1, f_2) : S^2 \amalg S^2 \rightarrow S^4$ into a *generic immersion* and then consider the Hurewicz maps

$$\pi_1(S^4 \setminus f_i) \rightarrow H_1(S^4 \setminus f_i) \cong \mathbb{Z}.$$

Even though the fundamental group of the complement changes during a homotopy of f_i , the first homology stays constant by Alexander duality and the fact that H_2 is infinite cyclic for the image of any generic immersion. One can thus consider Wall's intersection invariant λ with values in the group ring $\mathbb{Z}[\mathbb{Z}]$ to obtain two well-defined link homotopy invariants $\lambda(f_i, f_i) \in \mathbb{Z}[\mathbb{Z}]$. This was first observed by Paul Kirk in [17], hence we shall refer to these two Laurent polynomials as the *Kirk invariants*

$$\sigma_i(f_1, f_2) := \lambda(f_i, f_i) \in \mathbb{Z}[\mathbb{Z}].$$

Kirk realized (see also Section 6) that *both* his invariants vanish if only one of the components is an embedding and he asked whether Corollary 2 is true. In fact, our main result says that the Kirk invariants detect link homotopy in this dimension. This is extremely surprising, given the usual problems of deriving geometric information from algebraic intersection invariants in dimension four:

Theorem 3. *If $(f_1, f_2) : S^2 \amalg S^2 \rightarrow S^4$ is a link map with vanishing Kirk invariants $\sigma_1(f_1, f_2) = 0 = \sigma_2(f_1, f_2)$, then (f_1, f_2) is link homotopically trivial.*

John Milnor [21] had initiated the study of link homotopy for classical links in 3-space, introducing the now infamous *Milnor invariants*, which for non-repeating indices are link homotopy invariants. As the easiest example, consider the sets $LM_{p,q}^n$ of link homotopy classes of 2-component spherical link maps $S^p \amalg S^q \rightarrow S^n$. In the classical case $p = q = 1$ and $n = 3$, this set is easily seen to be detected by the linking number. Similarly, $LM_{1,n-2}^n \cong \mathbb{Z}$ for all $n \geq 3$.

The first unknown set is $LM_{2,2}^4$ and our main result Theorem 3 leads to its complete understanding as follows. Koschorke [18, Prop.2.3] showed that the ambient connected sum operation is well defined and makes $LM_{p,q}^n$ into an abelian monoid for $p, q \leq n - 2$.

Corollary 4. *For a link map $(f_1, f_2) : S^2 \amalg S^2 \rightarrow S^4$, let $-(f_1, f_2)$ denote its composition with a reflection of S^4 . Then the link map $(f_1, f_2) \# -(f_1, f_2)$ is homotopically trivial and $LM_{2,2}^4$ becomes a group under connected sum $\#$.*

This result follows directly from Theorem 3, observing that the Kirk invariants are additive under connected sum and change sign under reflection of S^4 . Alternatively, one could use the usual rotation argument and the fact that “link concordance implies link homotopy” which was proved by Bartels and the second author in this dimension [5].

Corollary 5. *$(\sigma_1, \sigma_2) : LM_{2,2}^4 \hookrightarrow \mathbb{Z}[\mathbb{Z}] \oplus \mathbb{Z}[\mathbb{Z}]$ is a group monomorphism.*

To describe the image of this monomorphism, fix a (multiplicative) generator x of \mathbb{Z} so that $\mathbb{Z}[\mathbb{Z}] = \mathbb{Z}[x^{\pm 1}]$ is the ring of Laurent polynomials. Here and throughout this paper we denote $z := (1 - x) \cdot (1 - x^{-1}) = (1 - x) + (1 - x^{-1})$.

Lemma 6. *For I the augmentation ideal in $\mathbb{Z}[\mathbb{Z}]$ and ι the usual involution on the group ring determined by $\iota(x) = x^{-1}$, we have*

$$I^k \cap \mathbb{Z}[\mathbb{Z}]^\iota = z^k \cdot \mathbb{Z}[z] \quad \forall k \in \mathbb{N},$$

The left hand side of the equation above consists of certain Laurent polynomials that are invariant under ι . Since Wall's intersection invariant is hermitian, it follows that $\lambda(f, f) \in \mathbb{Z}[\pi]^\iota$ for any fundamental group π . Moreover, the augmentation ideal I is the kernel of the augmentation map $\mathbb{Z}[\pi] \rightarrow \mathbb{Z}$ and $\lambda(f, f)$ is carried to the self-intersection of homology classes. Since $H_2(S^4) = 0$, it follows that $\lambda(f_i, f_i) \in I \cap \mathbb{Z}[\mathbb{Z}]^\iota = z \cdot \mathbb{Z}[z]$.

Theorem 7. *The Kirk invariants (σ_1, σ_2) fit into a short exact sequence of groups*

$$0 \longrightarrow LM_{2,2}^4 \longrightarrow z \cdot \mathbb{Z}[z] \oplus z \cdot \mathbb{Z}[z] \longrightarrow \mathbb{Z} \longrightarrow 0,$$

where we use the difference map to $\mathbb{Z} = z \cdot \mathbb{Z}[z]/z^2 \cdot \mathbb{Z}[z]$. In particular, $LM_{2,2}^4$ is a free abelian group of countably infinite rank.

With slightly different conventions, Kirk computed the cokernel of his invariant in [17]. We will reprove his result and Lemma 6 in Section 4.

We should recall that in the paper [19], a $\mathbb{Z}/2$ -valued invariant to detect nontrivial link maps in the kernel of the Kirk invariants was defined. However, Pilz [23] pointed out a computational error in the examples given in [19]. It was shown recently by Lightfoot [20] that this invariant vanishes identically on the kernel of the Kirk invariants. In fact, Lightfoot shows that the invariant is defined if $\sigma_1(f_1, f_2) = 0$ but is completely determined by $\sigma_2(f_1, f_2)$.

As will be explained in Section 2, our method for proving Theorem 3 is based on a 4-dimensional version of an *elementary link homotopy* in 3-dimensions as in Figure 3. The central idea is to consider a *Whitney sphere* corresponding to a Whitney disk for a pair of self-intersections in an immersion $f : S^2 \looparrowright S^4$. The Whitney sphere lies in the complement of f and is made out of four copies of the Whitney disk (see [14, §3.1, Ex.(2)], where these spheres were introduced as dual spheres to accessory disks).

In the case of a link map $(f_1, f_2) : S^2 \amalg S^2 \rightarrow S^4$ with vanishing Kirk invariants, we will use algebraic arguments involving the intersection form of $S^4 \setminus f_1$ and geometric constructions described in the proof of Proposition 22 to locate enough disjointly embedded (framed) Whitney disks. The latter is a long and hard part of the argument, but we found a shortcut in the setting of Corollary 2 that will be explained in Section 6. In both cases, a sequence of our *Whitney homotopies* along the corresponding Whitney spheres will finish the argument.

To arrange that the Whitney disks are embedded we apply Freedman's disk embedding theorem (in the manifold $S^4 \setminus f_1$), which needs a collection of algebraic dual spheres to the Whitney disks. Each such dual sphere will be constructed out of four copies of an accessory disk as in [14, §3.1] - we shall refer to such spheres as *accessory spheres*. Their existence follows from our algebraic computation and the fact that after finitely many finger moves one may assume that f_1 is in *standard position*, see Section 3. In particular,

the fundamental group is the (good) abelian group \mathbb{Z} , a fact which makes the algebraic calculations tractable, as well as Freedman’s embedding theorem hold.

We end this introduction by discussing a nice application of Theorem 3 to classical links. Let \mathcal{L} denote the set of links in \mathbb{R}^3 with two components, both of which are unknotted and have linking number 0. There is an additive map

$$\text{JK} : \mathcal{L} \longrightarrow LM_{2,2}^4$$

which seems to go back to Fenn, Rolfsen, Levine, Jin and Kirk. We shall refer to it as the *JK-construction* and it can be described as follows: Let $L = (l_1, l_2) \in \mathcal{L}$ and observe that $S^3 \setminus l_i$ are homotopy equivalent to S^1 because the knots l_i are trivial. The other component is null-homotopic in this complement by triviality of the linking number. Thus one can choose two disjoint cylinders $S^1 \times D^1 \rightarrow S^3 \times D^1$ by putting a null-homotopy of l_2 into $S^3 \times [-1, 0]$ keeping l_1 fixed, and by putting a null-homotopy of l_1 into $S^3 \times [0, 1]$ keeping l_2 fixed. The original classical link L is thought of as lying in $S^3 \times 0$, see Figure 2 (where the symmetry of the Whitehead link is used!).

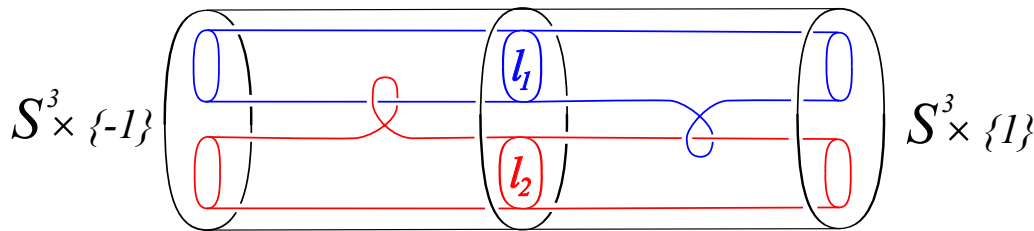


FIGURE 2. A schematic depiction of $\text{JK}(L)$ for $L = (l_1, l_2)$ the Whitehead link, with each self-intersection coming from a null-homotopy of an l_i .

Finally, one produces a link map $\text{JK}(L) : S^2 \amalg S^2 \rightarrow S^4$ by adding the standard disks to the unlinks in $S^3 \times \partial D^1$. This construction involves the choices of two null-homotopies but it gives a well defined link homotopy class because $\pi_2(S^3 \setminus l_i) \cong \pi_2(S^1) = 0$.

The additivity of JK means that *any* ambient connected sum of classical 2-component links is sent to the sum of the corresponding elements in the group $LM_{2,2}^4$. It was shown by Jin in his thesis [16] that the Kirk invariants of $\text{JK}(L)$ are Cochran’s β^i -invariants [8] of L . More precisely, in the above notation, we can write

$$\sigma_1(\text{JK}(L)) = \sum_{i=1}^N \beta^i(L) \cdot z^i \in z \cdot \mathbb{Z}[z]$$

and similarly for the second component (Cochran’s $\beta^i(L)$ also prefer one component). Cochran had shown that his invariants $\beta^i(L)$ are integer lifts of Milnor’s invariants $\mu_{1\dots 2i\dots 122}(L)$ for links with trivial linking numbers. In particular, the Sato-Levine invariant $\beta^1(L) = \mu_{1122}(L)$ is symmetric in the components 1 and 2, explaining again the cokernel of the Kirk invariants in Theorem 7.

It follows from Theorem 3 that $\text{JK}(L) = \text{JK}(L')$ if and only if L and L' share the same Cochran β -invariants. In particular:

Corollary 8. $\text{JK} : \mathcal{L} \rightarrow LM_{2,2}^4$ is onto; and $\text{JK}(L) = 0$ if and only if

$$\mu_{1\dots 2i\dots 122}(L) = 0 = \mu_{2\dots 2i\dots 211}(L) \quad \forall i \geq 2.$$

This gives a very satisfying 4-dimensional characterization of the vanishing of these Milnor invariants. The surjectivity of JK will be proven in Section 4 by writing down sufficiently many links $L \in \mathcal{L}$ to realize the image of the Kirk invariants. Alternatively, one could again use that “link concordance implies link homotopy”, or more precisely, that any (singular) link concordance $(S^1 \amalg S^1) \times D^1 \rightarrow S^3 \times D^1$ is link homotopic to a link homotopy.

The current paper is a much improved version of a manuscript that was circulated by the second author in the mid 1990’s but never published. That manuscript contained a gap in the proof of an immersed version of the current Whitney Homotopy Lemma 9 which is now filled by an application of Freedman’s disk embedding theorem. It remains an open problem whether Freedman’s infinite constructions can be replaced by an immersed version of our Whitney homotopies.

Theorem 3 was not even stated in the previous manuscript, only Corollary 2. The new ingredients for proving Theorem 3 are the manipulations of Whitney disks in Section 7. We only found these new constructions after developing an obstruction theory for *Whitney towers* over the last decade, see e.g. [9, 24, 25].

Acknowledgements: It is a pleasure to thank Tim Cochran and Mike Freedman for valuable discussions on the subject. The second author also thanks Colin Rourke for pointing out a gap in his original manuscript. The first author was supported by a Simons Foundation *Collaboration Grant for Mathematicians*, and both authors thank the Max Planck Institute for Mathematics, Bonn, where most of this work was carried out.

Outline of the paper: *Whitney homotopies* and *Whitney spheres* are introduced in Section 2. Throughout the course of the paper four geometric constructions of Whitney spheres will be given, all of which will be seen to be equivalent in section 5.7.

The translation of link homotopy into algebra begins in Section 3, which starts by presenting algebraic conditions for a link map to be trivial in terms of $\mathbb{Z}[\mathbb{Z}]$ -intersections between the second sphere and standard Whitney disks on the first sphere (Standard Unlinking Theorem 12). Most of Theorem 12 is then proved by examining the algebraic topology of the complement M of a standard sphere using Kirby diagrams (Lemma 13), and constructing a basis of standard Whitney spheres and accessory spheres for $\pi_2 M$.

Using Lemma 13, the structure of $LM_{2,2}^4$ is described in Section 4, which contains proofs of Lemma 6 and Theorem 7.

Section 5 returns to the path towards proving the main Theorem 3 by using immersed Whitney moves to define the notion of a *metabolic collection* of Whitney disks and accessory disks, with the corresponding generalization of Whitney spheres and accessory

spheres from Section 3 providing the input into the Metabolic Unlinking Theorem 20 which completes the proof of (and strengthens) Theorem 12. Whitney homotopies and Freedman’s disk embedding theorem play a central role in the proof of Theorem 20, which also depends on a geometric realization of metabolic isometries (Lemma 19) as well as a homotopy-theoretic characterization of Whitney spheres (Lemma 21).

Section 6 explains how Corollary 2 follows from the Metabolic Unlinking Theorem 20.

Section 7 completes the proof of Theorem 3 by showing in Proposition 22 that any link map in the kernel of the Kirk invariants satisfies the algebraic criteria of the Metabolic Unlinking Theorem 20. The proof of Proposition 22 involves multiple-step geometric manipulations of Whitney disks and accessory disks.

Technical details on Whitney disks and accessory disks are provided in the appendix Section 8.

2. THE WHITNEY HOMOTOPY IN DIMENSION 4

This section introduces the notion of a *Whitney homotopy*, which will play a key role in our ability to derive geometric conclusions from algebraic data. A Whitney homotopy is supported near a Whitney disk W on a generic immersion $f : S^2 \looparrowright X^4$, and involves shrinking an embedded *Whitney sphere* S_W to a point after performing a Whitney move on W , with S_W at all times remaining disjoint from f . Since the Whitney disks for our Whitney homotopies will be constructed via Freedman’s disk embedding machinery, we work in the (locally flat) topological category throughout this section, invoking the notions of 4-dimensional topological transversality from [14, chap.9].

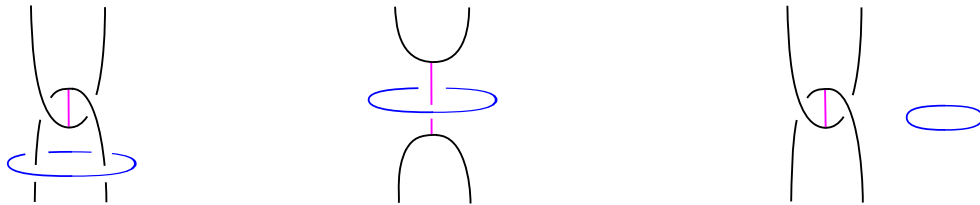


FIGURE 3. A 3-dimensional analogue of the Whitney homotopy.

2.1. A 3-dimensional elementary homotopy. As motivation towards a description of the Whitney homotopy of 2–spheres in dimension four, start by considering the analogous homotopy of 1–manifolds in 3–space shown in Figure 3. The sequence of pictures in Figure 3 describes a 3-dimensional link homotopy in which the black 1–manifold comes back to its original position while shrinking the blue circle to a small unknot. This homotopy keeps black and blue disjoint throughout, and has exactly two singularities, namely the black-black intersections from the un-clasping and re-clasping (guided by the purple arcs).

The 4-dimensional analogue of the link homotopy in Figure 3 is the composition of a Whitney move (“un-clasping”) and its reverse finger move (“re-clasping”) on a 2–sphere

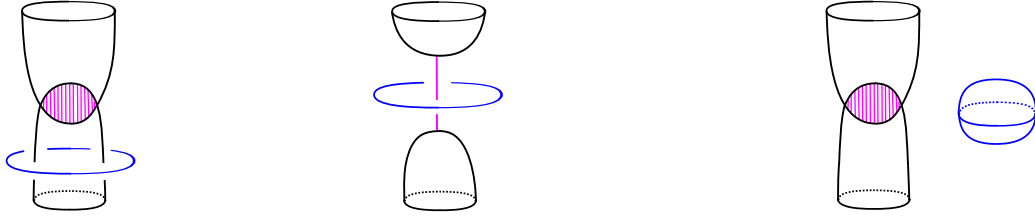


FIGURE 4. A schematic illustration of the 4-dimensional Whitney homotopy.

in a 4-manifold. The Whitney move is guided by its Whitney disk W whereas the finger move is again guided by an arc. Thus the analogue of the blue circle in Figure 3 is an embedded 2-sphere S_W which is the boundary of a 3-ball, normal to the arc guiding the finger move. We call S_W the *Whitney sphere*. Before starting a detailed description of this 4-dimensional Whitney homotopy, it may be helpful to consider the schematic description shown in Figure 4.

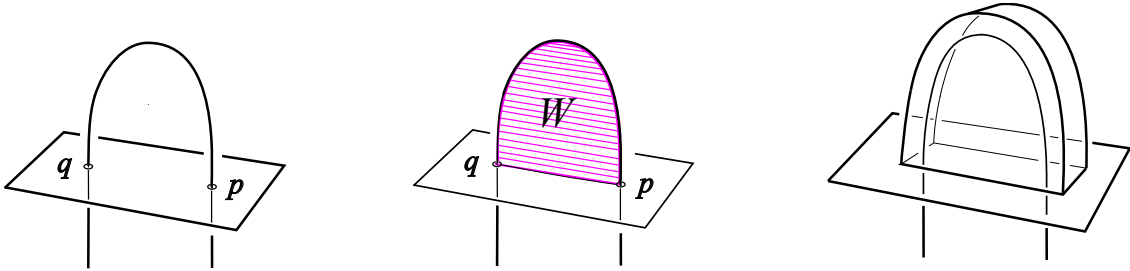


FIGURE 5. Left: A pair of transverse intersections p and q between surface sheets in a 3-dimensional slice of $B^4 = B^3 \times I$. By convention, the horizontal sheet is contained in the ‘present’ 3-dimensional slice, while the curved arc extends into ‘past’ and ‘future’ (cf. Figure 6). Center: A *Whitney disk* W pairing p and q . Right: A Whitney move on the horizontal sheet guided by W eliminates p and q by adding a *Whitney bubble* to this sheet.

2.2. Whitney moves and Whitney bubbles. Figure 5 describes a model *Whitney move* in a 4-ball neighborhood of a *Whitney disk* W : A pair of oppositely-signed transverse intersections between two surface sheets is eliminated by a homotopy which isotopes one of the sheets across W . The cut-and-paste effect of a Whitney move is to replace a disk neighborhood of an arc of the boundary ∂W in one surface sheet by a different disk, which we call a *Whitney bubble*, that has the same boundary and contains two parallel copies of W joined by a narrow embedded rectangle (Figure 5 right). Each of these copies of W is an extension of a normal *Whitney section* over ∂W which is defined by pushing ∂W tangentially in one sheet and normally to the other sheet. In general, a Whitney move is described by any embedding of this model into a 4-manifold which preserves the product structures and transversality of the sheets and W .

All Whitney disks in this section are embedded, and the reader may notice that they are also *framed* (which corresponds to the disjointness of parallel copies, as used in the Whitney bubble). Details on Whitney disks are given in Section 8.

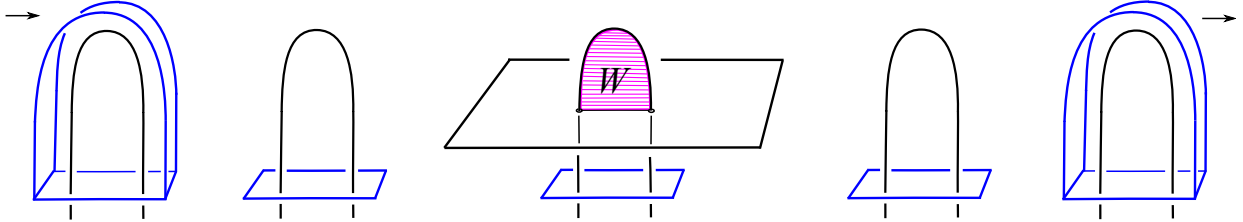


FIGURE 6. A *Whitney sphere* S_W (blue) for the Whitney disk W of Figure 5. With ‘time’ moving from left to right, the pictures in this figure explicitly show two each of the past and future 3-dimensional slices of 4-space on each ‘side’ of the center present slice. So S_W extends into past and future, while W and one of the sheets paired by W are contained in the present.

2.3. Whitney spheres. A *Whitney sphere* S_W is formed from a Whitney disk W by joining together the boundaries of two parallel copies of Whitney bubbles by an annulus as illustrated in Figure 6. This annulus (which appears “rectangular” in Figure 6) is formed by an interval’s worth of normal parallel copies of the boundary of a disk neighborhood around an arc of ∂W that would be exchanged for a Whitney bubble under a W -Whitney move. By construction S_W is contained in a 4-ball neighborhood of W , and S_W contains four parallel copies of W (two from each Whitney bubble).

(Note that the 4-ball described by the entire “movie” of Figure 6 is the accurate description of just the left-most schematic picture in Figure 4.)

2.4. The Whitney homotopy.

Lemma 9 (Whitney homotopy). *Let W be a (framed embedded) Whitney disk on $f : S^2 \looparrowright X^4$, such that the interior of W is disjoint from f . Then W determines a unique Whitney sphere S_W which is embedded in $X^4 \setminus f$, and the link map (f, S_W) is link homotopic to $(f, *)$ by a link homotopy which is supported in any neighborhood of W . Moreover, if $\#S_W$ denotes a connected sum of parallel copies of S_W along arbitrary tubes, then $(f, \#S_W)$ is also link homotopic to $(f, *)$.*

Proof. By construction, S_W is contained in a regular neighborhood of W , and is disjoint from f . The uniqueness of S_W will be shown in Lemma 21 (section 5.5) which gives a homotopy-theoretic definition of Whitney spheres. The existence of the link homotopy from (f, S_W) to $(f, *)$ follows from Figure 7, which shows that after a W -move on f there is a 3-ball in the complement of f which is bounded by S_W . After shrinking S_W to a

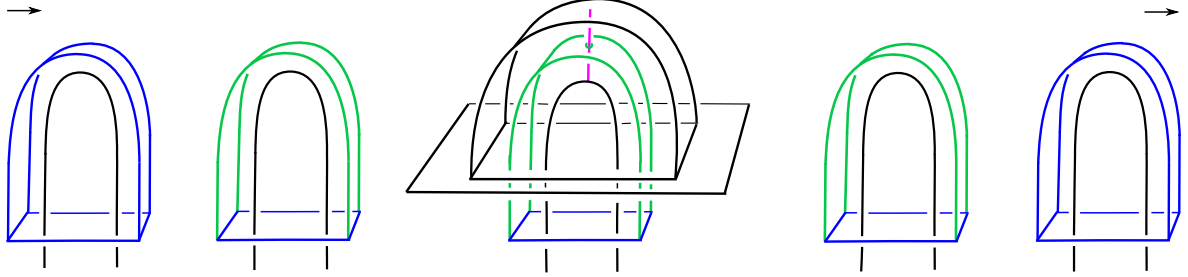


FIGURE 7. After the W -Whitney move on the horizontal sheet, the Whitney sphere S_W from Figure 6 bounds the green 3-ball formed by parallels of the Whitney bubble in the complement of f (black). Note that the green Whitney bubble is ‘inside’ the black Whitney bubble in the center picture.

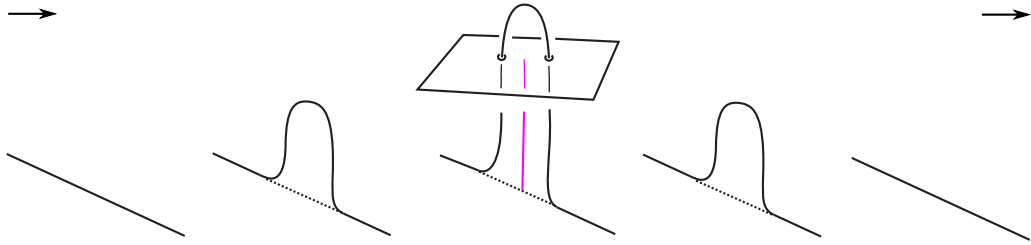


FIGURE 8. A *finger move* guided by the purple arc creates a pair of intersections between the sheet which extends into past and future as indicated and the rectangular sheet contained in the present. The dotted sub-arcs indicate the position of the lower sheet before the finger move.

point in $X^4 \setminus f$ one could, if desired, isotope f back to its original position using a finger move (Figure 8) guided by the purple arc in Figure 7.

The case of $\#S_W$ follows from the observation that there are k parallels of the green 3-balls in the complement of f that can be connected by arbitrary arcs, thickened into dimension 3. The boundary of the resulting 3-ball is by construction the tube sum $\#S_W$. \square

We remark that this proof of Lemma 9 is exactly as in the 3-dimensional case (Figure 3): The Whitney sphere shrinks after having done the Whitney move but it is a well defined nontrivial 2-sphere before the move.

3. THE STANDARD UNLINKING THEOREM

Let $(f_1, f_2) : S^2 \amalg S^2 \rightarrow S^4$ be a link map. After a small perturbation (which is a link homotopy) we may assume that both f_i are immersions whose singularities consist only of transverse self-intersection points. Furthermore, we may perform some cusp homotopies (again keeping f_i disjoint) to get the signed sum of the self-intersection points of each f_i to be zero. In S^4 this is the same as saying that the f_i have trivial normal bundle. By

[26, Thm.C], immersions $S^2 \looparrowright S^4$ as above, modulo regular homotopy, are the same as homotopy classes of maps $S^2 \rightarrow S^4$.

From now on, we will always assume that our maps $S^2 \looparrowright S^4$ are immersions with only transverse self-intersections whose signed sum is zero, i.e. with trivial normal bundle. Then we work modulo regular homotopy.

This approach has the following advantage: By general position, a regular homotopy is the composition of finitely many finger moves and then finitely many Whitney moves (up to isotopy). For example, since $\pi_2(S^4) = 0$ we may perform finger moves on f_1 (disjoint from f_2 by general position) to get f'_1 for which some Whitney moves lead to the standard unknotted embedding $f_0 : S^2 \subset S^4$. Conversely, f'_1 is obtained from f_0 by finitely many finger moves.

Definition 10. A map $f : S^2 \rightarrow S^4$ which is obtained from f_0 by finitely many finger moves is said to be in *standard position*. Here f_0 is the standard unknotted embedding $f_0 : S^2 \subset \mathbb{R}^3 \subset S^4$. Moreover, any collection of disjointly embedded Whitney disks for f which lead back to f_0 is called a *standard collection* of Whitney disks.

We have just proven the following result.

Lemma 11. *Any link map $(f_1, f_2) : S^2 \amalg S^2 \rightarrow S^4$ is link homotopic to one in which both components are in standard position. In particular, the fundamental groups of their respective complements are infinite cyclic, see Lemma 13.*

There is a simple sufficient condition for a link map $(f_1, f_2) : S^2 \amalg S^2 \rightarrow S^4$ to be link homotopically trivial: Assume that f_1 is in a standard position such that f_2 is disjoint from a standard collection of Whitney disks W_i for f_1 . Then one can do the Whitney moves on W_i in the complement of f_2 to get a link homotopy from (f_1, f_2) to (f_0, f_2) . But this link map is trivial since

$$\pi_2(S^4 \setminus f_0) \cong \pi_2(S^1 \times D^3) = 0.$$

The main result of this section is to give algebraic conditions that model the disjointness of f_2 and the W_i :

Theorem 12 (Standard Unlinking Theorem). *The following statements are equivalent:*

- (i) *The link map (f_1, f_2) is link homotopically trivial.*
- (ii) *There are finger moves on f_1 (disjoint from f_2) which bring f_1 into a standard position f with a standard collection of Whitney disks W_i for f such that*

$$\lambda(W_i, f_2) = 0.$$

- (iii) *There are finger moves on f_1 (disjoint from f_2) which bring f_1 into a standard position f with a standard collection of Whitney disks W_i for f such that*

$$\lambda(f_2, f_2) = 0 \quad \text{and} \quad \lambda(W_i, f_2) \in z \cdot \mathbb{Z}[x^{\pm 1}].$$

Here $z := (1-x)(1-x^{-1})$ where x is a generator of $\pi_1(S^4 \setminus f) \cong \mathbb{Z}$. The intersection numbers $\lambda(-, f_2)$ are measured in the group ring $\mathbb{Z}[\pi_1(S^4 \setminus f)] = \mathbb{Z}[x^{\pm 1}]$.

Proof that (i) \Rightarrow (ii) in Theorem 12. By general position we may arrange that the link homotopy from (f_1, f_2) to the unlink is of the following form: First finger moves on f_1 bring it into standard position f'_1 , then finger moves and Whitney moves on f_2 happen (in the complement of f'_1). Finally, Whitney moves on a standard collection of Whitney disks W_i for f'_1 (in the complement of $f'_2 = f_0$) lead to the unlink. Working in the complement of f'_1 , we clearly have $\lambda(f'_2, W_i) = 0$ since f'_2 is disjoint from the W_i . However, f'_2 differs from f_2 by a regular homotopy in the complement of f'_1 which leaves these intersection numbers unchanged, even though W_i and f_2 may intersect. Hence statement (ii) follows. \square

Proving the other parts of Theorem 12 will require more work. We start with the algebraic topology of the complement of a map $f : S^2 \looparrowright S^4$ in standard position. Along with the Whitney spheres from Section 2, the following lemma involves *accessory spheres*, which are introduced in the proof and described in further detail in section 5.2. Just as a Whitney sphere is constructed from four copies of a Whitney disk, an accessory sphere is constructed from four copies of an *accessory disk* bounded by a sheet-changing loop in f which passes through a self-intersection point (section 8.5).

Lemma 13. *Let W_1, \dots, W_n be a standard collection of Whitney disks for $f : S^2 \looparrowright S^4$ in standard position. Then the compact 4-manifold*

$$M := S^4 \setminus \text{small normal bundle of } f$$

has the following algebraic topological properties:

- (1) $\pi_1 M$ is infinite cyclic, generated by a meridian x . Set $\Lambda := \mathbb{Z}[x^{\pm 1}]$.
- (2) $\pi_2 M$ is a free Λ -module of rank $2n$ with a basis of the form

$$\{S_{W_1}, \dots, S_{W_n}, S_{A_1}, \dots, S_{A_n}\}$$

where S_{W_i} are the Whitney spheres corresponding to the Whitney disks W_i and the S_{A_i} are accessory spheres corresponding to positive accessory disks A_i .

- (3) Wall's intersection form $\lambda : \pi_2 M \times \pi_2 M \rightarrow \Lambda$ is metabolic in the sense that

$$\lambda(S_{W_i}, S_{W_j}) = 0 \quad \text{and} \quad \lambda(S_{A_i}, S_{A_j}) = z \cdot \delta_{ij} = \lambda(S_{W_i}, S_{A_j}).$$

- (4) Relative intersection numbers with the Whitney disks W_i induce a short exact sequence of free Λ -modules

$$0 \longrightarrow \langle S_{W_i} \rangle \longrightarrow \pi_2 M \xrightarrow{\lambda(W_i, -)} \Lambda^n \longrightarrow 0$$

Before proving Lemma 13, we use it to make some more progress towards completing the proof of Theorem 12:

Proof that (ii) \Rightarrow (iii)&(i) in Theorem 12. Statement 4 of Lemma 13 implies that any sphere $[f_2] \in \pi_2 M$ which satisfies $\lambda(W_i, f_2) = 0$ is homotopic (in the complement of f_1) to a Λ -linear combination of Whitney spheres S_{W_i} . Statement 3 then implies $\lambda(f_2, f_2) = 0$. Moreover, by applying Lemma 9 several times to the Whitney spheres S_{W_i} , we see that (f_1, f_2) is link homotopically trivial. \square

The harder work we have to do is to relax the strong conditions $\lambda(W_i, f_2) = 0$ to the much weaker condition $\lambda(W_i, f_2) \in z \cdot \Lambda$ of statement (iii) of Theorem 12. This will eventually be accomplished in Theorem 20.

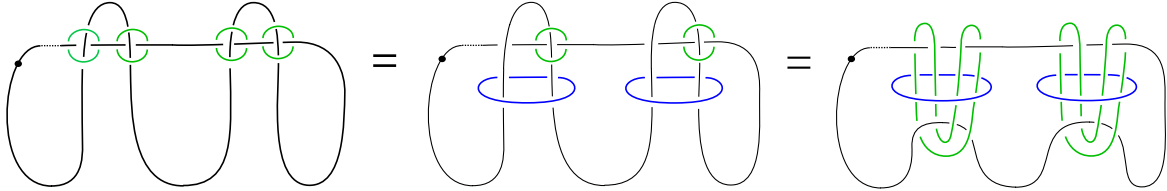


FIGURE 9. Equivalent Kirby diagrams in S^3 for the complement M of a regular neighborhood of a standard $f : S^2 \looparrowright S^4$: The dotted black unknot represents a 1-handle, and 0-framed 2-handles are attached along the green and blue circles.

Proof of Lemma 13. By assumption, f is obtained from f_0 by n finger moves which are the inverses of the Whitney moves along W_i . These finger moves depend on the isotopy classes of their guiding arcs which may be assumed to be trivial in the complement of the unknotted f_0 . Using standard Kirby calculus techniques (e.g. Chapter 6 of [15], in particular [15, Fig. 6.27]) a handle diagram for M can be derived as in the left-hand side of Figure 9. The dotted circle represents a 1-handle, and together with a 0-handle it forms the 4-manifold $S^1 \times D^3$ which is the complement of f_0 . Each finger move then adds a pair of (green) 2-handles.

Since the 2-handles' attaching circles are null homotopic, it follows that

$$M \simeq S^1 \vee \bigvee^{2n} S^2.$$

So $\pi_1 M = \langle x \rangle \cong \mathbb{Z}$, where x is a meridian to the 1-handle, and $\pi_2 M$ is a free Λ -module of rank $2n$. Sliding one of each pair of green 2-handles in the left-hand diagram of Figure 9 over the other yields the blue 2-handle attaching circles in the center diagram. After an isotopy to get the right-hand diagram, the unions of cores of the 2-handles attached to the blue circles with the evident disks bounded by these attaching circles form n generators S_{W_i} , which will be shown in section 5.7 to be Whitney spheres as constructed in section 2.3.

Figure 10 shows the construction of positive and negative *accessory spheres* $S_{A_i^\pm}$, which will be described in more detail in section 5.2.2. For Lemma 13 we only use the n positive accessory spheres $S_{A_i} = S_{A_i^+}$.

By construction it is clear that the S_{W_i} are disjointly embedded in M , and that their intersection numbers with S_{A_j} are as claimed: These spheres are disjoint for $i \neq j$, and for $i = j$ they intersect in precisely four points (two oppositely-signed pairs) as seen in the right-most picture of Figure 9. Choosing orientations and basings appropriately, one can check from Figure 9 that $\lambda(S_{W_i}, S_{A_i}) = 2 - x - x^{-1}$.

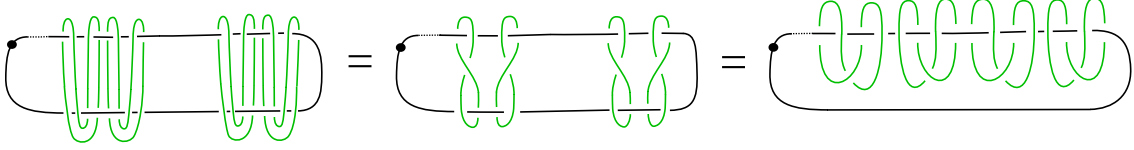


FIGURE 10. These Kirby diagrams are isotopic to the left side of Figure 9. Accessory spheres $S_{A_i^\pm}$ are formed from cores of the 2-handles together with null-homotopies of their green attaching circles. Null-homotopies can be seen on the right: The evident \mp -crossing change in each green circle corresponds to a self-intersection of $S_{A_i^\pm}$ whose associated group element is the generator x .

Again by construction, the spheres S_{A_i} are disjoint from each other and each have one self-intersection. By our convention of making the normal bundle of each immersion trivial, we add another oppositely-signed self-intersection with trivial group element. The self-intersection invariant $\lambda(S_{A_i}, S_{A_i})$ is computed from intersections between S_{A_i} and a pushoff, and it follows that it equals $2 - x - x^{-1} = z$ because the sum of the coefficients is the homological self-intersection number of a sphere in S^4 and hence must vanish.

To prove statement 3 note that the Whitney disks W_i are disjoint from S_{W_j} and have geometric intersections δ_{ij} with S_{A_j} . This can be read off from the center picture of Figure 9 (see also section 5.2.2), and implies statement 4. \square

For future reference, we note that the right-most picture of Figure 10 implies:

Lemma 14. *The set of positive and negative accessory spheres $S_{A_i^\pm}$ forms a basis of disjointly immersed 2-spheres for $\pi_2 M$ with $\lambda(S_{A_i^+}, S_{A_j^+}) = z \cdot \delta_{ij} = -\lambda(S_{A_i^-}, S_{A_j^-})$. \square*

4. PROOF OF THEOREM 7: THE GROUP OF DISJOINT 2-SPHERES

In this section we use Theorem 3 to compute the group $LM_{2,2}^4$, i.e. to derive the short exact sequence from Theorem 7:

$$0 \longrightarrow LM_{2,2}^4 \longrightarrow z \cdot \mathbb{Z}[z] \oplus z \cdot \mathbb{Z}[z] \longrightarrow \mathbb{Z} \longrightarrow 0.$$

Here the Kirk invariants are used for the first homomorphism and the difference map to $\mathbb{Z} = z \cdot \mathbb{Z}[z]/z^2 \cdot \mathbb{Z}[z]$ for the second. Recall that we fixed a (multiplicative) generator x of the fundamental group \mathbb{Z} so that $\mathbb{Z}[\mathbb{Z}] = \mathbb{Z}[x^{\pm 1}]$ and we set

$$z := (1 - x) \cdot (1 - x^{-1}) = (1 - x) + (1 - x^{-1}).$$

The first step is to show Lemma 6, namely that

$$I^k \cap \mathbb{Z}[\mathbb{Z}]^\iota = z^k \cdot \mathbb{Z}[z] \quad \forall k \in \mathbb{N}_0,$$

where I denotes the augmentation ideal in $\mathbb{Z}[\mathbb{Z}]$ and ι is the usual involution on the group ring determined by $\iota(x) = x^{-1} =: \bar{x}$.

Proof of Lemma 6. Since $\iota(z) = \bar{z} = z \in I$, one inclusion is clear. For the other, start with the case $k = 0$. If $P \in \mathbb{Z}[x^{\pm 1}]$ is invariant under ι then it is symmetric around x^0 and hence we can subtract an integer multiple of $z^n = (-1)^n(x^n + \cdots + x^{-n})$ to reduce the degree of P . By induction on n we see that $P \in \mathbb{Z}[z]$.

Now take $P \in I^k = (1-x)^k \cdot \mathbb{Z}[x^{\pm 1}]$ and assume $P = \bar{P}$. Then there is a $Q \in \mathbb{Z}[x^{\pm 1}]$ such that

$$(1-x)^k \cdot Q = P = \bar{P} = (1-x^{-1})^k \cdot \bar{Q}.$$

Since the group ring is a unique factorization domain, it follows that P is divisible by $z^k = (1-x)^k \cdot (1-x^{-1})^k$ and that the quotient is again invariant under ι . The case $k = 0$ now shows that $P \in z^k \cdot \mathbb{Z}[z]$. \square

Lemma 15. *For any link map $(f_1, f_2) : S^2 \amalg S^2 \rightarrow S^4$, the Kirk invariants satisfy the symmetry relation $\sigma_1(f_1, f_2) - \sigma_2(f_1, f_2) \in z^2 \cdot \mathbb{Z}[z]$.*

Proof. As in Lemma 11, we may assume that (f_1, f_2) is in general position and that f_1 is standard. By additivity of the Kirk invariants, it suffices to assume that $f_2 = \alpha \cdot S_A$ is a multiple of a single accessory sphere S_A , for some element $\alpha \in \mathbb{Z}[x^{\pm 1}]$, where we are using the basis of positive and negative accessory spheres described in Lemma 14. Assuming that S_A is a positive accessory sphere, we have:

$$\sigma_1(f_1, f_2) = \lambda(f_1, f_1) = 2 - x_2^{\epsilon(\alpha)} - x_2^{-\epsilon(\alpha)} \quad \text{and} \quad \sigma_2(f_1, f_2) = \lambda(f_2, f_2) = \alpha \cdot \bar{\alpha} \cdot z,$$

with $\epsilon : \mathbb{Z}[x^{\pm 1}] \rightarrow \mathbb{Z}$ the augmentation map. It suffices to set $x_2 = x$ and show that these two expressions become equal modulo z^2 . Let $k := \epsilon(\alpha)$ and $P_k := 1 + x + x^2 + \cdots + x^{k-1}$. Then

$$2 - x^k - x^{-k} = (1-x^k) \cdot (1-x^{-k}) = (1-x) \cdot P_k \cdot (1-x^{-1}) \cdot \bar{P}_k = z \cdot P_k \cdot \bar{P}_k.$$

Thus it suffices to show that for all $\alpha \in \mathbb{Z}[x^{\pm 1}]$, we have $P_k \cdot \bar{P}_k - \alpha \cdot \bar{\alpha} \in z \cdot \mathbb{Z}[z]$. Since this element is invariant under the involution ι , it suffices to show by Lemma 6 that it lies in the augmentation ideal I . But this is clearly true since $\epsilon(\alpha) = k = \epsilon(P_k)$. \square

To compute the cokernel of the Kirk invariant, we are left with proving that every element in $z \cdot \mathbb{Z}[z] \oplus z \cdot \mathbb{Z}[z]$ satisfying the symmetry relation of Lemma 15 is realized as the direct sum of the Kirk invariants of a link map.

Proof. Using linear combinations of the above example from the proof of Lemma 15 with $\sigma_1(f_1, f_2) = 2 - x_2^{\epsilon(\alpha)} - x_2^{-\epsilon(\alpha)}$, we see that the first component can be any element in $z \cdot \mathbb{Z}[z]$. Now we add link maps (g_1, g_2) with $\sigma_1(g_1, g_2) = 0$ to correct the second component. For $g_2 = \alpha \cdot S_A$, as in the above example, this just means that $\epsilon(\alpha) = 0$, i.e. $\alpha = (1-x) \cdot \beta$. Taking sums again, we need to realize any element in $z^2 \cdot \mathbb{Z}[z]$ by linear combinations of elements $\alpha \cdot \bar{\alpha} \cdot z = \beta \cdot \beta \cdot z^2$.

This is possible by an induction on degree, since we can use summands with $\beta = 1$ and $\beta = (1-x^k)$ for arbitrary k . \square

We leave it as a fun exercise for the reader to draw examples of classical links $L \in \mathcal{L}$ that realize these Kirk invariants in their JK-construction, proving surjectivity in Corollary 8. See also [11]. We note that the original Fenn-Rolfsen example with L the Whitehead link leads to $f_2 = S_A$ in the above notation!

5. THE METABOLIC UNLINKING THEOREM

It turns out that we will need a strengthening of the (as yet unproved) key implication $(iii) \Rightarrow (i)$ in the Standard Unlinking Theorem 12. This will involve using Whitney moves on *immersed* Whitney disks to construct more general versions of Whitney spheres and accessory spheres in a way that preserves the essential metabolic properties from the standard setting of Lemma 13. So with the goal of presenting this Metabolic Unlinking Theorem 20 later in this section, we start by re-examining the complement of a standard position $f : S^2 \looparrowright S^4$, and giving alternate constructions of Whitney spheres and accessory spheres using Whitney moves in local coordinates.

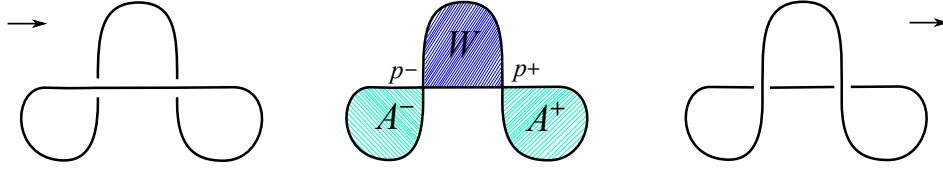


FIGURE 11. A standard Whitney disk W on f with standard accessory disks A^\pm in local coordinates $B^3 \times I$, with the ‘time’ interval moving from left to right into the 0-handle of S^4 . Changing the positive crossing corresponds to the positive self-intersection p^+ of f , and changing the negative crossing corresponds to the negative self-intersection p^- of f . The circle of f on the right shrinks to a point at future times and disappears with no further singularities.

5.1. Standard Whitney disk-accessory disk triples. Observe that for any $f : S^2 \looparrowright S^4$ in standard position, it can be arranged that each standard Whitney disk W pairing self-intersections p^\pm is contained in a 4-ball with local coordinates as in Figure 11. (E.g. choose the deleted slice disk representing the 1-handle in the left Kirby diagram of Figure 9 to have a minimum for each \pm -pair of green 2-handles.) The local model of Figure 11 defines what we call *standard accessory disks* A^\pm bounded by sheet-changing circles in f and having interiors disjoint from f . A standard W together with accessory disks A^\pm as in Figure 11 is called a *standard Whitney disk-accessory disk triple*.

5.2. Whitney spheres and accessory spheres in local coordinates. Using standard W and A , this section provides alternative constructions of the Whitney sphere S_W and accessory sphere S_A described in the proof of Lemma 13. Here we start with local 2-spheres that intersect f near ∂W , and then use Whitney moves on parallels of W and A

to remove the intersections with f . This approach has the advantage of generalizing the construction to the cases where W and A are not necessarily standard (section 5.3).

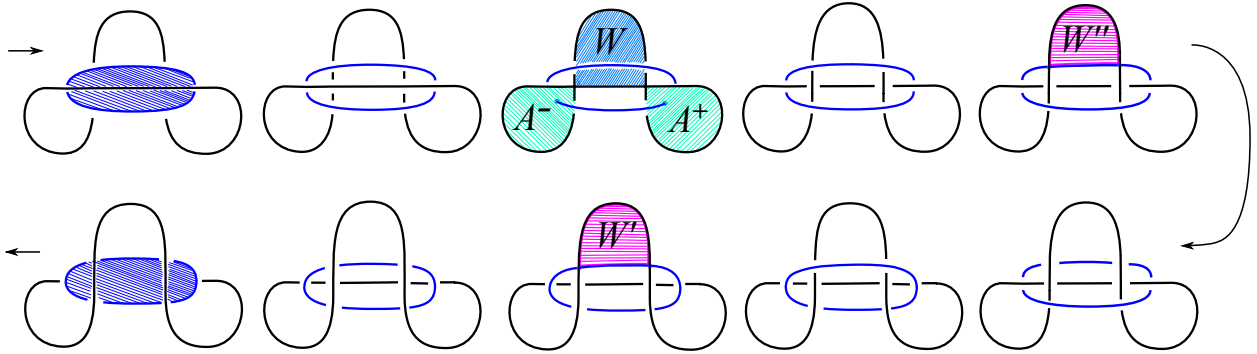


FIGURE 12. A *pre-Whitney sphere* for a standard Whitney disk W is the union of the left-most upper and lower blue disks together with the annulus traced out by the blue loop moving clockwise from left to right along the top row, then right to left along the bottom row. The two pairs of intersections between this pre-Whitney sphere and f (black) are paired by Whitney disks W' and W'' (purple) which are Whitney parallel to W (light blue). One sees that the pre-Whitney sphere is geometrically dual to each accessory disk in top middle picture (cf. Figure 11).

5.2.1. *Whitney spheres revisited.* Figure 12 shows an embedded *pre-Whitney sphere* for a standard Whitney disk W supported near a boundary arc of W . The two pairs of intersections between the pre-Whitney sphere and f are paired by Whitney disks W' and W'' which are parallel to W . Applying the W' - and W'' -Whitney moves to the pre-Whitney sphere yields the *Whitney sphere* S_W in the complement of f . Note that S_W is geometrically dual to each accessory disk, via an intersection inherited from the pre-Whitney sphere.

The two Whitney bubbles in the resulting S_W are the same as those in the first Whitney sphere description of Figure 6. It is an artifact of the different choices of local coordinates that in Figure 6 the Whitney bubbles appear to be “on different sides” of W , while in Figure 12 they appear to be “on the same side” of W : In both cases the bubbles “differ by meridian to f ”, meaning that any loop formed by a path between the bubbles in S_W followed by a path back through parallels of the interior of W will link f . It will follow from the homotopy-theoretic characterization given Lemma 21 that the description here yields the same Whitney spheres as in section 2 as well as in the proof of Lemma 13.

5.2.2. *Accessory spheres revisited.* Figure 13 shows an immersed positive *pre-accessory sphere* (green) supported near the corresponding self-intersection of f (black). The pair of green-black crossing changes in the top-right picture in the top row of the figure are paired by a Whitney disk V formed from a parallel copy of A . The pair of green-black

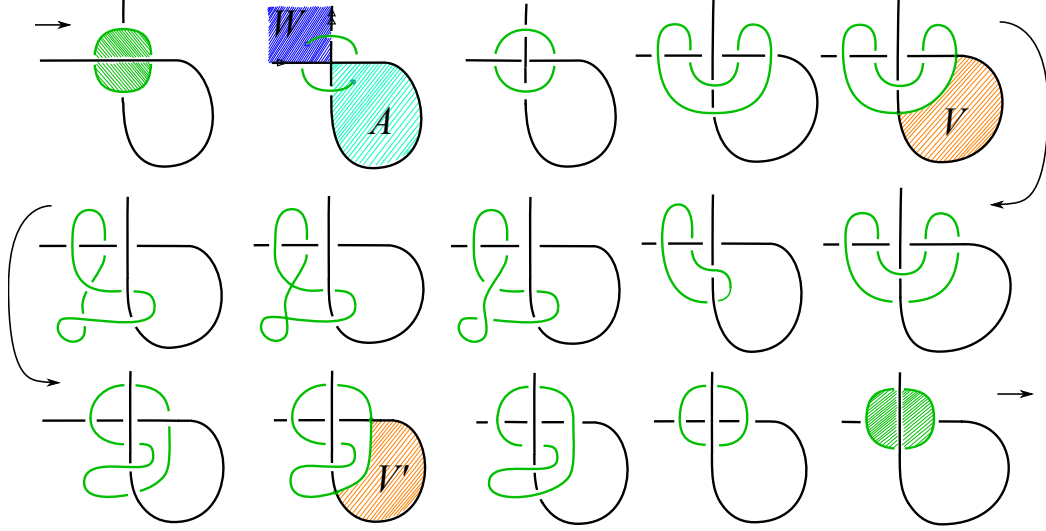


FIGURE 13. A green immersed *pre-accessory sphere* associated to a standard (positive) accessory disk A is the union of the two green disks (top left and bottom right) together with the homotopy of the green loop snaking from left to right along the top row, then right to left along the middle row, then left to right along the bottom row. The pre-accessory sphere is geometrically dual to each of W and A (top second-from-left picture).

crossing changes in the bottom second-from-left picture are paired by a Whitney disk V' formed from another parallel copy of A . Applying the V' - and V'' -Whitney moves to the pre-accessory sphere yields the positive *accessory sphere* S_A in the complement of f . (See section 8.7 for details on using parallel copies of accessory disks to guide Whitney moves.)

A pair of green-green self-crossing changes are visible in the second-from-left picture in the middle row of Figure 13. These self-crossing changes correspond to oppositely-signed self-intersections of S_A , and from the figure it can be computed that $\lambda(S_A, S_A) = 2 - x - x^{-1}$ as in the proof of Lemma 13.

From this description it is clear that S_A contains four parallel copies of A (two oppositely-oriented copies from each Whitney bubble), and that the oppositely-signed pair of self-intersections of S_A can be kept arbitrarily close to the self-intersection of f .

Note that S_A is geometrically dual to each of W and A , via intersections inherited from the pre-Whitney sphere.

5.2.3. *Whitney sphere-accessory sphere intersections.* Since the standard W and A (and parallel copies) have disjoint interiors, the intersections between S_W and S_A are the same as those between the pre-Whitney and pre-accessory spheres. Figure 14 shows that the only intersections between S_A and S_W occur near the self-intersection point of f in ∂A ;

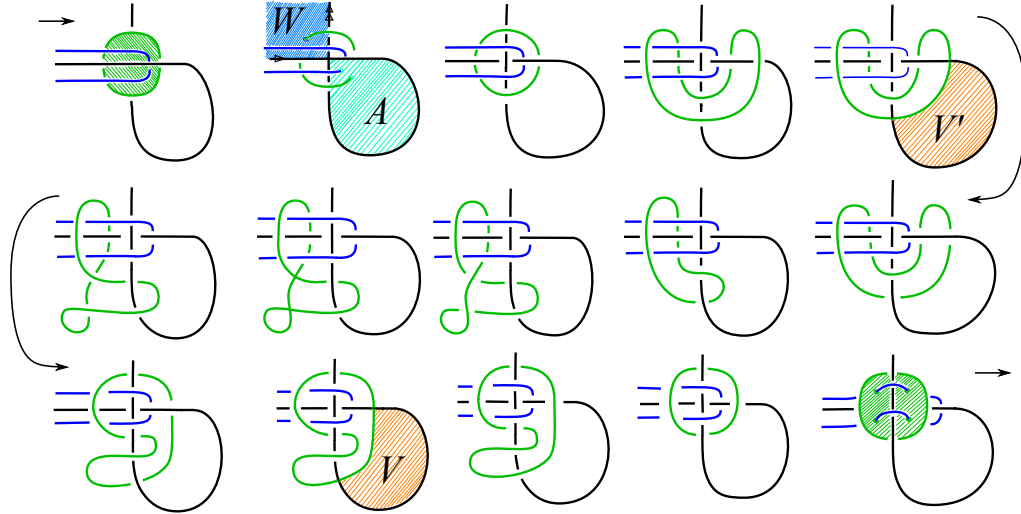


FIGURE 14. The 4 intersection points between a positive pre-accessory sphere S_A (green) and its pre-Whitney sphere S_W (blue) are contained entirely in the bottom right picture.

see the bottom right picture of Figure 14. It can be computed from the figure that $\lambda(S_A, S_W) = 2 - x - x^{-1}$, which is consistent with Lemma 13.

5.3. Cleanly immersed Whitney disks and accessory disks. An *immersed Whitney disk* W differs from a Whitney disk as described in section 2.2 in that the interior of W is allowed to have finitely many transverse self-intersections, and W is said to be *twisted* if the Whitney section over ∂W does not extend to a nowhere-vanishing normal section over W . In general, if the Whitney section over ∂W has normal Euler number $n \in \mathbb{Z}$ relative to the disk framing of W , then W is said to be *n-twisted*; with the case $n = 0$ corresponding to W being *framed*. See section 8.3 for details.

As in the framed embedded setting, an immersed Whitney bubble can be formed from two parallel oppositely-oriented copies of W , and a *Whitney move* guided by W is defined by the analogous cut-and-paste construction which replaces a neighborhood of an arc of ∂W in one sheet by this immersed Whitney bubble.

Each self-intersection of W gives rise to a self-intersection in any parallel copy of W and a pair of intersections between the two parallel copies of W which are part of the Whitney bubble. Moreover, if W is n -twisted, then there will be n additional intersections between the two parallel copies of W .

Definition 16. An immersed (possibly twisted) Whitney disk or accessory disk on f whose interior is disjoint from f is said to be *cleanly immersed*.

This leads to natural generalizations of Whitney spheres and accessory spheres: In section 5.2 the pre-Whitney and pre-accessory spheres are supported near f , so the constructions of Whitney spheres and accessory spheres in sections 5.2.1 and 5.2.2 can

be carried out using cleanly immersed Whitney disks and accessory disks which are not necessarily standard. From now on we take this more general definition of *Whitney spheres* and *accessory spheres*.

Remark. See [7] for alternative constructions of Whitney spheres and accessory spheres in the complements of immersed disks in the 4–ball, with applications to classical knot invariants.

5.4. Metabolic Whitney disks and accessory disks. The following definition gives criteria for cleanly immersed disks to be “sufficiently standard” so as to be useful in the upcoming Metabolic Unlinking Theorem 20:

Definition 17. A *metabolic collection* of disks for a standard position $f : S^2 \looparrowright S^4$ with $2n$ self-intersections consists of cleanly immersed Whitney disks W_1, \dots, W_n and cleanly immersed positive accessory disks A_1, \dots, A_n satisfying the following conditions:

- The boundaries of all W_i and A_j are disjointly embedded, except that ∂W_i intersects ∂A_i in the i th positive self-intersection p_i^+ of f . We also require that in a collar neighborhood of their boundaries, W_i and A_i are as in Figure 12, in particular, that there are no intersection points in these collars other than $p_i^+ = \partial W_i \cap \partial A_i$.
- The Λ -valued intersection invariants, computed in the complement of f , satisfy

$$\lambda(W_i, W_j) = 0 = \lambda(W_i, A_j),$$

where $\lambda(W_i, W_i)$ is computed using a Whitney section. We note that, as a consequence, each W_i is framed.

A Whitney or accessory disk for f is called *metabolic* if it is part of a metabolic collection.

Applying the constructions described in section 5.2 to a metabolic collection $\{W_i, A_i\}$ yields Whitney spheres S_{W_i} and accessory spheres S_{A_i} which have the same Λ -valued intersections as the Whitney and accessory spheres in Lemma 13 *except* that the intersections and self-intersections $\lambda(S_{A_i}, S_{A_j})$ of the accessory spheres are not controlled.

Lemma 13 shows that a metabolic collection always exists and the following result strengthens this statement:

Lemma 18. *Let $f : S^2 \looparrowright S^4$ be in standard position.*

- (1) *Any collection of the self-intersections of f in oppositely-signed pairs is induced from a standard collection of Whitney disks for f . Together with standard positive accessory disks, they form a metabolic collection.*
- (2) *In any metabolic collection $\{W_i, A_i\}$ for f , the corresponding Whitney and accessory spheres form a basis for the Λ -module $\pi_2(M)$. Moreover, the same sequence as in part (4) of Lemma 13 is exact.*

Here M denotes the complement of a regular neighborhood of f as in Lemma 13.

Proof. Claim (1) follows from the right-most Kirby diagram in Figure 10: Each green accessory handle attaching circle corresponds to a self-intersections of f , and these circles can be slid past each other to get the left-most diagram of Figure 9 for any choice of pairing. The metabolicity follows from Lemma 13.

For (2), consider the Λ -homomorphism $\varphi : \Lambda^{2n} \rightarrow \pi_2(M)$ that sends the free generators to the Whitney spheres and accessory spheres constructed from the metabolic collection. Then there is a commutative diagram

$$\begin{array}{ccc} \Lambda^{2n} & \xrightarrow{\varphi} & \pi_2(M) \\ \cong \downarrow & & \cong \downarrow \lambda/z \\ (\Lambda^{2n})^* & \xleftarrow{\varphi^*} & \pi_2(M)^* \end{array}$$

where $\lambda : \pi_2(M) \rightarrow \pi_2(M)^*$ is the intersection form and $z := 2 - x - x^{-1}$ is the factor arising in part (3) of Lemma 13. This lemma also implies that λ is divisible by z and after dividing it, becomes unimodular. The left vertical arrow is obtained by going around the diagram and hence is given by the intersection numbers (divided by z) of the Whitney and accessory spheres.

By the definition of a metabolic collection, this pairing is also unimodular. The diagram hence implies that φ^* is onto which stays true when tensoring it with \mathbb{Q} . Since $\pi_2(M)^*$ is a free Λ -module and $\Lambda \otimes \mathbb{Q} = \mathbb{Q}[x^{\pm 1}]$ is a principal ideal domain, it follows that φ^* is also injective, hence an isomorphism.

Again the commutativity of the diagram implies that φ is an isomorphism which proves both parts of our statement (2). \square

The following realization result for metabolic isometries will provide the starting point for the proof of the subsequent Metabolic Unlinking Theorem:

Lemma 19. *Let (f, f_2) be a link map with f in standard position, and with $\lambda(f_2, f_2) = 0$, such that $\lambda(W_i, f_2) \in z \cdot \Lambda$ for some metabolic collection $\{W_i, A_i\}$ for f . Denote by M_n the complement of a regular neighborhood of f , where n is the number of pairs of self-intersections. After two more finger moves on f (in the complement of f_2) there is an isometry Φ of the intersection form $(\pi_2 M_{n+2}, \lambda)$ such that:*

- (1) $\Phi \equiv \text{id} \pmod{z}$, i.e. for all $a \in \pi_2 M_{n+2}$ there is an element $b \in \pi_2 M_{n+2}$ such that $\Phi(a) - a = z \cdot b$, and
- (2) $\Phi^{-1}(f_2) \in \langle S_{W_i} \rangle$.

Proof. First observe that since Λ has no zero-divisors an isometry of $(\pi_2 M_n, \lambda)$ is the same as an isometry of the form $(\pi_2 M_n, \lambda')$ where

$$\lambda'(a, b) := \frac{1}{z} \cdot \lambda(a, b) \quad \forall a, b \in \pi_2 M_n.$$

This hermitian form λ' is well-defined and unimodular by part (3) of Lemma 13 and Definition 17. We prefer to work with λ' in place of λ throughout this proof.

By our assumption $\lambda(W_i, f_2) \equiv 0 \pmod{z}$ and part (4) of Lemma 13 (via Lemma 18) there is a sphere g with

$$[g] \in \langle S_{W_i} \rangle \leq \pi_2 M_n$$

such that $[g] \equiv [f_2] \pmod{z}$. It also follows that $\lambda(g, g) = 0$. We do one finger move on f along an arc which links f_2 precisely once. This link homotopy changes f_2 to $f_2 + S_{W_{n+1}}$ in $\pi_2 M_{n+1}$, where W_{n+1} is a local framed embedded Whitney disk inverse to the finger move. By changing g to $g + S_{W_{n+1}}$ we may assume that in $\pi_2 M_{n+1}$ we still have $[g] \equiv [f_2] \pmod{z}$ and in addition

$$\lambda'(g, g) = 0 = \lambda'(f_2, f_2) \text{ and } \lambda'(g, S_A) = 1 = \lambda'(f_2, S_A).$$

Here S_A is the accessory sphere constructed from the standard (positive) accessory disk $A = A_{n+1}$ corresponding to the finger move. Let C_1 be the orthogonal complement of the Λ -span $\langle g, S_A \rangle$ in $(\pi_2 M_{n+1}, \lambda')$. Similarly, let C_2 be the orthogonal complement of $\langle f_2, S_A \rangle$ in $(\pi_2 M_{n+1}, \lambda')$. Since the forms on $\pi_2 M_{n+1}$, $\langle g, S_A \rangle$ and $\langle f_2, S_A \rangle$ are unimodular the Λ -modules C_i are stably free and hence free. We define two bases \mathfrak{B}_i of $\pi_2 M_{n+1}$ by

$$\mathfrak{B}_1 := \{g, S_A, \text{ some basis for } C_1\} \quad \text{and} \quad \mathfrak{B}_2 := \{f_2, S_A, \text{ some basis for } C_2\}.$$

Let J be the $(2n+2, 2n+2)$ -matrix with entries in Λ which represents the identity map on $\pi_2 M_{n+1}$ in terms of the basis \mathfrak{B}_1 and \mathfrak{B}_2 . Then J is the matrix for an isometry between the *abstract* hermitian forms

$$\begin{pmatrix} 0 & 1 \\ 1 & 1 \end{pmatrix} \perp (C_1, \lambda') \text{ and } \begin{pmatrix} 0 & 1 \\ 1 & 1 \end{pmatrix} \perp (C_2, \lambda').$$

Moreover, since $[g] \equiv [f_2] \pmod{z}$ we know that C_1 equals $C_2 \pmod{z}$, and by choosing the above bases for C_i to be equal in $\pi_2 M_{n+1}/z$ we may assume that

$$J_{ij} \equiv \delta_{ij} \pmod{z}.$$

Now we introduce one further trivial finger move to f , leaving f_2 and g unchanged in $\pi_2 M_{n+1} \subset \pi_2 M_{n+2}$. The new orthogonal complements D_i to $\langle g, S_A \rangle$ and $\langle f_2, S_A \rangle$ in $(\pi_2 M_{n+2}, \lambda')$ are then given by

$$D_i = \langle S_{W_{n+2}}, S_{A_{n+2}} \rangle \perp C_i.$$

Since λ' restricted to the first summand is just the form $\begin{pmatrix} 0 & 1 \\ 1 & 1 \end{pmatrix}$ we conclude that the matrix J induces an isometry from D_1 to D_2 which is the identity modulo z . But this isometry can be extended to the desired isometry of $(\pi_2 M_{n+2}, \lambda)$ by sending g to f_2 and leaving S_A fixed. \square

5.5. The Metabolic Unlinking Theorem. The following result gives the promised strengthening of the implication $(iii) \Rightarrow (i)$ in Theorem 12:

Theorem 20 (Metabolic Unlinking). *A link map (f_1, f_2) is link homotopically trivial if there are finger moves on f_1 (disjoint from f_2) which bring f_1 into a standard position f such that $\lambda(f_2, f_2) = 0$ and there is a metabolic collection $\{W_i, A_i\}$ for f with*

$$\lambda(W_i, f_2) \in z \cdot \Lambda.$$

Proof. By Lemma 19 we may assume that we have a link map (f, f_2) , with f in standard position, such that the 4-manifold $M = S^4 \setminus$ small normal bundle of f allows an isometry Φ of the intersection form $(\pi_2 M, \lambda)$ such that

- (1) $\Phi \equiv \text{id} \pmod{z}$ and
- (2) $\Phi^{-1}(f_2) \in \langle S_{W_i} \rangle$

for some metabolic collection $\{W_i, A_i\}$ for f . We want to use Lemma 9 several times to conclude that (f, f_2) is link homotopically trivial. Therefore, we need to express f_2 as a linear combination of Whitney spheres formed from disjoint framed embedded Whitney disks. Define spheres

$$T_i := \frac{1}{z} \cdot (\Phi(S_{W_i}) - S_{W_i}) \in \pi_2 M.$$

This definition makes sense since $\Phi \equiv \text{id} \pmod{z}$ and Λ has no zero divisors. Then define Whitney disks

$$V_i := W_i \# T_i$$

which are the interior connected sum of the metabolic Whitney disks W_i with the spheres T_i . We assert that the V_i are cleanly immersed Whitney disks for f with $S_{V_i} = \Phi(S_{W_i})$, satisfying $\lambda(V_i, V_j) = 0$, and with algebraically transverse spheres $V_i^\dagger := \Phi(S_{A_i})$ satisfying $\lambda(V_i, V_j^\dagger) = \delta_{ij}$.

To prove this assertion, first note that by our convention we represent the spheres T_i by immersions with trivial normal bundle. In particular, adding them to W_i does not change the relative Euler number of the Whitney disks. By Lemma 21 below, the class in $\pi_2 M$ of any Whitney sphere S_W is equal to $z \cdot [W]$ in the relative homotopy group $\pi_2(M, \partial M)$, so we have

$$S_{V_i} = z \cdot [V_i] = z \cdot [W_i] + z \cdot T_i = S_{W_i} + \Phi(S_{W_i}) - S_{W_i} = \Phi(S_{W_i}).$$

It follows that $\lambda(V_i, V_j) = 0$ because Φ is an isometry, and thus

$$0 = \lambda(S_{W_i}, S_{W_j}) = \lambda(S_{V_i}, S_{V_j}) = z \cdot z \cdot \lambda(V_i, V_j).$$

A similar comparison shows that V_j^\dagger are algebraically transverse spheres for V_i :

$$\lambda(V_i, V_j^\dagger) = \lambda(W_i, S_{A_j}) = \delta_{ij}.$$

Since $\pi_1 M$ is cyclic and thus a good group, we can apply Freedman's embedding theorem [14, Cor.5.1B] to obtain disjoint topologically framed embedded Whitney disks, regularly

homotopic to V_i and with algebraically transverse spheres. We continue to call the resulting collection of Whitney disks V_i .

The corresponding Whitney spheres S_{V_i} are disjointly embedded and the condition $\Phi^{-1}(f_2) \in \langle S_{W_i} \rangle$ from Lemma 19 translates into

$$[f_2] \in \langle S_{V_i} \rangle \leq \pi_2 M \text{ i.e. } [f_2] = \sum_{i=1}^n \alpha_i \cdot S_{V_i} \text{ with } \alpha_i \in \mathbb{Z}[x^{\pm 1}].$$

We will next apply the Whitney Homotopy Lemma 9 to (f, f_2) n times. The first application is the link homotopy which does the Whitney move on V_1 , then shrinks $\alpha_1 \cdot S_{V_1}$, and finally does the finger move that reverses the Whitney move and returns f to its original position. We get the link map

$$(f, f_2 - \alpha_1 \cdot S_{V_1}) = (f, \sum_{i=2}^n \alpha_i \cdot S_{V_i}).$$

Then we apply the same moves using the disjointly embedded Whitney disks V_2, V_3, \dots, V_n to get a link homotopy from (f, f_2) to $(f, *)$. But now f shrinks in $S^4 \setminus * = \mathbb{R}^4$ and Theorem 20 is proven. \square

We note that in the above argument, we brought f_2 into a position where it's the geometric sum of embedded Whitney spheres S_{V_i} , and is in particular disjoint from the embedded Whitney disks V_i . So we could do Whitney moves on f along all the V_i , in the complement of f_2 , to arrive at an embedded link map (f', f_2) with possibly knotted components. If this embedding was smooth one could conclude that (f', f_2) is trivial from the main result of [5], which uses singular handles and stratified Morse theory.

Our proof here works in the topological category and is more explicit: We see step by step how f_2 becomes geometrically the sum of fewer and fewer Whitney spheres since each S_{V_i} shrinks after doing the Whitney move on V_i by a Whitney homotopy, until f_2 eventually becomes trivial.

5.6. Homotopy theoretic definition of a Whitney sphere. The next lemma completes the proof of Theorem 20, and gives a purely homotopy-theoretic definition of a Whitney sphere S_W in terms of the cleanly immersed W on a generic immersion $f : S^2 \looparrowright X^4$. Assuming that X has no boundary, the boundary ∂M of

$$M := X \setminus \text{small normal bundle of } f$$

only depends on the double points of f and is a standard 3-manifold: In any of the Kirby diagrams of Figures 9 and 10 replace the dots on circles by 0-framings to get a framed link description. It is not hard to show that ∂M is prime because $\pi_1 M$ is infinite and not a free product. If f is a framed embedding then $\partial M = S^1 \times S^2$, and if it isn't then $\pi_2(\partial M) = 0$.

In the presence of a Whitney disk W for f we are in the latter case and hence the homotopy class of a Whitney sphere S_W is determined by its homotopy class in the

relative group $\pi_2(M, \partial M)$. But this group contains as an element $[W]$ represented by the Whitney disk (with a small collar removed so that its boundary lies in ∂M).

In the following lemma we use the natural action of $\pi_1(\partial M)$ on $\pi_2(M, \partial M)$:

Lemma 21. *Suppose that W is a cleanly immersed Whitney disk on $f : S^2 \looparrowright X^4$. Then the monomorphism $\pi_2(M) \rightarrow \pi_2(M, \partial M)$ sends $[S_W]$ to $(1 + gh^{-1} - g - h^{-1}) \cdot [W]$, where $g, h \in \pi_1(\partial M)$ both map to the same meridian of f in $\pi_1 M$ via $\partial M \hookrightarrow M$.*

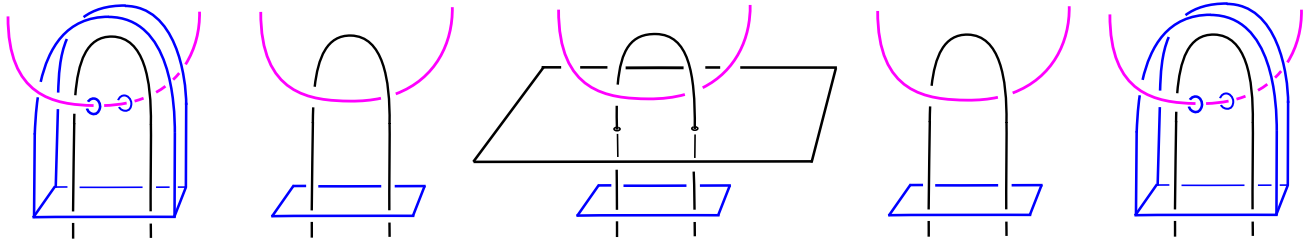


FIGURE 15. The (pre-image of) the sphere-minus-four-disks S_W^0 (blue) in the 4-ball domain of $W \times D^2$. The purple arc traces out (the pre-image of) a disk which is dual to W . Compare Figure 6.

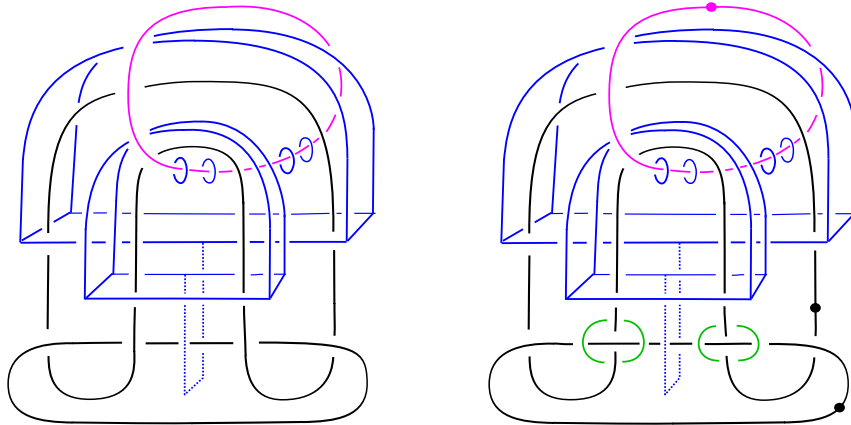


FIGURE 16. Left: The black and purple sheets form a Borromean rings in the boundary 3-sphere of Figure 15. The two twice-punctured Whitney bubbles in $S_W^0 \subset M'$ are also shown, but suppressed from view (apart from the dotted PL arc) is the embedded annulus in S_W^0 connecting the Whitney bubbles' boundaries (cf. Figure 15). Right: A Kirby diagram of M' , the complement of a neighborhood of f in a $S^1 \times B^3$ neighborhood of $\partial W \subset X^4$. The green circles are 0-framed 2-handles which realize the black-black crossing changes in the boundary. Part of the annulus (again suppressed from view) in S_W^0 passes over the green 2-handles, as shown in the left picture of Figure 17.

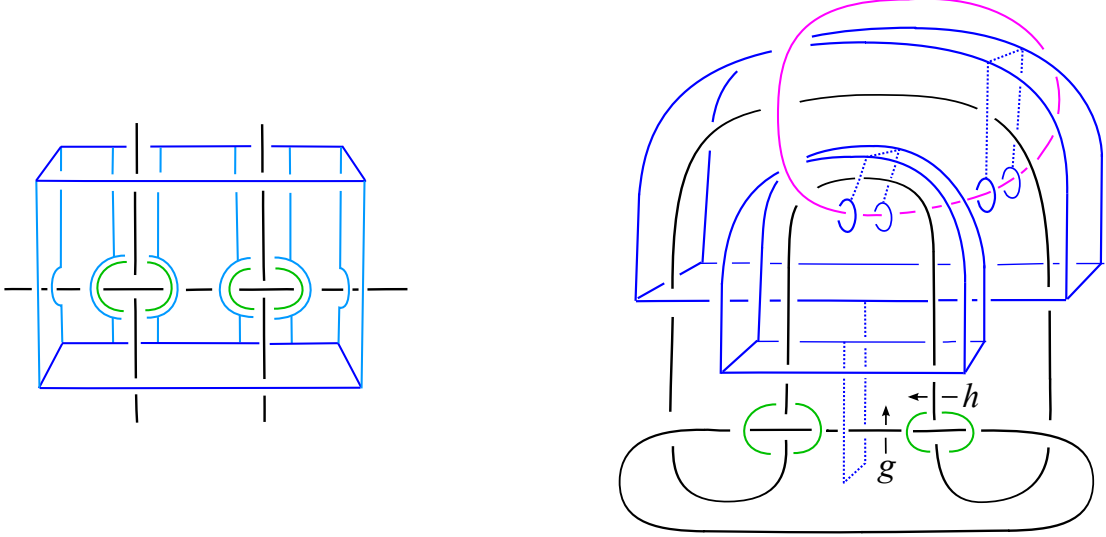


FIGURE 17. Left: The part of the embedded annulus in S_W^0 connecting the Whitney bubbles' boundaries near the green 2-handles. Right: The 3-manifold $\partial M' \subset \partial M$, described by replacing the dotted circles in Figure 16 by 0-framed 2-handles.

Proof. Deleting from S_W the interiors of the four parallel copies of W yields a sphere-minus-four-disks S_W^0 embedded in ∂M , so in the relative homotopy group S_W maps to four copies of W . By Seifert–Van Kampen, it suffices to carry out the computation of the group elements in the intersection M' of M with a $S^1 \times B^3$ neighborhood of $\partial W \subset X^4$. Starting with the description of S_W in Figure 6, Figure 15 explains the Kirby diagram for M' shown in Figure 16, with $S_W^0 \subset M'$.

The right-hand side of Figure 17 shows two elements $g, h \in \pi_1 \partial M'$ which each map to the same generator x of $\pi_1 M$ by the inclusion $\partial M \hookrightarrow M$. The group elements for the image of S_W in $\pi_2(M, \partial M)$ are represented by loops through the punctures of S_W^0 that run along S_W^0 and return along the purple circle dual to W . Taking the basepoint at the second puncture from the left, yields the elements h^{-1} , 1 , g and gh^{-1} , respectively, for the four punctures (from left to right). The signs of these elements alternate from left to right, so orienting S_W appropriately yields $(1 + gh^{-1} - g - h^{-1}) \cdot [W]$ as its image in $\pi_2(M, \partial M)$. \square

5.7. Comparing Whitney sphere descriptions. We close this section by observing how the various descriptions of Whitney spheres given so far are all homotopic via Lemma 21.

For the descriptions of S_W given in local coordinates (Figure 6 and Figure 12) it suffices to check that each bubble contains a pair of oppositely-oriented copies of W which differ by a meridian to one sheet of f , and that the bubbles differ from each other by a meridian

to the other sheet, as in Figure 17. The same goes for the generalization of the Figure 12 construction using cleanly immersed W .

For the Kirby diagram description of S_W in the right-most picture of Figure 9, the embedded disk in S_W bounded by the unknotted blue attaching circle contains four normal disks to a green circle, each of which is a parallel of W as can be seen from the left-most picture of Figure 9. The group elements and orientations can be computed from the figure.

6. PROOF OF COROLLARY 2: PULLING AWAY AN EMBEDDED SPHERE

In this section we derive Corollary 2 from Theorem 20. So we have to show that for any embedding $f_1 : S^2 \hookrightarrow S^4$, the link map (f_1, f_2) is link homotopic to (f, f_2) where f is in standard position with a metabolic collection $\{W_i, A_i\}$ such that

$$\lambda(W_i, f_2) \in z \cdot \Lambda \quad \text{and} \quad \lambda(f_2, f_2) = 0.$$

Recall that $\Lambda = \mathbb{Z}[x^{\pm 1}]$ and $z = 2 - x - x^{-1}$, so $z \cdot \Lambda = (1 - x)^2 \cdot \Lambda$.

Alexander duality holds for any embedding, so we know that

$$H_1(S^4 \setminus f_1) \cong H^2(S^2) \cong \mathbb{Z} \quad \text{and} \quad H_2(S^4 \setminus f_1) \cong H^1(S^2) = 0.$$

In particular, we have an infinite cyclic cover Y of this 2-knot complement and denote by $t \in \pi_1(S^4 \setminus f_1)$ any embedded loop that maps to a generator in H_1 . Using the coefficient exact sequence

$$0 \longrightarrow \Lambda \xrightarrow{\cdot(1-t)} \Lambda \xrightarrow{\epsilon} \mathbb{Z} \longrightarrow 0$$

we get the corresponding Bockstein exact sequence

$$\cdots \longrightarrow H_2(Y) \xrightarrow{\cdot(1-t)} H_2(Y) \longrightarrow 0$$

The map $f_2 : S^2 \rightarrow S^4 \setminus f_1$ lifts to Y and hence we get a representative $[f_2] \in H_2(Y)$. For any $N \in \mathbb{N}$, the above exact sequence says that there is an $a_N \in H_2(Y)$ such that $(1 - t)^N \cdot a_N = [f_2]$. The equality is given by a (compact) 3-chain c and hence we can find an open neighborhood U_N of $f_1(S^2)$ in S^4 such that $S^4 \setminus U_N$ contains the compact sets $f_2(S^2)$ and t , and the induced infinite cyclic covering Y_N contains the compact sets a_N and c .

Now pick a generic approximation f of f_1 inside U_N and do finger moves (away from f_2) until f is standard. We have a pair of inclusions

$$S^4 \setminus f_1 \supset S^4 \setminus U_N \subset S^4 \setminus f$$

and by construction of U_N , the objects t, f_2, a_N, c do exist in $S^4 \setminus f$. Since f is standard, $\pi_1(S^4 \setminus f) \cong \mathbb{Z}$ and so t is homologous to some power x^k of the generator x of this fundamental group. If Z is the infinite cyclic covering of $S^4 \setminus f$, then we arrive at the equation

$$f_2 = (1 - x^k)^N a_N \in H_2(Z) = \pi_2(S^4 \setminus f).$$

As a consequence, we see that for a standard collection of Whitney disks W_i on f the polynomial $(1-x)^N$ divides both of the expressions

$$\lambda(W_i, f_2) = \lambda(W_i, (1-x^k)^N a_N) \quad \text{and} \quad \lambda(f_2, f_2) = \lambda((1-x^k)^N a_N, (1-x^k)^N a_N).$$

This implies for $N = 2$ that our I^2 -conditions hold and by increasing N arbitrarily, we also get $\lambda(f_2, f_2) = 0$. \square

7. PROOF OF THEOREM 3

This section completes the proof of Theorem 3 via the following proposition which shows that a link map with vanishing Kirk invariant satisfies the algebraic intersection condition of the Metabolic Unlinking Theorem 20:

Proposition 22. *If (f, f_2) is a link map with vanishing Kirk invariant, then after a link homotopy it can be arranged that f is in standard position with metabolic Whitney disks W_i satisfying $\lambda(W_i, f_2) \in z \cdot \Lambda$ for all i .*

Recall that $\Lambda = \mathbb{Z}[x^{\pm 1}]$ for $\pi_1(S^4 \setminus f) = \langle x \rangle \cong \mathbb{Z}$, and $z = 2 - x - x^{-1}$, so $z \cdot \Lambda = I^2$ for I the augmentation ideal of Λ .

An outline of the proof of Proposition 22 will be given in section 7.2 after introducing some terminology to facilitate the discussion:

7.1. Primary and secondary multiplicities. Let (f, f_2) be an oriented link map with $\pi_1(S^4 \setminus f) = \langle x \rangle \cong \mathbb{Z}$, for x a positive meridian to f , and let $D \looparrowright S^4$ be an oriented immersed disk with $\partial D \subset f$ such that the interior of D is disjoint from f , e.g. D is a cleanly immersed Whitney disk or accessory disk on f .

Then we can write

$$\lambda(D, f_2) = m + n(1-x) + P \in \mathbb{Z}[x^{\pm 1}],$$

for $m \in \mathbb{Z}$, $n \in \mathbb{Z}$, and $P \in I^2$ (by choosing a basing of D appropriately). We call the integers m and n the *primary multiplicity* and *secondary multiplicity*, respectively, of D . Note that this notion of ‘‘multiplicity’’ always refers to intersections with f_2 .

The primary multiplicity is just the linking number of ∂D and f_2 , and hence can also be used in the case that $\partial D \cap f_2 = \emptyset$, even if ∂D is not contained in f .

The secondary multiplicity only depends on a push-off $\overline{\partial D}$ of ∂D into the interior of D : After (perhaps) some disjoint finger moves, we may assume that $\pi_1(S^4 \setminus (f \cup f_2))$ is isomorphic to the free Milnor group on (positive) meridians x and x_2 . Then $\overline{\partial D}$ represents $x_2^m [x, x_2]^n \in \pi_1(S^4 \setminus (f \cup f_2))$, with the commutator exponent n equal to the secondary multiplicity of D .

7.2. Outline of the proof of Proposition 22. In this terminology the conclusion of Proposition 22 says that f admits a metabolic collection whose Whitney disks all have vanishing primary and secondary multiplicities.

It will not be difficult to arrange the vanishing of the Whitney disks’ primary multiplicities, but killing the secondary multiplicities will involve some work!

The proof will proceed by an eight-step construction which starts with a standard collection and creates many more new Whitney disks and accessory disks. This will involve the creation and manipulation of Whitney disks whose interiors are temporarily not disjoint from f , but disjointness will eventually be recovered using carefully constructed “secondary” Whitney disks. Keeping track of the different types of new disks and the progress towards controlling their intersections and multiplicities will involve some tricky book-keeping, so the following outline is provided for guidance:

- (a) Before starting the construction, f_2 will be expressed as a linear combination of standard accessory spheres which intersect an initial collection of Whitney disks W_i on f in a controlled way (Lemma 23, section 7.5). In particular, these W_i will have primary multiplicity zero.
- (b) The goal of Step 1 through Step 6 (sections 7.7–7.12) of the construction is to reduce to 0 or 1 the primary multiplicities of all accessory disks whose corresponding Whitney disks have possibly non-zero secondary multiplicity. This reduction will allow the secondary multiplicities of the corresponding Whitney disks to be killed in the Step 7 and Step 8.
 - Step 1 eliminates pairs of intersections between initial Whitney disks W_i and f_2 which represent non-zero secondary multiplicity, at the cost of creating new pairs of self-intersections of f . This step also constructs Whitney disks (the U in Lemma 24) in preparation for cleaning up new Whitney disks that will be created during later steps.
 - Step 2 constructs Whitney disks V_0, V_1 for each new pair of self-intersections created in Step 1, such that V_0 and V_1 have interior intersections with f . These V_0 and V_1 have accessory disks with primary multiplicities 0 and 1, respectively, that were created in Step 1 (Lemma 24).
 - Step 3 creates even more intersections between f and V_0 by tubing V_0 and f into standard accessory and Whitney spheres on f_2 . This tubing is a key part of the construction as it serves to reduce the primary multiplicities on the new accessory disks that will be created when f is later pushed off of the interior of V_0 (in Step 5). This step also constructs temporary bigon disks B^j that will be used to form these new accessory disks.
 - Step 4 applies the analogous tubing from Step 3 but to V_1 , and constructs quadrilateral disks Q^j that will be used to form secondary Whitney disks for later making f disjoint from the interior of V_1 (in Step 6).
 - Step 5 pushes f off of the interior V_0 at the cost of creating new self-intersections of f paired by controlled Whitney disks W^j whose associated accessory disks A^j (formed from the B^j in Step 3) have primary multiplicity 0 or 1.

Here the super-script notation serves to differentiate these new W^j, A^j from the initial collection W_i, A_i .

The interior of each W^j intersects f , but these intersections are paired by parallels U^j of the previously constructed U from Step 1. At this point only those W^j whose A^j has primary multiplicity 1 are made cleanly embedded by U^j -moves.

- Step 6 removes all interior intersections between f and V_1 using secondary Whitney disks R^j that were created during Step 5 from the quadrilaterals Q^j constructed in Step 4.

A summary of the result of Step 1–Step 6 is given in section 7.14.

- (c) In Step 7 (section 7.15) each Whitney disk whose associated accessory disk has primary multiplicity 1 will be made to have secondary multiplicity 0 by a “double boundary-twisting” operation. It temporarily creates intersections between the Whitney disk and f which are then eliminated via a secondary Whitney move guided by a parallel copy of the accessory disk. More generally, this operation can change the secondary multiplicity of a Whitney disk by any integral multiple of the primary multiplicity of an associated accessory disk (Lemma 26).
- (d) Step 8 (section 7.16) deals with the remaining W^j from Step 5 whose A^j have primary multiplicity 0. First, the vanishing of $\lambda(f_2, f_2)$ is used to show that there are an even number of such W^j . Then a “double transfer move” is used to collect the U^j in pairs that yield canceling contributions to the secondary multiplicities of the W^j after making them cleanly embedded by U^j -Whitney moves.

This step also creates more self-intersections of f which are paired by local Whitney disks which are arranged to have vanishing secondary multiplicity. Constructing accessory disks for these local Whitney disks requires the full generality of the definition of a metabolic collection (Definition 17).

These eight steps are carried out first in a low-multiplicity base case, which is then checked in section 7.18 to be extendable to the general case. The definition of a metabolic collection stipulates *positive* accessory disks, but this will be easily arranged after Step 8 in section 7.17.

Throughout the constructions f and f_2 will only be changed by disjoint finger moves (and isotopy), hence f will always be in standard position.

Details on techniques used in the constructions are given in Section 8.

As an illustration of a technique that will be used repeatedly during the proof, we have the following observation on how using Whitney moves to make disks’ interiors disjoint from f affects the resulting primary and secondary multiplicities:

7.3. Observation: Let $D \looparrowright S^4$ be an oriented immersed disk, with $D \cap f_2 = \emptyset$, such that $D \pitchfork f$ consists of two oppositely-signed intersections paired by a Whitney disk U which has interior disjoint from f . Then the result D' of doing the U -Whitney move on D has interior disjoint from f , and satisfies

$$\lambda(D', f_2) = (1 - x) \cdot \lambda(U, f_2) \in \mathbb{Z}[x^{\pm 1}]$$

for an appropriate orientation and basing choice on U .

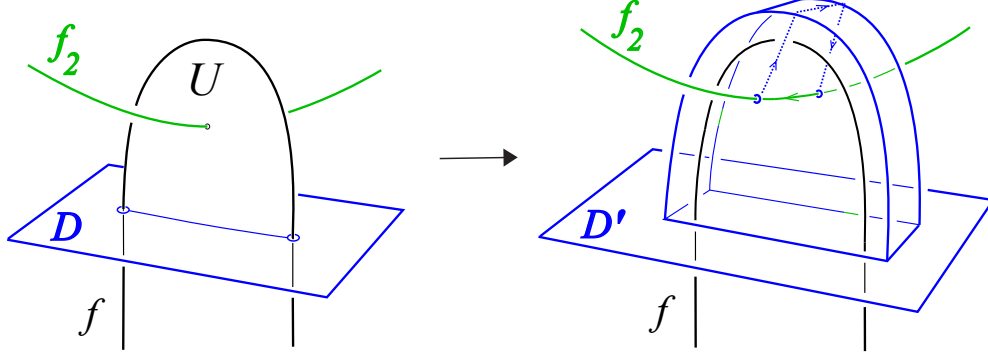


FIGURE 18. Left: A Whitney disk U pairing intersections between D (blue) and f (black), such that U has an interior intersection with f_2 (green). Right: The result D' of doing the U -Whitey move on D has a pair of oppositely-signed intersections with f_2 whose group elements differ by a meridian to f (indicated by the dotted blue arc).

To see why this equation holds, observe that the U -Whitney move forms D' from D by adding two oppositely oriented copies of U , so each each intersection in $U \cap f_2$ gives rise to two oppositely-signed intersections between D' and f_2 with group elements that differ by the generator x represented by a meridian to f (Figure 18). Any self-intersections or non-trivial twisting of U will yield self-intersections in D' , but will not affect $\lambda(D', f_2)$.

The same equation holds if U is a *union* of Whitney disks (connected by basings in D) pairing $D \pitchfork f$ under the same other assumptions. In particular, *the primary multiplicity of such a D' is always zero, and the secondary multiplicity of D' is equal to the primary multiplicity of U .*

If the assumption that D is disjoint from f_2 is weakened to just requiring that $\partial D \cap f_2 = \emptyset$, then the right side of the equation will give the contributions to $\lambda(D', f_2)$ coming from the new intersections $\{D' \cap f_2\} \setminus \{D \cap f_2\}$ created by the U -Whitney move(s).

7.4. Orientation conventions. A Whitney disk W pairing $\{p^+, p^-\} \in f \pitchfork f$ is oriented by choosing a *positive boundary arc* $\partial_+ W \subset \partial W$ which is oriented from the negative self-intersection p^- towards the positive self-intersection p^+ , and a *negative boundary arc* $\partial_- W \subset \partial W$ running back to p^- in the other sheet of f . This choice of orientation on ∂W together with the usual “outward first” convention orients W . Any positive and negative accessory disks A^+ and A^- associated to such an oriented Whitney disk W are oriented according to the convention indicated in Figure 19: The boundaries ∂A^\pm are oriented to run from the negative sheet of f at p^\pm to the positive sheet of f at p^\pm (again using the outward first convention).

On the other hand, given a pair of oriented accessory disks A^\pm for p^\pm , section 8.8 shows how a Whitney disk W for p^\pm can be constructed by half-tubing together A^+ and A^- (perturbed rel p^\pm) along f so that the resulting triple W, A^+, A^- satisfies the orientation convention of the previous paragraph. If the A^\pm are standard, or more generally framed

and disjointly cleanly embedded, then a 4–ball neighborhood of the triple W, A^+, A^- will be diffeomorphic to Figure 19. (*Framed* accessory disks are discussed in section 8.6.)

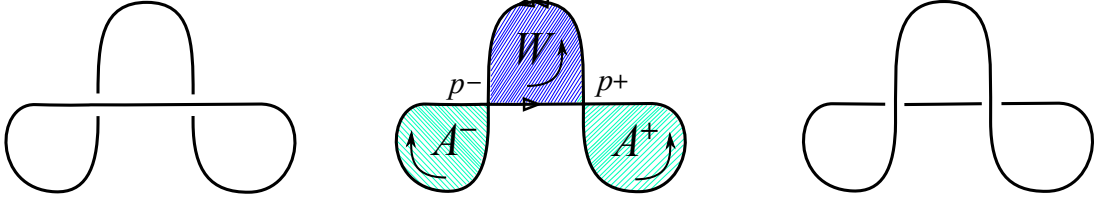


FIGURE 19. Orientation conventions for Whitney disks and accessory disks.

7.5. Initial form for the proof of Proposition 22: We may assume that f is in standard position, admitting standard Whitney disk–accessory disk triples W_i, A_i^+, A_i^- as in section 5.1 (framed, cleanly embedded, only intersecting at the self-intersections of f). Since $\lambda(f, f) = 0 \in \mathbb{Z}[x_2^\pm]$, we may also assume by Lemma 18(1) that A_i^+ and A_i^- have the same primary multiplicity m_i , for each i , with orientations on the A_i^\pm such that $m_i \geq 0$, and W_i oriented as in section 7.4, with a neighborhood of $W_i \cup A_i^+ \cup A_i^-$ diffeomorphic to Figure 19.

We fix orientations on the basis of standard accessory spheres $S_{A_i^\pm}$ from Lemma 14 so that $\lambda(W_i, S_{A_i^\pm}) = \pm 1$, and write f_2 as a $\mathbb{Z}[x^{\pm 1}]$ -linear combination of the $S_{A_i^\pm}$:

$$(1) \quad f_2 = \sum \alpha_i^+ \cdot S_{A_i^+} + \alpha_i^- \cdot S_{A_i^-}$$

where each α_i^\pm is of the form

$$(2) \quad \alpha_i^\pm = m_i + n_i^\pm(1 - x) + P_i^\pm$$

with $n_i^\pm \in \mathbb{Z}$ the secondary multiplicities of A_i^\pm , and P_i^\pm Laurent polynomials in I^2 .

Since W_i is dual to each of $S_{A_i^+}$ and $-S_{A_i^-}$, we have

$$(3) \quad \lambda(W_i, f_2) = (m_i - m_i) + (n_i^+ - n_i^-)(1 - x) + P_i^+ - P_i^- = 0 + n_i(1 - x) + P_i$$

with $P_i = P_i^+ - P_i^- \in I^2$, and $n_i = n_i^+ - n_i^- \in \mathbb{Z}$. It follows that each W_i has primary multiplicity $0 = m_i - m_i$, and the integer n_i is the secondary multiplicity of W_i . The starting point for the proof of Proposition 22 is the observation that the tubes and parallels of $S_{A_i^\pm}$ realizing f_2 as the connected sum in Equation (1) can be chosen so that the intersections in $W_i \cap f_2$ contributing to the secondary multiplicities n_i admit the “controlled” Whitney disks illustrated in Figure 20 and described in the following lemma:

Lemma 23. *The connected sum decomposition of f_2 in Equation 1 can be realized so that for each i the following three conditions are satisfied:*

- (a) *The m_i -many copies of each $S_{A_i^\pm} \subset f_2$ which contribute the canceling primary multiplicities in Equation (3) are disjoint from W_i .*

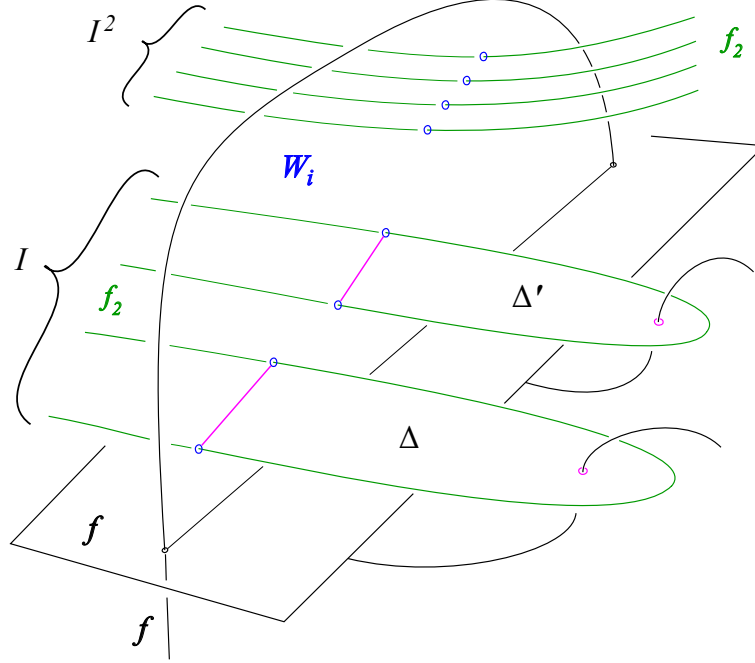


FIGURE 20. Illustration of Lemma 23: The pairs in $W_i \cap f_2$ which contribute the terms $n_i(1-x) \in I$ to $\lambda(W_i, f_2)$ admit Whitney disks (here Δ and Δ') which each contain just a single intersection with f , as in Item (b).

- (b) *The intersections in $W_i \cap f_2$ which contribute the terms $n_i(1-x) \in I$ to $\lambda(W_i, f_2)$ in Equation (3) come in $|n_i|$ -many pairs, each of which admits a framed embedded Whitney disk containing only a single interior intersection with f .*
- (c) *The rest of the intersections in $W_i \cap f_2$ contribute the terms $P_i \in I^2$ to $\lambda(W_i, f_2)$ in Equation (3).*

Proof. Condition (a): The m_i -many pairs of parallel copies of each of $S_{A_i^+}$ and $S_{A_i^-}$ corresponding to the coefficients m_i in Equation 2 can be made disjoint from W_i by tubing each pair of parallels of $S_{A_i^+}$ and $S_{A_i^-}$ together at their dual \pm -intersections with W_i along a tube of normal circles to W_i . (Each connected sum of parallels of $S_{A_i^\pm}$ is an embedded Whitney sphere S_{W_i} which is disjoint from the framed embedded W_i .)

Condition (b): Each pair of terms $(1-x) \cdot S_{A_i^+} \subset f_2$ contributing $+1$ to n_i^+ , or pair of terms $-(1-x) \cdot S_{A_i^+} \subset f_2$ contributing -1 to n_i^+ , (resp. $\pm(1-x) \cdot S_{A_i^-} \subset f_2$ contributing ± 1 to n_i^-), can be represented by taking two oppositely-oriented parallel copies of $S_{A_i^+}$ (resp. $S_{A_i^-}$) close to each other, and connecting them by a tube near W_i that runs around a meridian to f (see the $S_{A_i^-}$ case in Figure 21). As can be read off from Figure 21, each of these pairs of intersections in $W_i \cap f_2$ contributes $\pm(1-x)$ to $\lambda(W_i, f_2)$, and we choose the orientations of the copies of $S_{A_i^\pm}$ to yield the desired signs. As shown in Figure 21,

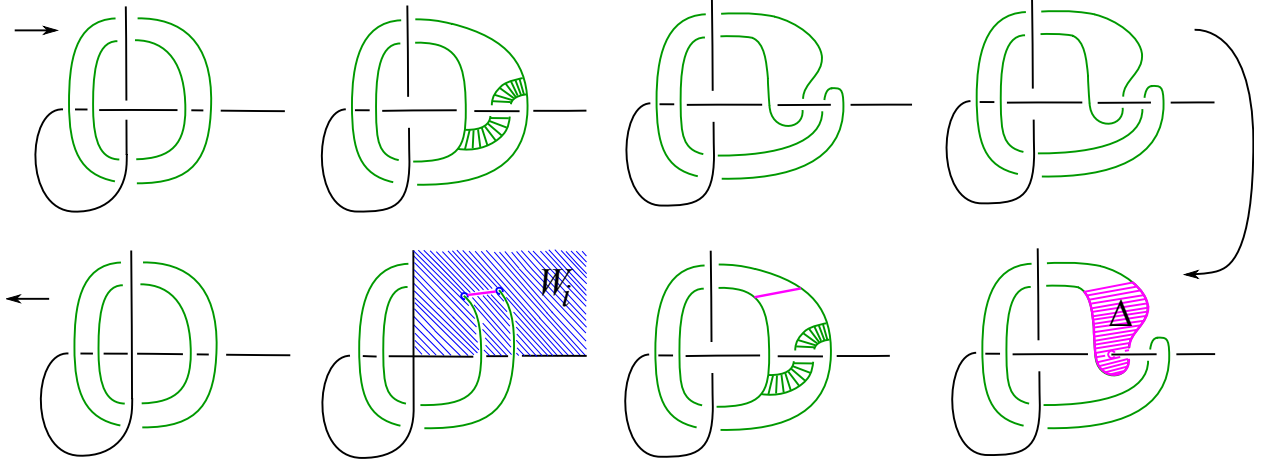


FIGURE 21. From Item (b) of Lemma 23: Near the i th negative self-intersection of f (black) (with time coordinate moving clockwise from left to right along the top row, then right to left along the bottom row), the Whitney disk W_i (blue) intersects $\pm(1-x) \cdot S_{A_i^-} \subset f_2$ (green) in two points paired by an order 2 Whitney disk Δ (purple). The intersection point between Δ and f is visible in the bottom right picture. The negative accessory disk A_i^- is suppressed from view in this figure, but could be shown in the same picture as (the corner of) W_i (bottom row, second-from-left). Any copies of the $S_{A_i^\pm} \subset f_2$ corresponding to the terms of m_i and P_i^\pm are also not shown. In the positive accessory sphere case $\pm(1-x) \cdot S_{A_i^+} \subset f_2$ the analogous figure would look the same as this figure near Δ (compare the right-hand part of Figure 39).

each of these pairs of intersections in $W_i \cap f_2$ admits a framed embedded Whitney disk whose interior is disjoint from all surfaces except for a single interior intersection with f . We only need $|n_i|$ -many of these pairs since any cancellation between n_i^+ and n_i^- in $n_i = n_i^+ - n_i^-$ gets absorbed into P_i , as described in next paragraph.

Condition (c): The rest of the copies of $S_{A_i^\pm}$ in $P_i^\pm \cdot S_{A_i^\pm} \subset f_2$ (and their connecting tubes) corresponding to the terms of P_i^\pm in Equation 2 can be chosen to have no intersections with the spheres of the previous two items in the neighborhood of the self-intersection of f described by Figure 21 (they would appear as constant parallel green circles in Figure 21, tubed together outside the neighborhood). The intersections of these factors of f_2 with W_i correspond to the $P_i \in I^2$ term of $\lambda(W_i, f_2)$ in Equation 3. We don't need to do any further clean-up on these intersections since our goal is to arrange for all metabolic Whitney disks to intersect f_2 in I^2 .

Since tubes are supported near arcs, the sums of accessory spheres described so far in this proof can be connected into the single sphere f_2 without creating any other intersections. (Since $S_{A_j^\pm} \cap W_i = \emptyset$ for $j \neq i$, all of $W_i \cap f_2$ has been accounted for.) \square

7.6. Proof of Proposition 22.

Proof. Starting with (f, f_2) as in section 7.5 satisfying Lemma 23, we will **first prove the special case that each accessory disk A_i^\pm has primary multiplicity $0 \leq m_i \leq 2$, and each Whitney disk W_i either has secondary multiplicity $-1 \leq n_i \leq 1$, or has arbitrary n_i if $m_i = 1$.** The proof will involve a construction that eliminates the pairs of intersections from Item (b) of Lemma 23 which contribute $n_i(1-x) \cdot S_{A_i^\pm} \cap W_i$ at the cost of creating new metabolic Whitney disk–accessory disk pairs satisfying the criteria of Proposition 22. This construction will be presented in eight steps in sections 7.7 through 7.17. Then we complete the proof of Proposition 22 in section 7.18 by describing how the construction can be extended to the general case of arbitrary n_i and arbitrary (non-negative) m_i .

Before starting the construction for this special case, note that any initial pair W_i, A_i^+ such that $n_i = 0$ already satisfies Proposition 22 (since W_i has vanishing primary multiplicity by Lemma 23). Also, any initial W_i, A_i^+ with $m_i = 1$ will be left “as is” for the first six steps of the construction (since Step 7 below will show how such unit primary multiplicity can be used to arrange that $n_i = 0$).

So the first six steps of the construction for this special case will be applied simultaneously to all W_i such that $n_i = \pm 1$, with $m_i = 2$ or $m_i = 0$. Since these steps of the construction are supported near each $W_i \cup A_i^-$ inside the 4–ball neighborhood described by Figure 19, and since these 4–balls can be taken to be disjoint, it suffices to describe these steps locally.

We will assume that $m_i = 2$ during the first six steps, with modifications for the easier $m_i = 0$ case pointed out in section 7.13 just after Step 6.

7.7. Step 1. To start the construction, consider a pair $\pm(1-x) \cdot S_{A_i^\pm} \cap W_i$ of intersections between f_2 and a W_i corresponding to the secondary multiplicity $n_i = \pm 1$ of W_i . By Lemma 23 this intersection pair admits a framed embedded Whitney disk Δ having only a single interior intersection with f as in Figure 21. Note that Figure 21 shows the negative accessory sphere case $\pm(1-x) \cdot S_{A_i^-} \cap W_i$, with all other parallel copies of $S_{A_i^-}$ suppressed from view (including the two copies of $S_{A_i^-}$ corresponding to primary multiplicity $m_i = 2$ of A_i^- , which would appear as constant arcs parallel to the green circle strands passing through the accessory circle ∂A_i^- , c.f. Figure 25). Subsequent figures will illustrate the construction details specifically for this negative accessory sphere case, and it will be pointed out how the same constructions also work for the positive accessory sphere case $\pm(1-x) \cdot S_{A_i^+} \cap W_i$. In both cases the construction will leave the positive accessory disk A_i^+ unchanged.

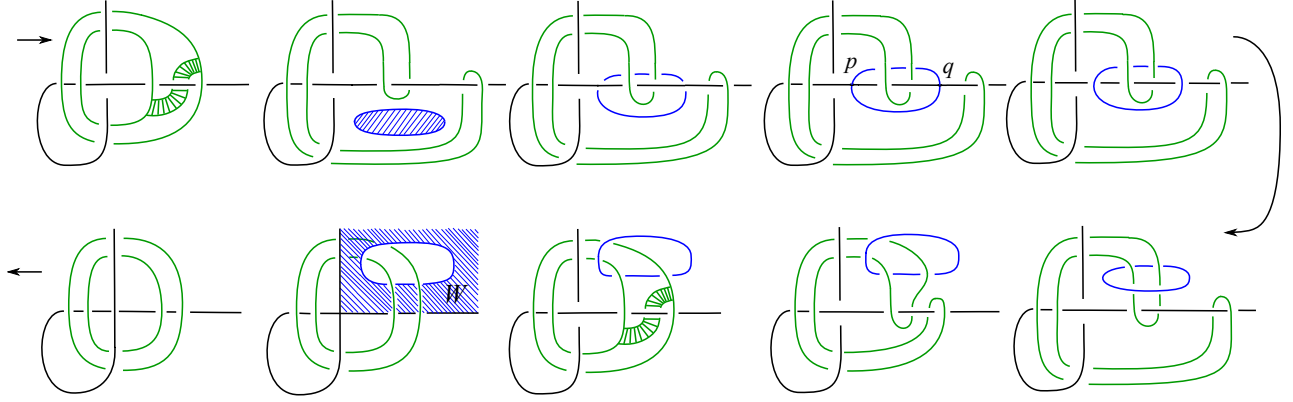


FIGURE 22. The Whitney disk W_i (blue) after eliminating the pair of intersections between W_i and f_2 (green) by a Whitney move guided by Δ from Figure 21: Zooming in here all on but the top-left picture in Figure 21, the pair of interior intersections p, q that W_i now has with f (black) corresponds to the blue-black crossing changes shown in the second-from-right picture of the top row. Both the intersections p and q will be eliminated by the finger moves shown in Figure 23.

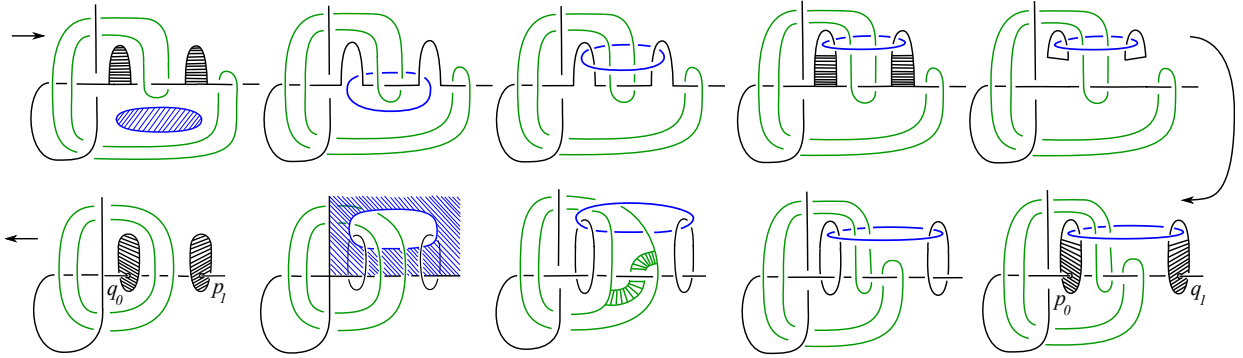


FIGURE 23. This figure shows the result of eliminating the interior intersections $p, q \in W_i \cap f$ (from Figure 22) by two finger moves on f along W_i (across $\partial_+ W_i$): Zooming in on all but the top-left picture in Figure 22, two of the new self-intersections $q_0, p_1 \in f \cap f$ are visible in the lower left-most picture, while the other two $p_0, q_1 \in f \cap f$ are visible in the lower right-most picture. The finger move that eliminated p created the pair p_0, q_0 , and the finger move that eliminated q created p_1, q_1 .

Change W_i by doing the Whitney move guided by Δ (and keep the same notation for W_i). This Whitney move eliminates the pair of intersections between f_2 and W_i , and creates a new pair of intersections p, q between f and the interior of W_i , as shown in Figure 22.

Next, use two finger moves on f to push each of $p, q \in W_i \cap f$ off of W_i (across $\partial_+ W_i$), creating two new pairs p_0, q_0 and p_1, q_1 of self-intersections of f , as illustrated in detail in Figure 23.

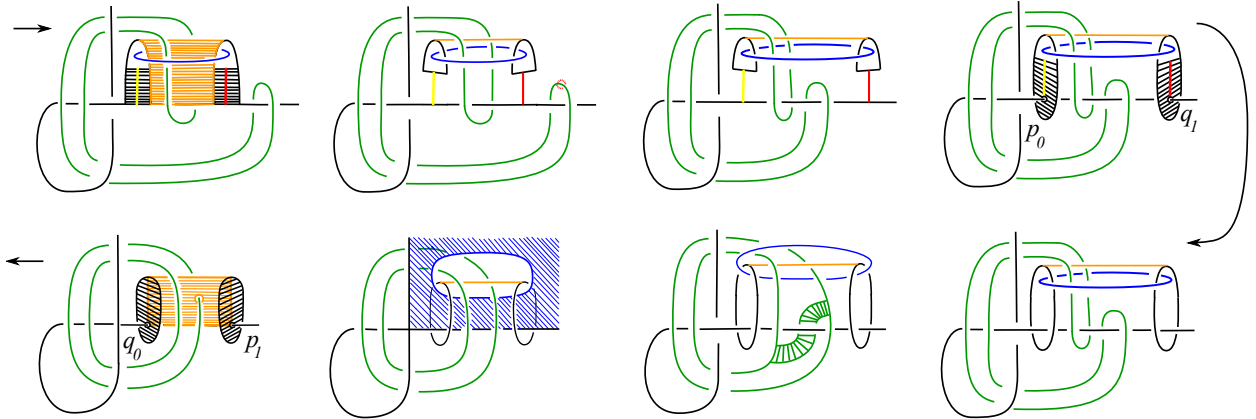


FIGURE 24. Proof of Lemma 24: These coordinates correspond to the last seven 3-ball slices pictured in Figure 23, here with an additional slice inserted between the 5th and 6th slice. The Whitney disk U for p_1 and q_0 is shown in orange. The intersection point between U and f_2 is visible in the left-most slice in the bottom row. Across the top row, the accessory disk A^{p_0} for p_0 is shown in yellow, and the accessory disk A^{q_1} for q_1 is shown in red. The intersection point (indicated schematically by the small dotted red circle in the second from left slice in the top row) between A^{q_1} and f_2 corresponds to the red-green crossing change between the center two slices in the top row. (Compare Figure 25.)

The disks described by the following lemma will be used repeatedly during constructions in subsequent steps:

Lemma 24. *The self-intersections p_0, q_0 and p_1, q_1 of f satisfy the following three conditions:*

- (i) p_0 admits a framed embedded accessory disk A^{p_0} such that the interior of A^{p_0} is disjoint from both f and f_2 , and from all other Whitney and accessory disks.
- (ii) q_1 admits a framed embedded accessory disk A^{q_1} such that the interior of A^{q_1} has a single intersection with f_2 , but is disjoint from f , and from all other Whitney and accessory disks.
- (iii) p_1 and q_0 admit a framed embedded Whitney disk U such that the interior of U has a single intersection with f_2 , but is disjoint from f , and from all other Whitney and accessory disks.

Proof. The disks A^{p_0} , A^{q_1} and U are explicitly described in local coordinates in Figure 24 (see also Figure 25). The positive accessory sphere case $\pm(1-x) \cdot S_{A_i^+} \cap W_i$ is covered by essentially the same figures. \square

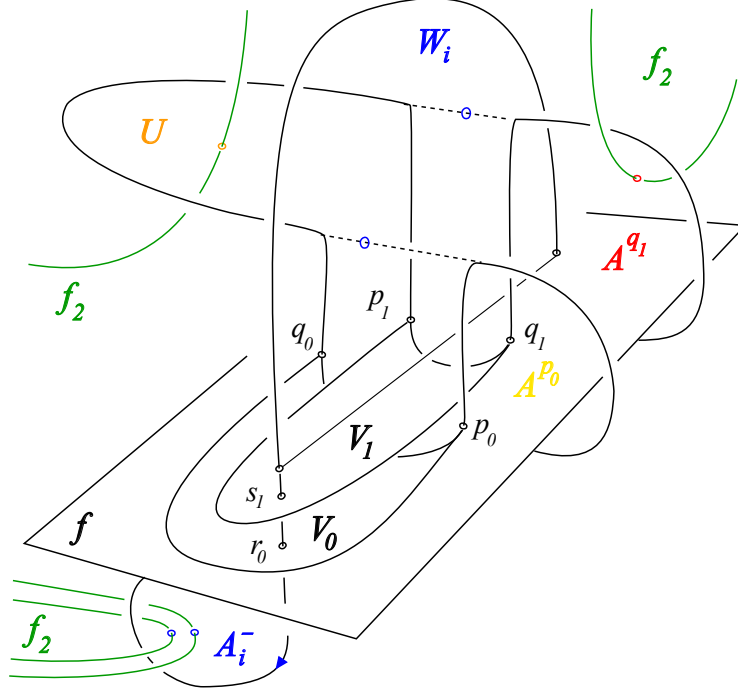


FIGURE 25. From **Step 2**: The Whitney disks V_0 and V_1 (nested along $\partial_+ W_i$) pairing p_0, q_0 and p_1, q_1 .

7.8. **Step 2.** As shown in Figure 25, the two new pairs p_0, q_0 and p_1, q_1 of self-intersections of f created by the finger moves in Figure 23 admit framed embedded Whitney disks V_0 and V_1 whose interiors each have only a single transverse intersection with f (near the negative self-intersection of f paired by W_i). By construction these points $r_0 = V_0 \cap f$ and $s_1 = V_1 \cap f$ lie on the accessory circle ∂A_i^- . Even if we had started with a positive accessory sphere pair $\pm(1-x) \cdot S_{A_i^+} \cap W_i$, we would still use these same nested V_0 and V_1 near the negative self-intersection of f .

Since the Whitney and accessory disks are framed and embedded, the 4-ball pictured in Figure 25 is accurate except that any pairs of oppositely-signed intersections that W_i and A_i^- may have with f_2 are suppressed from view. The two sheets of f_2 shown intersecting A_i^- are like-oriented copies of $S_{A_i^-}$ corresponding to $m_i = 2$ (these were suppressed in Figures 21, 22, 23 and 24).

Figure 26 shows a different view of V_0 and V_1 . Note that r_0 and s_1 admit a *generalized Whitney disk* which is the quadrilateral Q bounded by the indicated arcs running from s_1 along f to r_0 then down V_0 and back along f to V_1 and back up through V_1 to s_1 (section 8.10). Also, r_0 admits the *generalized accessory disk* B which is the bigon bounded by an arc from r_0 along f then back up through V_0 to r_0 (section 8.10). This B consists of most of the standard accessory disk A_i^- (which we do not need, since W_i also has the standard A_i^+), and contains all the intersections with f_2 that A_i^- had.

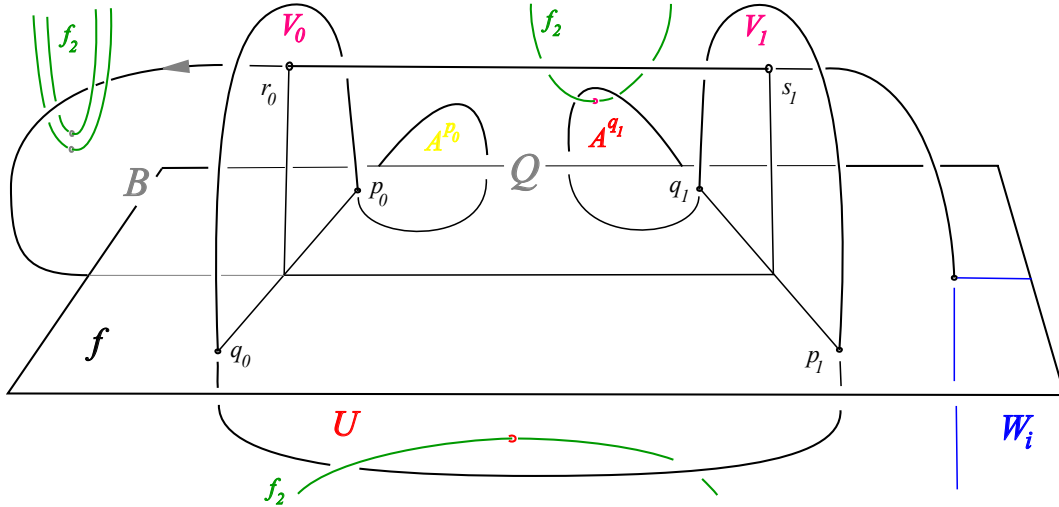


FIGURE 26. **From Step 2:** A slightly different view of V_0 and V_1 , from ‘underneath’ the horizontal sheet of f shown in Figure 25 and after ‘straightening’ ∂V_0 and ∂V_1 by an ambient isotopy (of the 2-complex).

In Figure 26 the accessory disks A^{p_0} (yellow) and A^{q_1} (red) are visible behind the quadrilateral Q . A corner of W_i is visible in the lower right. The (non-canceling) pair of intersections between f_2 and the bigon B visible in the upper left are inherited from the intersections $f_2 \cap A_i^-$ corresponding to $m_i = 2$ shown in the lower left of Figure 25. Any canceling pairs of intersections between B and f_2 (corresponding to canceling pairs in $A_i^- \cap f_2$) are suppressed, but otherwise the 4-ball picture in Figure 26 is accurate since all disks are framed and embedded.

Note that the union $B \cup Q$ equals the standard A_i^- with a small corner removed near the self-intersection of f . The subsequent steps 3–6 will be supported in a 4-ball neighborhood of A_i^- .

At this point the primary multiplicity of B (the linking number of ∂B with f_2 in S^4) is the same as the primary multiplicity of A_i^- , namely 2, but the construction will next exchange r_0 for new intersections between f and V_0 , each equipped with a generalized accessory disk whose boundary has linking number 0 or 1 with f_2 . These new generalized accessory disks will be modified parallels of B , and will become metabolic accessory disks later in the construction.

7.9. Step 3. After isotoping a small disk of f_2 into the 4-ball neighborhood of A_i^- , perform a local trivial finger move on f_2 , creating a local Whitney sphere $S_{f_2}^W$ and accessory spheres $S_{f_2}^\pm$, and tube V_0 into the new positive accessory sphere $S_{f_2}^+$ on f_2 via a tube that starts near r_0 . This creates four new intersection points $r_0^1, r_0^2, r_0^3, r_0^4$ between V_0 and $S_{f_2}^W$, as shown in the left side of Figure 27.

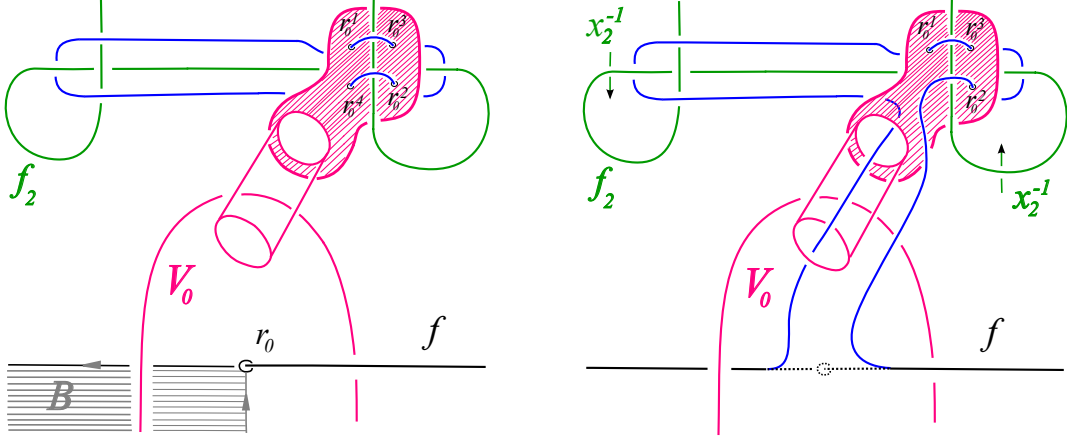


FIGURE 27. **From Step 3:** Left: The Whitney disk V_0 (red) is tubed into the local accessory sphere $S_{f_2}^+$ (also red), creating four intersections $r_0^1, r_0^2, r_0^3, r_0^4$ between V_0 and the local Whitney sphere $S_{f_2}^W$ (blue). The disk in $S_{f_2}^+$ near where the tube attaches corresponds to the bottom right-most picture in Figure 14 except that colors are different. Right: f (black) is tubed (blue) along V_0 into $S_{f_2}^W$ to eliminate r_0 and r_0^4 .

Now r_0 can be removed by tubing f into $S_{f_2}^W$ via a tube of normal circles to V_0 that also eliminates r_0^4 , as shown in the right side of Figure 27. Note that this is a link homotopy since a Whitney sphere for f_2 has been added to f . This link homotopy is an isotopy on f , since the Whitney sphere is trivial (it comes from the local embedded Whitney disk which is inverse to the finger move on f_2).

The next step is to check that parallels of B can be extended to give generalized accessory disks B^1, B^2, B^3 for the new intersections $\{r_0^1, r_0^2, r_0^3\} = V_0 \pitchfork f$ which are framed, and disjointly embedded, with interiors disjoint from f . This is carried out in Figure 28, Figure 29 and Figure 30. The primary multiplicities of B^1, B^2 and B^3 are 1, 1 and 0, respectively, as can be computed from the figures, using that B had primary multiplicity 2.

It will be important that B^1, B^2 and B^3 do not intersect each other, but this is easy to see in (the slightly schematic) Figure 30 as even the projections to the present are disjointly embedded, with B^1 appearing in front of B^2 , which is in turn in front of B^3 . And the parts of B^1, B^2 and B^3 coming from parallels of B are disjointly embedded since B was framed and embedded.

At this point in the construction (after the implementations of Figure 28, Figure 29 and Figure 30) we have disjointly embedded framed generalized accessory disks B^1, B^2, B^3 for r_0^1, r_0^2, r_0^3 , with respective primary multiplicities 1, 1, 0. These will eventually be converted into metabolic accessory disks on f having these same primary multiplicities.

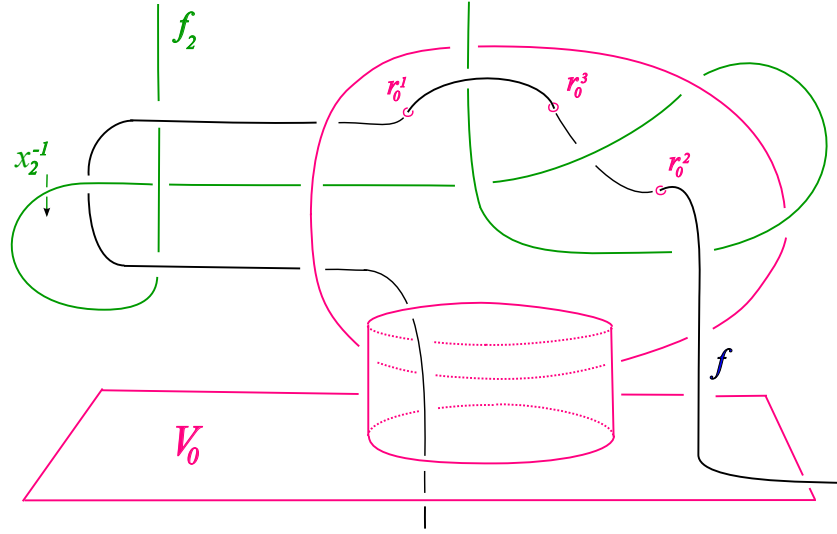


FIGURE 28. **From Step 3:** In preparation for extending parallels of B to create generalized accessory disks for r_0^1, r_0^2, r_0^3 , this figure shows a close up of the right hand side of Figure 27, with the disk in $S_{f_2}^+$ now shown as transparent, and the original part of V_0 now shown as horizontal, and perpendicular to the tube.

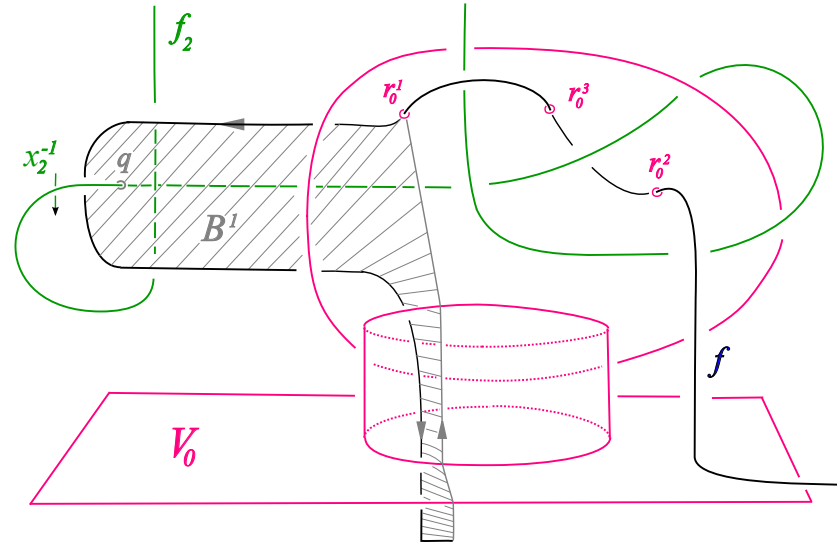


FIGURE 29. **From Step 3:** This figure shows the same view as Figure 28, now including part of a generalized accessory disk B^1 (grey) for r_0^1 . The grey arc running up along V_0 indicates part of one boundary arc of B^1 , while the other boundary arc of B^1 runs from r_0^1 to the left along f and down inside the tube of V_0 . A single intersection point $q \in B^1 \cap f_2$ is visible on the left, and the rest of B^1 (not visible) consists of a parallel copy of B . The primary multiplicity of B^1 is 1, since the boundary of the grey sub-disk added to B to form B^1 represents x_2^{-1} , so B^1 has primary multiplicity one less than the primary multiplicity of B .

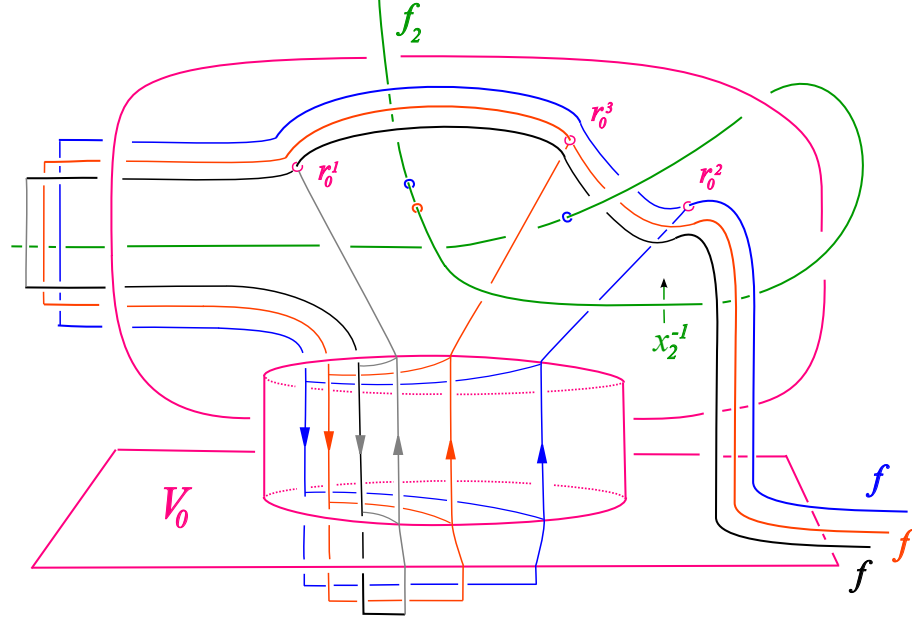


FIGURE 30. **From Step 3:** The same view as Figure 29, but now indicating parts of all three generalized accessory disks B^1 (grey-black), B^2 (blue) and B^3 (orange) for r_0^1, r_0^2 and r_0^3 . The picture is schematic in that two of the arcs of f really lie slightly in the past and future, respectively, along with small neighborhoods in V_0 and the B^j near the corresponding intersections $V_0 \pitchfork f$. The primary multiplicities of B^2 and B^3 can be computed from this figure, keeping in mind that each of B^2 and B^3 also has an intersection with f_2 parallel to $q \in B^1 \cap f_2$ as on the left of Figure 29 which is not visible in this figure, and these intersections correspond to factors of x_2^{-1} in ∂B^2 and ∂B^3 . The single orange intersection in $B^3 \cap f_2$ visible here corresponds to another factor of x_2^{-1} in ∂B^3 , hence the primary multiplicity of B^3 is 0 (two less than that of B). The blue positive-negative pair in $B^2 \cap f_2$ indicates no further change in the linking of ∂B^2 with f_2 , so the primary multiplicity of B^2 is 1 (one less than that of B).

Note that V_0 has a new oppositely-signed pair of self-intersections inherited from $S_{f_2}^+$, but with group elements that are trivial in $\pi_1(S^4 \setminus f)$.

7.10. **Step 4.** Now we work on V_1 in a similar way as the modification of V_0 in Step 3 (7.9): Perform another trivial finger move on f_2 to create another local Whitney sphere $S_{f_2}^{W'}$ and accessory sphere $S_{f_2}^{+'}$ on f_2 , and eliminate $s_1 = V_1 \pitchfork f$ by tubing V_1 into $S_{f_2}^{+'}$, and f into $S_{f_2}^{W'}$, yielding new intersections $\{s_1^1, s_1^2, s_1^3\} = V_1 \pitchfork f$ (analogously to Figure 27 and Figure 28).

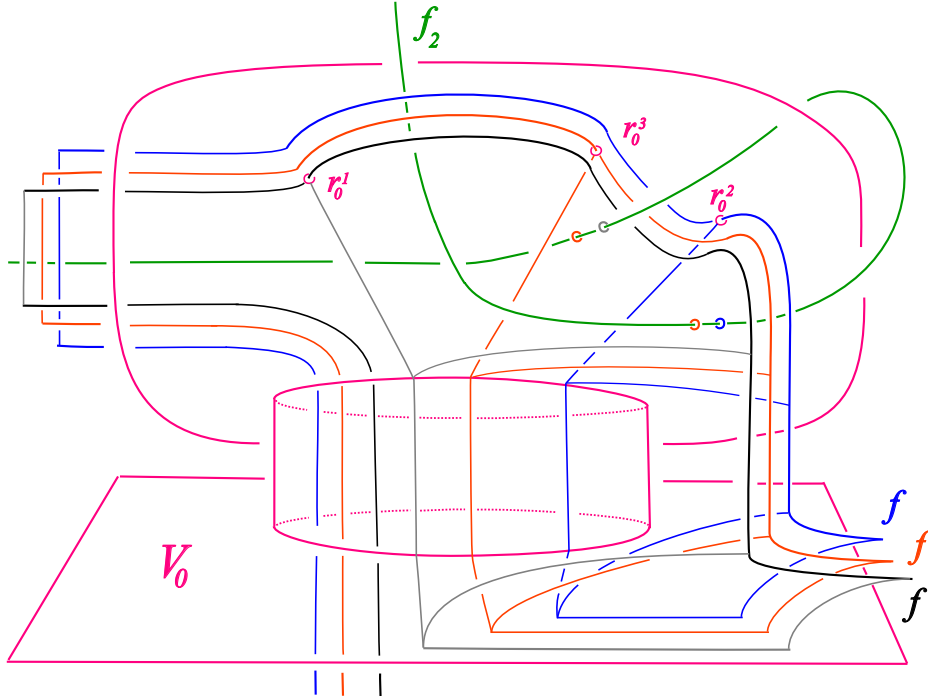


FIGURE 31. **From Step 4:** A partially schematic picture of the construction of Q^1, Q^2, Q^3 near r_0^1, r_0^2, r_0^3 using the same boundary arcs along V_0 as for B^1, B^2, B^3 in Figure 30. (Again, the picture is schematic in that two of the arcs of f really lie slightly in the past and future, respectively, along with small neighborhoods in V_0 and the Q^j of the corresponding intersections $V_0 \cap f$.) There is a single (grey) intersection between Q^1 and f_2 ; and a single (blue) intersection between Q^2 and f_2 ; as well as a pair of (orange) intersections between Q^3 and f_2 . Note that the interiors of the Q^j and the B^k are all disjointly embedded (the Q^j are ‘outside’ the tube, while the B^k are ‘inside’).

Parallel copies of the embedded quadrilateral Q can now be extended to create generalized Whitney disks Q^j for the pairs r_0^j, s_1^j in the following way:

Near $\{s_1^1, s_1^2, s_1^3\} = V_1 \cap f$ this is accomplished by the same kind of parallel local extensions that were used to create the B^j from B (as in Figure 30 but with V_1 and s_1^j replacing V_0 and r_0^j , and with Q and Q^j replacing B and B^j).

Near $\{r_0^1, r_0^2, r_0^3\} = V_0 \cap f$, it is possible to extend the parallels of Q on the “other side” of V_0 from the B^j (“outside” instead of “inside” the tube in the 3-ball slice of local coordinates) in a way that does not create any intersections between the Q^j and any previously created B^k , as shown in Figure 31.

The resulting Q^j are disjointly embedded, and have interiors disjoint from all surfaces other than f_2 . It will not be necessary to keep track of multiplicities of the Q^j .

Observe that, similarly to V_0 , now V_1 has a new oppositely-signed pair of self-intersections inherited from $S_{f_2}^{+'}$, with group elements that are trivial in $\pi_1(S^4 \setminus f)$.

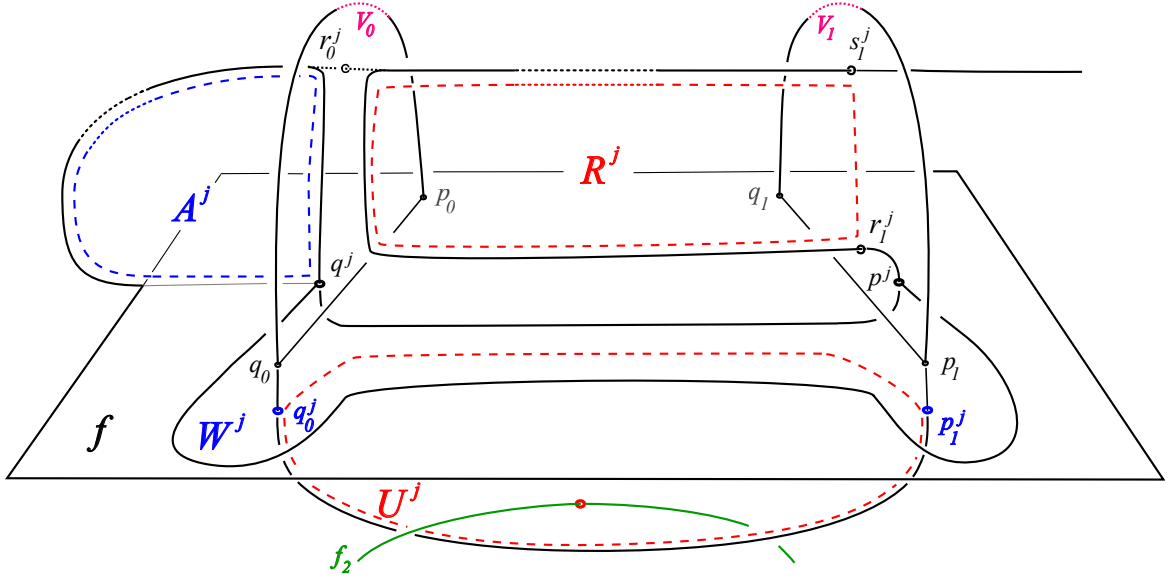


FIGURE 32. **From Step 5:** A partially condensed view of the result of ‘transferring’ an intersection $r_0^j \in V_0 \cap f$ to $r_1^j \in V_1 \cap f$. The new self-intersections $q^j, p^j \in f \cap f$ are paired by the local Whitney disk W^j . A parallel copy of the Whitney disk U^j from Lemma 24 pairs $q_0^j, p_1^j \in W^j \cap f$. Suppressed from view are intersections A^j and R^j have with f_2 , as well as the self-intersections of V_0 and V_1 inherited from $S_{f_2}^+$ and $S_{f_2}^{+'}$. Also not shown are the other intersection pairs r_0^k, s_1^k (or r_1^k, s_1^k) that V_0 and V_1 have with f , and their corresponding parallels of the embedded B^k and Q^k (or A^k and R^k).

7.11. **Step 5.** Now we make the interior of V_0 disjoint from f : This is accomplished by three *transfer moves*, pushing down each of r_0^1, r_0^2, r_0^3 into f , then across f and into V_1 by finger moves, creating new intersections r_1^1, r_1^2, r_1^3 between V_1 and f as in Figure 32 (see also Section 8.10).

Each transfer move also creates a pair p^j, q^j of self-intersections of f which are paired by a local Whitney disk W^j which comes equipped with a cleanly embedded, framed accessory disk A^j which is formed from B^j . Each A^j has interior disjoint from all other Whitney and accessory disks, and primary multiplicity equal to 0 or 1 since each B^j had primary multiplicity 0 or 1 (Step 3). Each W^j has a single pair of interior intersections q_0^j, p_1^j with f that can be paired by a parallel copy U^j of the framed embedded Whitney disk U from Lemma 24. Note that these W^j can be nested disjointly, as were V_0, V_1 in Figure 26 (see also Figure 40).

Since each U^j has just a single intersection with f_2 , performing a U^j -Whitney move on W^j would make W^j cleanly embedded with interior disjoint from all other disks, and with primary multiplicity 0 and secondary multiplicity equal to ± 1 (by Observation 7.3).

At this point, we go ahead and do the U^j -Whitney moves **only on those W^j whose A^j has primary multiplicity 1**. (For each i such that $m_i = 2$ there are two such W^j , corresponding to B^1 and B^2 each having primary multiplicity 1 in Step 3.)

In Step 8 below, the remaining W^j having A^j with primary multiplicity 0 will be made cleanly imbedded in a way that “collects” the non-zero secondary multiplicities into canceling pairs so that the resulting metabolic Whitney disks each have secondary multiplicity 0. (For each i such that $m_i = 2$ there is one such W^j , corresponding to B^3 having primary multiplicity 0 in Step 3.)

At this point V_0 is cleanly immersed, framed, and with interior disjoint from f_2 and all other disks. The only self-intersections of V_0 are the oppositely-signed pair inherited from tubing into the accessory sphere $S_{f_2}^+$ on f_2 in (Step 3), and the group elements of these self-intersections are both trivial in $\pi_1(S^4 \setminus f)$, so $\lambda(V_0, V_0) = 0 \in \mathbb{Z}[x^{\pm 1}]$.

By construction, the accessory disk A^{p_0} for V_0 from Lemma 24 is framed and cleanly embedded with interior disjoint from all other Whitney and accessory disks.

Note that V_0 and A^{p_0} both have vanishing primary and secondary multiplicities (and in fact are both disjoint from f_2).

7.12. Step 6. The transfer moves in the previous Step 5 (Figure 32) convert the quadrilaterals Q^j into framed disjointly embedded Whitney disks R^j pairing s_1^j and r_1^j (section 8.10). The interior of each R^j intersects f_2 (near $S_{f_2}^+$ and $S_{f_2}^{+'}$ from Step 4), but is disjoint from f and all other disks. So the interior of V_1 can be made to be disjoint from f and all other disks via Whitney moves on V_1 guided by the R^j .

By construction, V_1 is now cleanly immersed, framed and disjoint from all other Whitney disks and from the interiors of all accessory disks. Also, V_1 satisfies $\lambda(V_1, V_1) = 0 \in \mathbb{Z}[x^{\pm 1}]$, since the only self-intersections of V_1 come from tubing into accessory spheres on f_2 which contribute oppositely-signed self-intersections with trivial group elements in $\pi_1(S^4 \setminus f)$.

The accessory disk A^{q_1} for V_1 (from Lemma 24) is framed and embedded with interior disjoint from all other Whitney and accessory disks. From Lemma 24, A^{q_1} has primary multiplicity 1.

Since the only intersections that V_1 has with f_2 come from the R^j -Whitney moves, it follows from Observation 7.3 that V_1 has vanishing primary multiplicity. (At this point we do not need to control the secondary multiplicity of V_1 , since Step 7 will deal with each Whitney disk whose accessory disk has primary multiplicity 1.)

7.13. The case $m_i = 0$: The six steps so far have been described for the case $m_i = 2$. If we had started with W_i with $m_i = 0$, then the construction is simplified as follows: Step 1 and Step 2 proceed exactly the same as above. Observe that in this $m_i = 0$ case, at the end of Step 2 the bigon B has primary multiplicity 0 (the same as A_i^-), so Step 3 and

Step 4 can be skipped entirely, and in Step 5 the transfer move is applied to the single intersection $r_0 = B \pitchfork f$. So Step 5 yields just a single W^j , with accessory disk A^j having primary multiplicity 0. (This A^j is formed from B , which is a sub-disk of the original A_i^- , since we didn't have to do the tubing of Step 3 and Step 4 to reduce the primary multiplicity.) As in Figure 32, the intersection pair $W^j \pitchfork f$ admits U^j intersecting f_2 in a single point, and will be made cleanly embedded in Step 8 along with the other W^j having A^j with primary multiplicity 0.

7.14. Summary of Steps 1–6. Recall that we are assuming the base case that each initial Whitney disk W_i has secondary multiplicity $-1 \leq n_i \leq 1$, and each initial accessory disk A_i^\pm has primary multiplicity $0 \leq m_i \leq 2$. Simultaneously carrying out the above constructions of Steps 1 through 6 on all the initial W_i with $n_i = \pm 1$ and $m_i = 0, 2$ has yielded the following:

- (a) All the initial pairs W_i, A_i^+ either had $m_i = 1$ to start with, or now have $n_i = 0$ from Step 1. Each of these initial W_i, A_i^+ are still cleanly embedded and disjoint from all other Whitney and accessory disks.
- (b) Each new Whitney disk V_0 created in Step 2 and modified in Step 5 is cleanly immersed, with $\lambda(V_0, V_0) = 0 \in \mathbb{Z}[x^{\pm 1}]$, and has interior disjoint from all other disks. The accessory disk A^{p_0} for V_0 is framed and embedded with interior disjoint from all other Whitney and accessory disks. By construction both V_0 and A^{p_0} have vanishing primary and secondary multiplicities, and are in fact disjoint from f_2 .
- (c) Each new Whitney disk V_1 created in Step 2 and modified in Step 6 is cleanly immersed, with $\lambda(V_1, V_1) = 0 \in \mathbb{Z}[x^{\pm 1}]$. The accessory disk A^{q_1} for V_1 is framed and embedded with interior disjoint from all other Whitney and accessory disks. The primary multiplicity of V_1 is 0 by Observation 7.3, and the primary multiplicity of A^{q_1} is 1 by Lemma 24.
- (d) The new disk pairs W^j, A^j created in Step 5 **such that A^j has primary multiplicity 1** are (after the U^j -Whitney moves) all cleanly embedded and disjoint from all other disks. These W^j each have primary multiplicity 0, and each W^j also has secondary multiplicity ± 1 , coming from the unit primary multiplicities of the U^j which were used to get $W^j \pitchfork f = \emptyset$ (by Observation 7.3).
- (e) Those new disk pairs W^j, A^j created in Step 5 **such that A^j has primary multiplicity 0** are embedded and disjoint from all other disks but still have $W^j \pitchfork f$ paired by U^j .

So the **remaining “problems”** to be dealt with are

- the Whitney disks which have possibly non-zero secondary multiplicity and have accessory disks with primary multiplicity 1, as in items (a), (c) and (d), and
- the W^j which still intersect f and have accessory disks with primary multiplicity 0, as in item (e).

These problems will be taken care of in Step 7 and Step 8 respectively.

7.15. **Step 7.** In this step we use a local construction to kill the secondary multiplicity of each Whitney disk whose accessory disk has unit primary multiplicity. At this point in the proof such Whitney disks are either from the initial collection with arbitrary secondary multiplicity (as in 7.14a), or are a V_1 created in Step 2 (as in 7.14c), or are from the W^j created in Step 5 with unit secondary multiplicity (as in 7.14d). In each of these cases the corresponding accessory disk is framed and cleanly embedded, with interior disjoint from all other disks.

Let W, A be one of these Whitney disk–accessory disk pairs with A having primary multiplicity 1. This step will describe how to replace W by a new Whitney disk V with secondary multiplicity 0 such that $\partial V = \partial W$, with V supported near $W \cup A$ and disjoint from the interior of A . Since all the accessory disks at this point are disjointly embedded and with interiors disjoint from all Whitney disks, this construction can be carried out simultaneously to replace all such W, A by V, A without creating any new intersections among disks.

First we construct V in the case that A is a positive accessory disk, and has just a single positive intersection with f_2 . The construction described in Figure 33 and Figure 34 shows how to add $+(1-x)$ to $\lambda(W, f_2) \bmod I^2$ by changing the interior of W by two boundary-twists and a Whitney move guided by a Whitney disk formed by a parallel copy of A . Since the boundary-twists are oppositely-handed, W is still framed (for details on the boundary-twisting construction see e.g. [14, sec.1.3]).

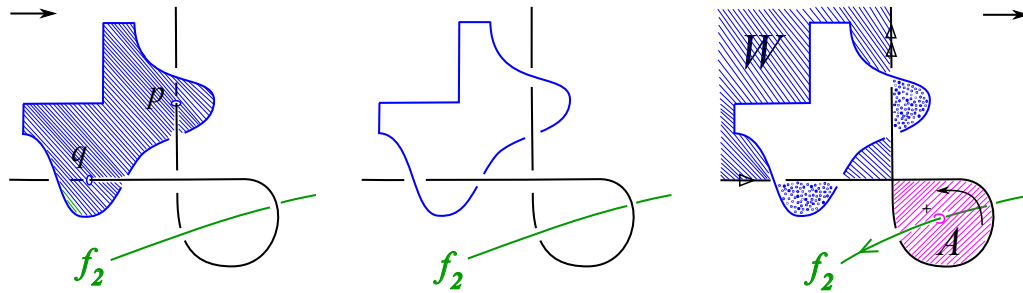


FIGURE 33. Near the framed embedded positive accessory disk A for W : A left-handed boundary-twist along $\partial_- W$ and a right-handed boundary-twist along $\partial_+ W$ creates a pair of oppositely-signed intersections p and q in $W \cap f$.

The construction is supported in an arbitrarily small neighborhood of A , and also leaves a smaller neighborhood of A unchanged; so this construction can be iterated to increase $\lambda(W, f_2) \bmod I^2$ by $n(1-x)$ for any $n \geq 1$. If the left-handed and right-handed boundary-twists are switched in the construction, or if the construction is carried out using a negative accessory disk, then $\lambda(W, f_2) \bmod I^2$ is changed by $-(1-x)$, so the secondary multiplicity of W can be changed by any $n \in \mathbb{Z}$ and the desired V can be created in this case. Note that the construction of V from W is supported near $W \cup A$, so no new intersections are created between any Whitney or accessory disks.

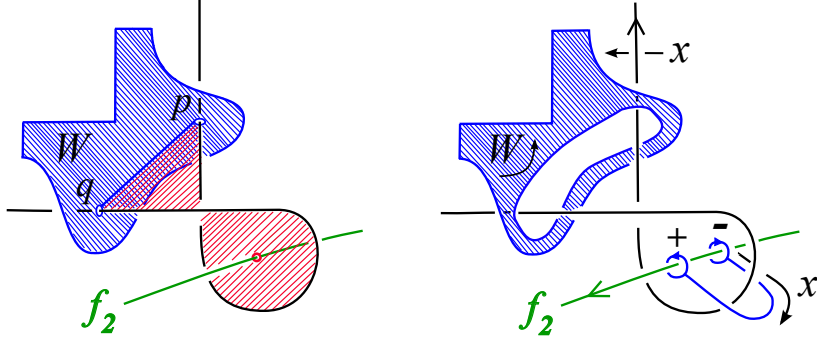


FIGURE 34. Both of these pictures correspond to the right-most 3-dimensional slice of 4-space shown in Figure 33. Left: The intersections p and q created by the boundary-twists can be paired by the red Whitney disk formed from a parallel of A (as in section 8.7). Right: The result of performing the red Whitney move on W . The Whitney bubble added to W by the Whitney move is suppressed from view, except for an arc (blue) connecting the new intersection points between W and f_2 . The intersections $p, q \in W \cap f$ have been eliminated, and (as per Observation 7.3) the change in $\lambda(W, f_2) \bmod I^2$ is equal to $+(1-x)$.

Now consider the general case where A has possibly more than one intersection with f_2 (corresponding to $P \cdot S_A$ terms in f_2 , for $P \in I^2$ as in Lemma 23, and/or oppositely-signed intersection pairs created Step 3): Each intersection between A and f_2 will contribute a term $\pm(1-x) \bmod I^2$ via the construction shown in Figures 33 and 34. Since $\lambda(A, f_2) = 1$ modulo I , the net affect of each iteration of the construction is still to change $\lambda(W, f_2)$ by $\pm(1-x)$ modulo I^2 , again by Observation 7.3, so the secondary multiplicity of W can be reduced to zero, yielding V with secondary multiplicity zero and with the same vanishing primary multiplicity as W .

Remark 25. The reader might wonder why this construction of V does not contradict the fact (from Lemma 13) that $\lambda(g, f_2) \in I^2$ for any $g : S^2 \hookrightarrow S^4 \setminus f$? After all, it seems that such a g could be formed from the two framed and cleanly immersed Whitney disks W and V with $\partial W = \partial V$ in the above construction, yielding $\lambda(g, f_2) = \pm(1-x) \notin I^2$? But the subtlety here is that although W and V are each framed, they have different (relative) framings along each of the positive and negative boundary arcs, so perturbing $W \cup V$ to be disjoint from f would create intersections near $\partial W = \partial V$, and eliminating these intersections would effectively “undo” the construction.

The general effect of the double boundary-twisting construction in this step is summarized by the following lemma:

Lemma 26. *Suppose W, A is a cleanly immersed Whitney disk–accessory disk pair on f in standard position such that A has primary multiplicity m . Then for any integer k , there exists a cleanly immersed Whitney disk V supported in a neighborhood of $W \cup A$,*

with $\partial V = \partial W$, such that V has the same primary multiplicity as W , and the secondary multiplicity of V differs from the secondary multiplicity of W by km .

7.16. Step 8. After Step 7, all Whitney disks have vanishing primary and secondary multiplicities except for those W^j created in Step 5 whose accessory disks A^j have primary multiplicity 0 (cf. 7.14e). Each of these W^j still has a single pair of interior intersections with f which are paired by a Whitney disk U^j . Since each U^j has just a single interior intersection with f_2 , doing a U^j -move on W^j would make W^j cleanly embedded with secondary multiplicity ± 1 (by Observation 7.3), so this final step of the construction will first collect these U^j in “canceling” pairs so that doing the U^j -moves will yield cleanly embedded W^j with secondary multiplicity 0.

To start this construction we need the following:

Claim: There are an even number of these U^j .

Proof of Claim: Doing the U^j -moves on these W^j would yield cleanly embedded pairs W^j, A^j . Just for this proof of the claim denote by $\{W_i, A_i\}$, the collection consisting of these resulting cleanly embedded pairs W^j, A^j together with the initial Whitney disk–accessory disk pairs and all the other Whitney disk–accessory disk pairs constructed so far in the previous steps.

Note that the number of U^j in the claim equals the number of pairs in $\{W_i, A_i\}$ such that W_i has non-zero secondary multiplicity, and all of these non-zero secondary multiplicities are ± 1 . Also, the corresponding A_i all have primary multiplicity 0.

Convert all the pairs in $\{W_i, A_i\}$ into accessory disk pairs A_i^\pm (see section 8.9), and then use these A_i^\pm to construct a basis of accessory spheres $S_{A_i^\pm}$ for $\pi_2(S^4 \setminus f)$. Since the A_i are all framed and pairwise disjointly embedded, and the W_i all have vanishing $\mathbb{Z}[x^{\pm 1}]$ -intersections, this basis of accessory spheres has the same $\mathbb{Z}[x^{\pm 1}]$ -intersections as the standard accessory spheres in Lemma 14.

Write f_2 in terms of the $S_{A_i^\pm}$:

$$f_2 = \sum \alpha_i^+ \cdot S_{A_i^+} + \alpha_i^- \cdot S_{A_i^-},$$

with

$$\alpha_i^\pm = m_i^\pm + n_i^\pm(1-x) + q_i^\pm z \quad \text{mod } I^3$$

for integers $m_i^\pm, n_i^\pm, q_i^\pm$, where m_i^\pm and n_i^\pm are the primary and secondary multiplicities of A_i^\pm , respectively, and $z := (2 - x - x^{-1})$.

Since the W_i all had primary multiplicity 0, the construction of section 8.9 has yielded A_i^\pm such that $m_i^+ = m_i^-$ for each i . Denoting these primary multiplicities by m_i , we have the following formula for the coefficient of z^2 in the expansion of $\lambda(f_2, f_2)$ in powers of z :

$$\sum [((n_i^+)^2 - (n_i^-)^2) + (n_i^+ - n_i^-)m_i + 2m_i(q_i^+ - q_i^-)]$$

This sum must vanish since $\lambda(f_2, f_2) = 0$ from the Kirk invariant hypothesis of Proposition 22. Note that $n_i^+ - n_i^-$ is the secondary multiplicity of W_i , because $\lambda(W_i, f_2) = \lambda(A_i^+, f_2) - \lambda(A_i^-, f_2)$ by construction. And recall that for $m_i = 1$, we have $n_i^+ - n_i^- = 0$;

while for $m_i = 0$, we have $n_i^+ - n_i^- = \pm 1$ (and $0, 1$ are the only values of m_i). So setting the sum equal to zero modulo 2 shows that $\sum(n_i^+ - n_i^-)$ is even, which proves the claim. \square

Remark 27. An alternate proof of this claim can be made using Lightfoot's main result in [20].

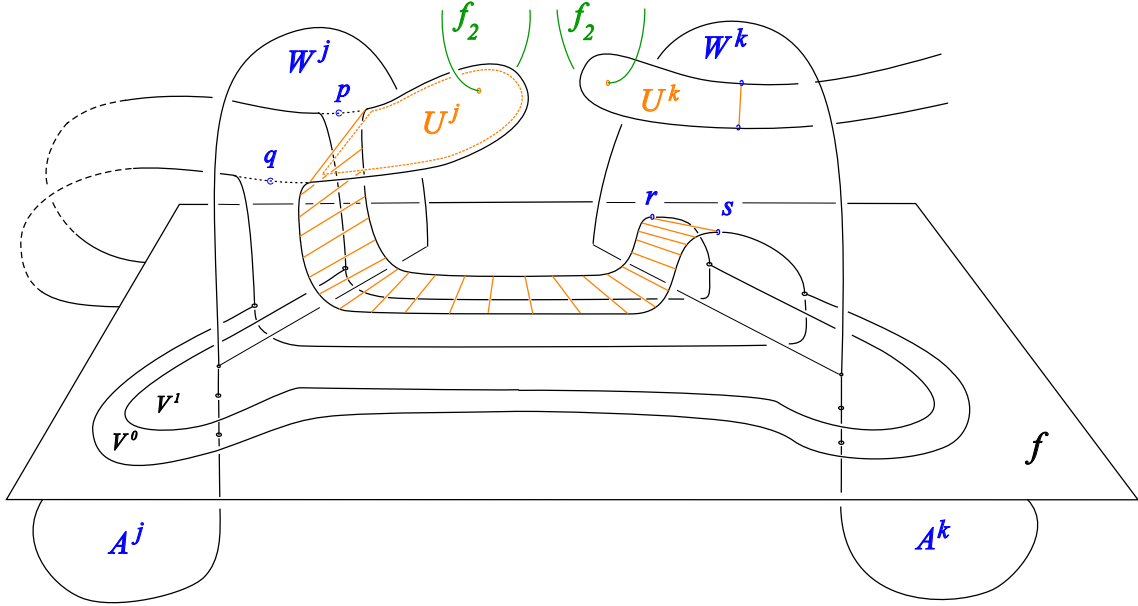


FIGURE 35. The *double transfer move*: Two parallel finger moves exchange $\{p, q\} = W^j \pitchfork f$ paired by the Whitney disk U^j for $\{r, s\} \subset W^k \pitchfork f$ paired by an extension of U^j by a band. Two new local Whitney disks V^0 and V^1 pair the self-intersections of f created by the finger moves.

The double transfer move. Having established the claim that there are an even number of the W^j created in Step 5 whose accessory disks A^j have primary multiplicity 0, each with a single U^j pairing $f \pitchfork W^j$, Step 8 will proceed using a construction which “transfers” any U^j off of its W^j and onto a different W^k . As a result of this *double transfer move*, W^j will be cleanly embedded and disjoint from f_2 , and after making W^k cleanly embedded via both the “new” U^j -move and the original U^k -move, W^k will have vanishing secondary multiplicity (and primary multiplicity). This double transfer move of a Whitney disk from one Whitney disk to another is an enhancement of the move transferring a single point from one Whitney disk to another as above in Figure 32 of Step 5 (see also section 8.10). At certain points it will be necessary to keep careful track of orientations, and discussion of some of these details will be deferred to section 7.16.1 so as not to break the flow of the geometric descriptions.

The construction starts as described in Figure 35, and is carried out simultaneously to all such pairs W^j, W^k : The intersections $\{p, q\} = W^j \pitchfork f$ paired by U^j are exchanged for

$\{r, s\} \subset W^k \pitchfork f$ via a parallel pair of finger moves guided by an embedded arc from ∂W^j to ∂W^k in f . This new pair r, s admits an embedded Whitney disk formed by extending U^j (minus a collar in U^j of $\partial U^j \subset W^j$) by an embedded band near the arc (shown in the figure as the orange band just above the horizontal sheet of f). This Whitney disk, which we continue to denote U^j , still has only a single interior intersection with f_2 .

The parallel pair of finger moves also creates two new pairs of self-intersections of f which can be paired by embedded Whitney disks V^0 and V^1 , which each have a pair of interior intersections with f as shown in Figure 35 (where both V^0 and V^1 hang down below the horizontal sheet of f). As is evident in Figure 35, the boundaries ∂V^0 and ∂V^1 intersect the accessory disk boundaries ∂A^j and ∂A^k , but these intersections can be eliminated by adding half-tubes to A^j and A^k near f as in Figure 36. Adding these half-tubes creates two pairs of intersections between f and each of A^j and A^k near r, s that admit Whitney disks parallel to U^j .

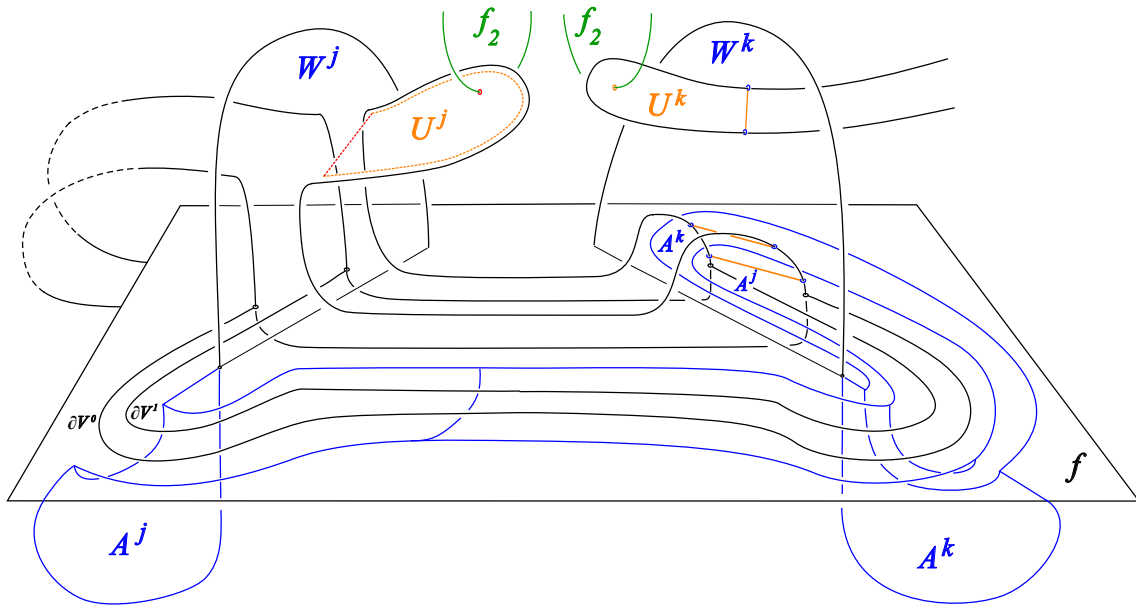


FIGURE 36. After adding half-tubes to make all of ∂V^0 , ∂V^1 , ∂A^j and ∂A^k disjointly embedded: These half-tubes appear ‘below’ the present sheet of f near A^j and A^k , but then rotate (through the future) ‘above’ the horizontal present sheet of f near W^k , where they each have a pair of transverse intersections with f which can be paired by parallels of the Whitney disk U^k pairing r, s in Figure 35 (here r and s are suppressed from view). These parallels of U^k are suppressed from view except for the boundary arcs lying in A^j and with A^k , (and only part of U^k is shown). Pushing the interiors of V^0 and V^1 into the past keeps them disjoint from the half-tubes.

Now do the Whitney moves on these two parallel copies of U^j to get A^j and A^k cleanly embedded, and do both the U^k -move and U^j -move to get W^k cleanly embedded (but keep the same notation for A^j , A^k and W^k).

At this point W^j has vanishing primary and secondary multiplicities (in fact $W^j \cap f_2 = \emptyset$), and is equipped with the cleanly embedded accessory disk A^j . Also $W^j \cup A^j$ is disjoint from all other disks by construction.

As explained below in section 7.16.1 the freedom in choosing the guiding arc between ∂W^j and ∂W^k allows for control of whether or not the orientation (relative to W^k) of the resulting U^j is preserved or flipped by the double transfer move, and as a result it can be arranged that the effect of then doing the U^j -move on W^k creates a canceling contribution to that of the U^k -move on the secondary multiplicity of the resulting cleanly embedded W^k . So, assuming this, we also now have that W^k has vanishing primary and secondary multiplicities, and is equipped with the cleanly embedded accessory disk A^k . Also $W^k \cup A^k$ is disjoint from all other disks by construction.

Before converting V^0 and V^1 into metabolic Whitney disks with vanishing primary and secondary multiplicities we first need to construct appropriate accessory disks A^0 and A^1 for V^0 and V^1 . Recall that the $\mathbb{Z}[x^{\pm 1}]$ -intersections among metabolic accessory disks can be arbitrary (Definition 17). We describe the construction of A^0 ; the same steps yield A^1 :

Choose an embedded accessory circle $a^0 \subset f$ for the self-intersection of f at the corner of V^0 near ∂W such that a^0 is disjoint from all other boundaries of Whitney and accessory disks. Since $\pi_1(S^4 \setminus f) \cong \mathbb{Z}$, there exists an immersed disk A^0 bounded by a^0 such that the interior of A^0 is disjoint from f . Then make the interior of A^0 disjoint from each Whitney disk (including W^j and W^k) by tubing A^0 into parallel copies of the dual accessory sphere as needed. Observe that the interior of A^0 can be assumed to be disjoint from V^0 and V^1 (even though they don't yet have accessory spheres), since V^0 and V^1 are supported near arcs in f . (As usual, we do not rename A^0 after changing its interior by adding these spheres.)

Now make A^0 disjoint from A^j and A^k by adding parallel copies of the Whitney spheres S_{W^j} and S_{W^k} to A^0 as needed. This disjointness will allow us to form secondary Whitney disks from A^j and A^k that will be used to get f disjoint from the interiors of V^0 and V^1 .

Simultaneously carry out the same steps to construct an accessory disk A^1 for V^1 such that A^1 is disjoint from A^j and A^k as well as all Whitney disks (except the corner-point $\partial A^1 \cap \partial V^1$).

It remains to clean up V^0 and V^1 . To get the interiors of V^0 and V^1 disjoint from f , form Whitney disks U^0 for $V^0 \cap f$ and U^1 for $V^1 \cap f$ by connecting parallels of (the framed cleanly embedded) A^j and A^k as in Figure 37. (Note that the interior of V^0 can be perturbed to be disjoint from U^1 .) Here we need that the interior intersections V^0 and V^1 have with f are of opposite signs, as can be assumed by the discussion in section 7.16.1.

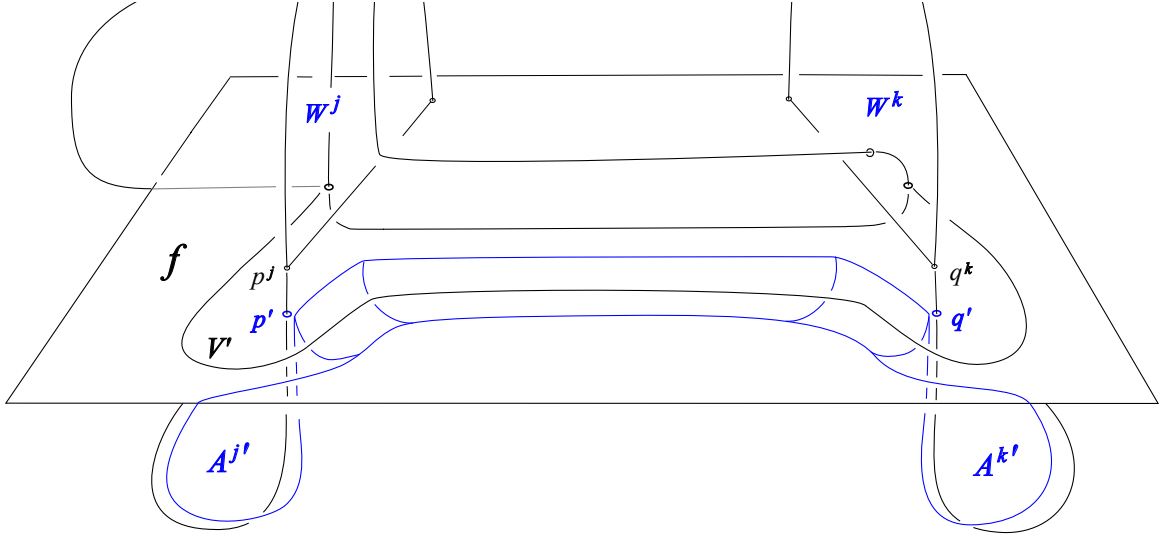


FIGURE 37. In the setting of Figures 35 and 36, here with V', U' denoting V^0, U^0 and/or V^1, U^1 : The Whitney disk V' intersects f in p^j and q^k , which are paired by a secondary Whitney disk U' (blue) formed by combining parallels $A^{j'}, A^{k'}$ of the accessory disks A^j, A^k for $p^j, q^k \in f \cap V'$.

Note that U^0 and U^1 each have primary multiplicity 0, since A^j and A^k both have primary multiplicity 0 (the Whitney moves done on A^j and A^k did not affect their primary multiplicities by Observation 7.3).

Now doing the U^0 - and U^1 -Whitney moves on V^0 and V^1 makes V^0 and V^1 both cleanly embedded with vanishing primary and secondary multiplicities (by Observation 7.3).

Since A^j and A^k are disjoint from the new A^0 and A^1 by construction, and were already disjoint from all previous Whitney disks and accessory disks, it follows that V^0 and V^1 have vanishing $\mathbb{Z}[x^{\pm 1}]$ -intersections with all Whitney and accessory disks, as required for metabolic Whitney disks.

To complete Step 8 of the construction it remains to check that this double transfer move can be simultaneously carried out for all pairs W^j, A^j and W^k, A^k created in Step 5 with A^j and A^k having primary multiplicity 0. To see this, observe that the parallel finger moves in Figure 35 (and the bands added to U^j and parallels of U^j) are supported near an arc a^{jk} in f from W^j to W^k (together with short arcs in W^j and W^k). Such an a^{jk} always exists because the complement in f of the disjointly embedded boundaries of all the Whitney disk-accessory disk pairs and all U^j is *connected* (the inverse image of each union of a Whitney disk boundary with the boundary of one of its accessory disks is an embedded arc in the domain 2-sphere of f , as is the inverse image of each U^j , and these arcs are all pairwise disjoint).

7.16.1. *Controlling orientations and signs in the double transfer move.* In the setting of Step 8, we have Whitney disks W^j such that each $W^j \pitchfork f$ is paired by an embedded Whitney disk U^j which contains only a single interior intersection with f_2 . The link map $(f, f_2) \looparrowright S^4$ is oriented, and by convention the positive generator x of $\pi_1(S^4 \setminus f) \cong \mathbb{Z}$ is represented by any positive meridian to f . Fix orientations on the W^j , and then orient the U^j by taking the boundary arc $\partial U^j \subset f$ to run from the negative to the positive intersection in W^j . With this convention, if $\lambda(U^j, f_2) = \pm x^N$, then performing the U^j -move on W^j makes W^j cleanly embedded with $\lambda(W^j, f_2) = \pm(1-x)x^N$, with the signs preserved. That is, the sign \pm of the intersection between U^j and f_2 equals the sign of the secondary multiplicity ± 1 of W^j after the U^j -move.

So given such W^j and W^k (with orientations as in the previous paragraph) we want to control the double transfer move so that after U^j has been moved onto W^k the sign of $U^j \cap f_2$ is *opposite* to the sign of $U^k \cap f_2$. Then doing the U^j - and U^k -moves on W^k will result in W^k having secondary multiplicity 0. We also need to arrange that the interior intersections V^0 and V^1 have with f are of opposite signs. We describe next how this can be accomplished with the configuration shown in Figure 35.

The choice of guiding arc $a^{jk} \subset f$ for the double transfer move determines whether the sign of $U^j \cap f_2$ is preserved or switched after U^j transferred onto W^k , depending on which boundary arcs $\partial_{\pm} W^j$ or $\partial_{\pm} W^k$ are joined by a^{jk} , and also on which sides in f of $\partial_{\pm} W^j$ or $\partial_{\pm} W^k$ are connected by a^{jk} . Also, observe from Figure 35 that if the signs of the self-intersections of f at A^j and A^k are of opposite sign, then so are the interior intersections that V^0 and V^1 have with f . By the construction in section 8.9, we may assume that the signs of the self-intersections of f at A^j and A^k are of opposite sign, so by choosing a^{jk} appropriately it can be arranged that the sign of $U^j \cap f_2$ is opposite to the sign of $U^k \cap f_2$ after the double transfer move, and that the interior intersections that V^0 and V^1 have with f are of opposite sign, with the configuration as in Figure 35.

7.17. **Checking metabolic properties.** The constructions in Step 7 and Step 8 resolved the remaining problems listed in items (a), (c) and (d), and in item (e) of section 7.14 without affecting any other disks. So the only remaining property of the W_i, A_i constructed so far that needs to be adjusted is that the definition of a metabolic collection requires *positive* accessory disks. This adjustment can be carried out using the construction in section 8.9 which forms a positive accessory disk out of a negative accessory disk together with a parallel of the Whitney disk.

This completes the proof of Proposition 22 in the special case that each accessory disk A_i^{\pm} has primary multiplicity $0 \leq m_i \leq 2$, and each Whitney disk W_i either has secondary multiplicity $-1 \leq n_i \leq 1$, or has arbitrary n_i if $m_i = 1$. To complete the proof we explain next how the eight steps of the construction can be extended to handle accessory disks with arbitrary (positive) primary multiplicities and Whitney disks with arbitrary secondary multiplicities.

7.18. **Extending the construction to the general case.** To handle the case that the A_i from the initial collection $\{W_i, A_i\}$ may have primary multiplicity $m_i > 2$, still

assuming that the W_i have secondary multiplicity $-1 \leq n_i \leq 1$, observe first that the above construction can proceed “as is” through Step 1 (7.7) and Step 2 (7.8) with 2 replaced by m_i . (So instead of two, there would be m_i strands of f_2 visible in the lower left of Figure 25 and the upper left of Figure 26.) In Step 3 (7.9), the construction (Figure 27) replaces $r_0 \in V_0 \pitchfork f$ admitting framed embedded B with the three $r_0^j \in V_0 \pitchfork f$ admitting parallel framed embedded B^j having primary multiplicities decreased by 1 or 2 from that of B . So iterating this step as needed on the r_0^j will eventually lead to many intersections in $V_0 \pitchfork f$ all admitting framed embedded generalized accessory disks with primary multiplicities 1 or 0. After applying the same iterations to $s_1^j \in V_1 \pitchfork f$ in Step 4 (7.10), the rest of the construction proceeds as in the $m_i = 2$ case above: We have as many disjoint framed embedded parallels of B and Q as we want, since they all come from the original standard accessory disk A_i^- . And in this $m_i > 2$ case the construction at Step 5 will yield more of the new W^j, A^j pairs, and there will be more R^j -Whitney moves on V_1 in Step 6, but these last two steps can proceed as before. The local construction of Step 7 proceeds as before on each Whitney disk whose accessory disk has primary multiplicity 1, there will just be more of them now. And similarly, both the claim and the double transfer moves in Step 8 proceed as before, now applied to more Whitney disks.

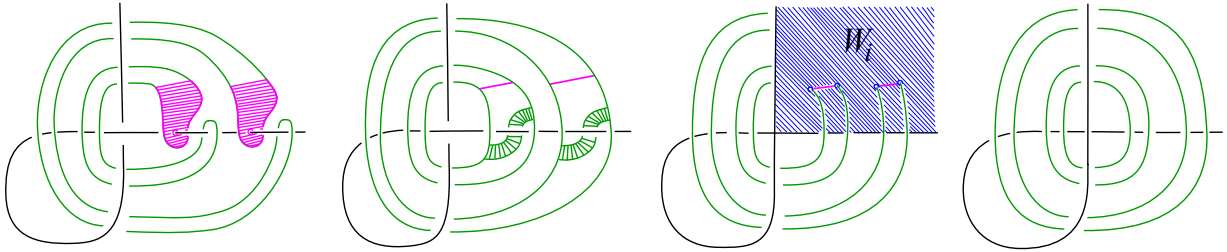


FIGURE 38. This figure corresponds to the bottom row in Figure 21, but here with two intersection pairs $\pm(1-x) \cdot S_{A_i^-} \cap W_i$ (the case $n_i = \pm 2$), each admitting a framed embedded Whitney disk (purple) having only a single interior intersection with f .

Now considering the case that the secondary multiplicity of an initial W_i has absolute value $|n_i| > 1$, there will be $|n_i|$ intersection pairs $\pm(1-x) \cdot S_{A_i^\pm} \cap W_i$, each admitting a framed embedded Whitney disk (like Δ in Figure 22) which has only a single interior intersection with f . See Figure 38 for the case of two negative accessory sphere pairs, and Figure 39 for an additional positive accessory sphere pair. It is not difficult to see that Step 1 (including Lemma 24) can be applied simultaneously to each intersection pair disjointly: Through Figure 23, the construction of Step 1 is supported in a neighborhood of the Whitney disk Δ together with an arc along W_i running from $\partial\Delta$ to ∂_+W_i (Δ itself is contained in the neighborhood of an arc). And the accessory and Whitney disks of Lemma 24 in Figure 24 can be constructed “side by side” along the boundary of W_i when

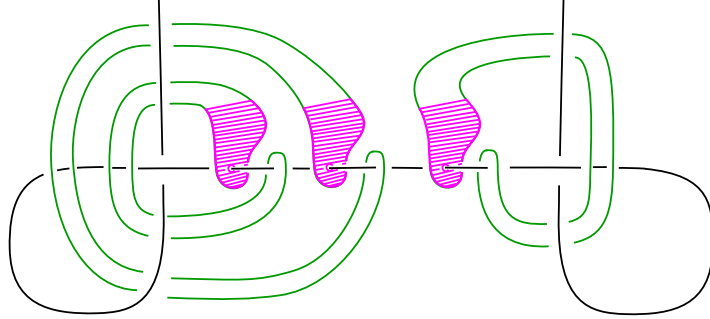


FIGURE 39. This figure corresponds to the left-most picture in Figure 38, but showing here the case of an additional positive accessory sphere pair along with the two negative accessory sphere intersection pairs.

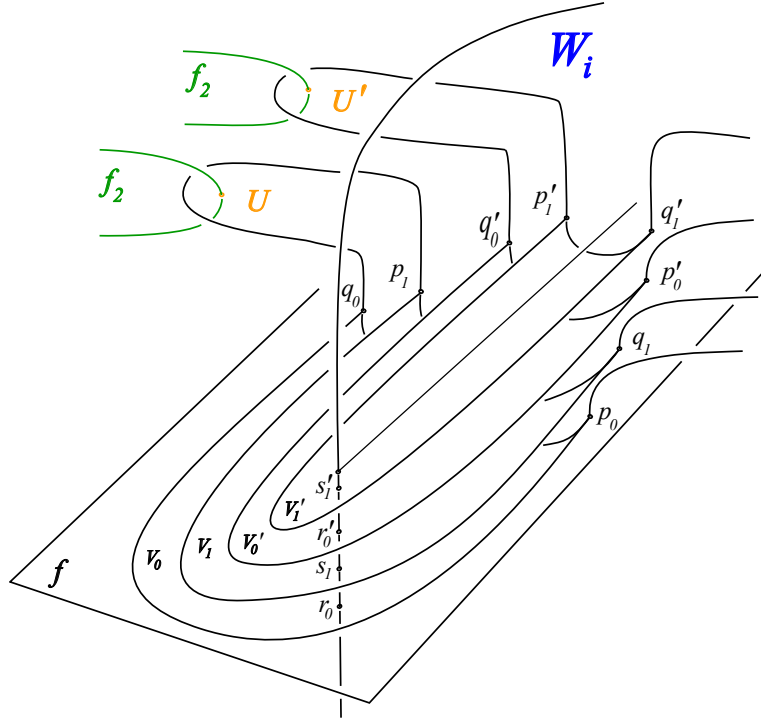


FIGURE 40. After simultaneously applying the constructions of Figures 22, 23 and 24 to Figure 38, the resulting four pairs of self-intersection pairs of f admit two pairs of nested Whitney disks as in Figure 25. Shown here is the case $n_i = 2$, but nested Whitney disks exist for any number of pairs of pairs; e.g. starting with Figure 39 would yield three nested pairs of Whitney disks. Recall that by construction we take these nested Whitney disks around the negative self-intersection of f , even when starting with intersections including pairs coming from positive accessory spheres $\pm(1-x) \cdot S_{A_i^+} \cap W_i$ (as in Figure 39).

starting with more pairs $\pm(1-x) \cdot S_{A_i^\pm} \cap W_i$ as in Figure 38. To visualize this it may be helpful to consider the $n_i = 2$ case and compare the input to Step 1 shown in Figure 20 and Figure 38 with the result that would be input to Step 2 shown in Figure 40.

Considering the situation at the start of Step 2, it is clear that an additional pair of self-intersection pairs p'_0, q'_0 and p'_1, q'_1 , to the pair p_0, q_0 and p_1, q_1 in Figure 25, admits nested pairs of Whitney disks V'_0 and V'_1 parallel to V_0 and V_1 , as shown in Figure 40. It is also clear that such nested Whitney disks exist for any number of such additional self-intersection pairs.

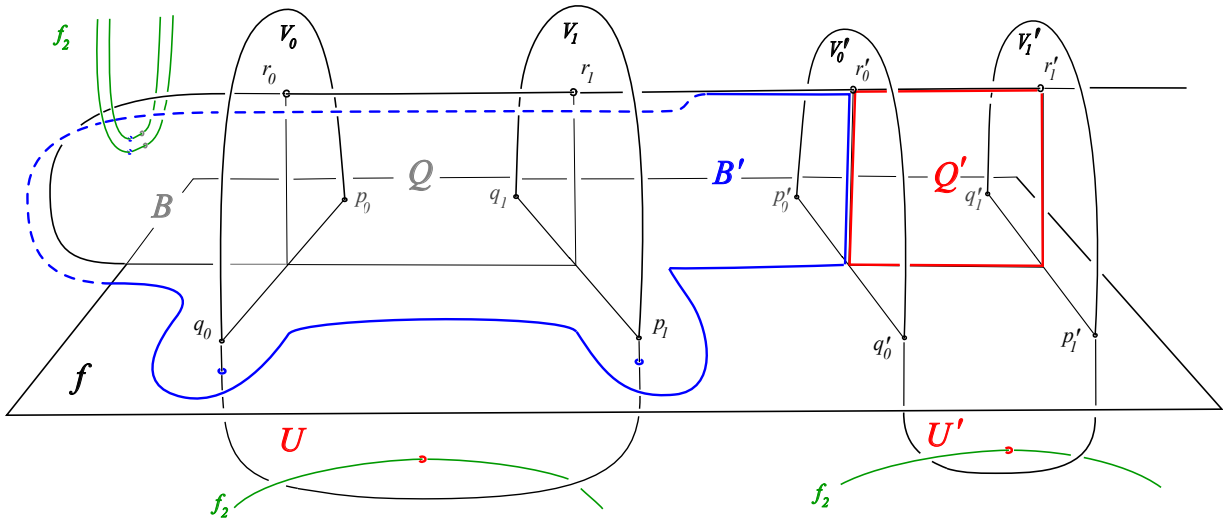


FIGURE 41. The boundary of B' is shown in blue, with the dotted sub-arcs indicating where $\partial B'$ has been pushed out of the present time coordinate along with most of the interior of B' (to avoid intersecting V_0 and V_1). Near q_0 and p_1 the interior of B' ‘hangs down underneath’ f (in the present), and the pair of transverse intersections between f and B' (near q_0 and p_1) can be removed by a Whitney move on B' guided by a parallel of the Whitney disk U from Lemma 24.

In order to continue with Step 2 we need to find an appropriate Q' and B' for $r'_0 = V'_0 \cap f$ and $s'_1 = V_1 \cap f$. The quadrilateral Whitney disk Q' sits between V'_0 and V'_1 , the same as Q sits between V_0 and V_1 , but a little work is required to find an appropriate generalized accessory disk B' for r'_0 : The problem is that forming B' from a parallel copy of A_i^- will yield intersections between $\partial B'$ and both ∂V_0 and ∂V_1 , which are transverse (in f) to ∂A_i^- . This problem is solved by first pushing $\partial B'$ off of ∂V_0 and ∂V_1 , which creates interior intersections between B' and f , and then using a parallel copy of the Whitney disk U to get the interior of B' disjoint from f , as shown in Figure 41 (recall from Lemma 24 that U is framed and embedded, with interior disjoint from f). This Whitney move does not change the primary multiplicity of B' by Observation 7.3. Now

r'_0 and s'_1 admit framed embedded B' and Q' disjoint from B and Q , and the subsequent steps 3 through 6 can be carried out as before.

Although Figure 41 only illustrates the case $n_i = 2$, the $n_i > 2$ cases are similar: If there was another pair of Whitney disks V''_0, V''_1 to the right of V'_0, V'_1 in Figure 41, then another generalized accessory disk B'' could be constructed by extending a parallel of B' , pushing $\partial B''$ off of $\partial V'_0$ and $\partial V'_1$, and then using a parallel of U' to get the interior of B'' disjoint from f . (The existence of Q'' between V''_0 and V''_1 is clear.) Repeating this process as needed yields disjointly embedded framed generalized accessory and Whitney disks for any n_i , and the rest of the steps can be carried out as before.

This completes the proof of Proposition 22. \square

8. APPENDIX: WHITNEY DISKS AND ACCESSORY DISKS

This section contains some details on techniques of immersed surfaces in 4-manifolds that are used throughout the paper, especially in Section 7. More information can be found in [14]. For further details and generality on Whitney disks and Whitney moves see e.g. [22, Thm.6.6].

Unless otherwise specified, submanifolds are assumed to intersect generically. Orientations are also assumed, but usually not specified explicitly. The discussion here holds in the flat topological category via the notions of 4-dimensional topological transversality from [14, chap.9].

8.1. Generic boundary-interior intersections. In the case that the boundary ∂D of an immersed disk D is contained in the interior of an immersed surface A , we require and assume that ∂D is embedded, and also that the interior of D is disjoint from A near ∂D , i.e. that there exists a collar in D of ∂D such that the intersection of this collar with A is equal to ∂D . In the case where the boundary of a disk W passes through an interior intersection p between surfaces A and B , the three sheets are required to meet near p as illustrated for the model Whitney disk W in Figure 42. (A *sheet* of a surface is a subdisk, open or closed.)

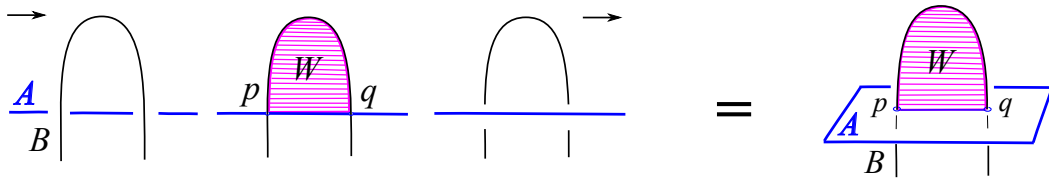


FIGURE 42. An embedded model Whitney disk W pairing intersections between surface sheets A and B : In the right-most picture the A -sheet is contained in the ‘present’ 3-dimensional slice of 4-space (along with W), while the black arc extends into ‘past’ and ‘future’ to describe the B -sheet, as in the 3-picture ‘movie’ on the left (with ‘time’ moving from left to right).

8.2. Whitney disks. Let p and q be oppositely-signed transverse intersections between connected immersed surfaces A and B in a 4-manifold X (in this paper such p and q are called a *canceling pair* of intersections), with p and q joined by embedded interior arcs $a \subset A$ and $b \subset B$ which are disjoint from all other singularities in A and B . Here we allow the possibility that $A = B$, in which case the circle $a \cup b$ must be embedded and change sheets at p and q . Any generic immersed disk $W \looparrowright X$ bounded by such a *Whitney circle* $a \cup b$ is a *Whitney disk* pairing p and q . Figure 42 shows a model Whitney disk in 4-space.

From the assumption of genericity (8.1), all Whitney disks in this paper are required to have embedded boundary. The adjective “immersed” will occasionally be attached to “Whitney disk” to remind the reader that a Whitney disk interior may not be embedded.

Throughout the following discussion of Whitney disks and Whitney moves the immersed surfaces A and B are allowed to have boundary in the interior of X , and either may itself be a Whitney disk, as in the constructions of Section 7.

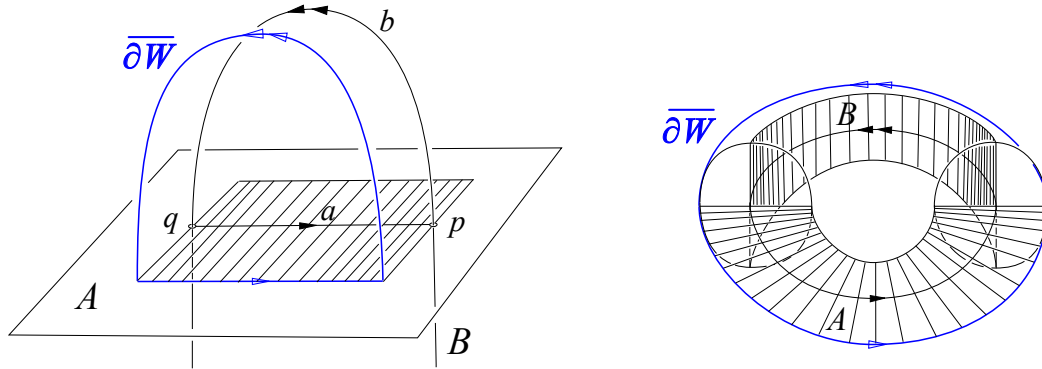


FIGURE 43. Left: Near a Whitney disk W pairing $p, q \in A \pitchfork B$, with $\partial W = a \cup b$, a Whitney section $\overline{\partial W}$ is shown in blue. This picture is accurate near ∂W ; in general, the evident (but not explicitly indicated) embedded W bounded by $a \cup b$ may have self-intersections as well as intersections with other surfaces. The line segments transverse to a in A indicate the correspondence with the right-hand picture of the normal disk-bundle $\nu_{\partial W}$ over ∂W . Right: The blue Whitney section $\overline{\partial W}$ is shown inside an embedding into 3-space of $\nu_{\partial W} \cong S^1 \times D^2$, with the sheets of A and B indicated by line segments transverse to ∂W . The A -sheet cuts the front solid torus horizontally, while the B -sheet cuts the back of the solid torus vertically.

8.3. Framed Whitney disks. For oriented immersed surfaces $A, B \looparrowright X$ in a 4-manifold X , let W be an immersed Whitney disk pairing intersections $p, q \in A \pitchfork B$, with boundary $\partial W = a \cup b$, for embedded arcs $a \subset A$ and $b \subset B$. Denote by $\nu_{\partial W}$ the restriction to ∂W of the normal disk-bundle ν_W of W in X . Since p and q have opposite

signs, $\nu_{\partial W}$ admits a nowhere-vanishing *Whitney section* $\overline{\partial W}$ defined by taking vectors tangent to A over a , and extending over b by vectors which are normal to B , as shown in the left of Figure 43.

The right side of Figure 43 shows $\overline{\partial W}$ inside an embedding into 3-space of $\nu_{\partial W} \cong S^1 \times D^2$. Although this choice of embedding has $\overline{\partial W}$ corresponding to the 0-framing of $D^2 \times S^1 \subset \mathbb{R}^3$ (as can always be arranged), the section of $\nu_{\partial W}$ determined (up to homotopy) by the canonical framing of ν_W will in general differ by $(\omega(W)$ -many) full twists relative to $\overline{\partial W}$. (If p and q had the same sign then there would have to be a half-twist in the sheets of A and B , so the (continuous) Whitney section $\overline{\partial W}$ could not exist.)

If $\overline{\partial W}$ extends to a nowhere-vanishing section \overline{W} of ν_W , then W is said to be *framed* (since the disk-bundle over a disk ν_W has a canonical framing, and a nowhere-vanishing normal section over an oriented surface in an oriented 4-manifold determines a framing up to homotopy). In general, the obstruction to extending $\overline{\partial W}$ to a nowhere vanishing section of ν_W is the relative Euler number $\chi(\nu_W, \overline{\partial W}) \in \mathbb{Z}$, called the *twisting* of W and denoted $\omega(W)$, so W is framed if and only if $\omega(W) = 0$. The twisting $\omega(W)$ can be computed by taking the intersection number of the zero section W with any extension \overline{W} of $\overline{\partial W}$ over W , so it does not depend on an orientation choice for W (since switching the orientation on W also switches the orientation of \overline{W}). And $\omega(W)$ is also unchanged by switching the roles of a and b in the construction of $\overline{\partial W}$, since interchanging the “tangent to...” and “normal to...” parts in the construction yields an isotopic section in $\nu_{\partial W}$ (isotopic through non-vanishing sections).

Remark 28. The twisting $\omega(W)$ of W , which is the element of $\pi_1(\mathrm{SO}(2)) \cong \mathbb{Z}$ determined by a Whitney section as described above, can be computed using *any section* $\overline{\partial W}$ of $\nu_{\partial W}$ such that $\overline{\partial W}$ is in the complement of the tangent spaces of both A and B , since such $\overline{\partial W}$ will have the same number of rotations as a Whitney section (relative to the longitude determined by the canonical framing of ν_W); see Figure 43. Parallel copies of W extending such nowhere-tangent sections are used, for instance, in the constructions of Whitney spheres and accessory spheres in section 5.2.

The adjective “parallel” applied to a Whitney circle or Whitney disk in this paper always refers to one of the constructions described above.

8.4. Whitney moves. Given a Whitney disk W pairing $p, q \in A \pitchfork B$, a *Whitney move on A guided by W* (also called a *W -Whitney move on A*) eliminates p and q by the construction illustrated in Figure 44: A small neighborhood of $\partial W \cap A$ in A is deleted, and a *Whitney bubble* consisting of two oppositely-oriented parallel copies of W and a parallel of a small neighborhood of $\partial W \cap B$ is added to A .

The result of a W -Whitney move on A is the same as changing A by a regular homotopy supported near W , and we frequently keep the same name/notation for a surface that has been changed by a Whitney move.

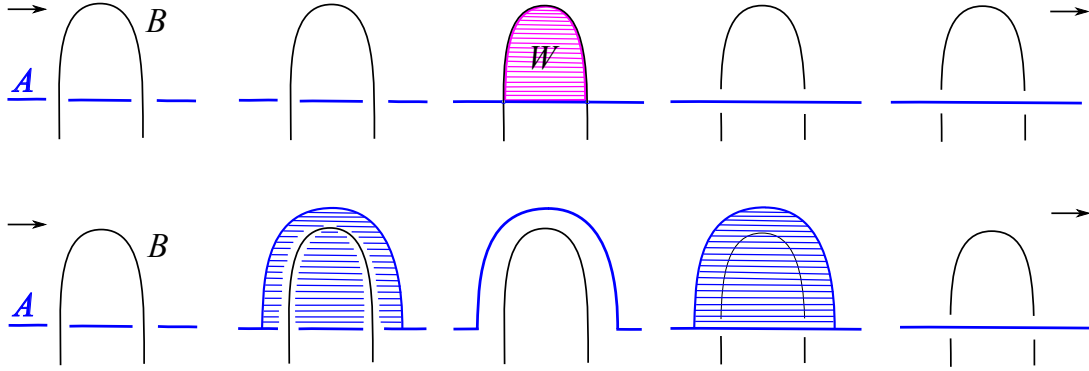


FIGURE 44. Before and after a model Whitney move: The top and bottom rows of pictures show the same slices of a 4-ball neighborhood containing surface sheets A (blue) and B (black). Before the Whitney move (top row), the intersections between A and B are paired by the framed embedded Whitney disk W (purple). After applying the W -Whitney move to A (bottom row), A and B are disjoint, and the Whitney bubble added to A is visible in the three center pictures.

8.5. **Accessory disks.** Let p be a transverse self-intersection in a connected immersed surface $f : \Sigma \looparrowright X$, where as usual we blur the distinction between f and its image in the 4-manifold X . An embedded circle in f which changes sheets at p and is disjoint from the boundary and all other singularities of f is called an *accessory circle* for p . Any generically immersed disk bounded by an accessory circle for p is called an *accessory disk* for p .

In this paper accessory disks will only be used in the case that $\Sigma = S^2$ and $X = S^4$, so every $p \in f \pitchfork f$ admits an accessory disk, for any choice of accessory circle.

8.6. **Framed accessory disks.** Let p be a self-intersection of f admitting an accessory disk A with (embedded) boundary ∂A . Denote by $\nu_{\partial A}$ the restriction to ∂A of the normal disk-bundle ν_A of A in X . The tangent space to f along ∂A determines a 1-dimensional subspace of $\nu_{\partial A}$ at each point other than p , and at p the two sheets of f determine a pair of transverse 1-dimensional subspaces of $\nu_{\partial A}$ (Figure 45). Let $\overline{\partial A}$ be any nowhere-vanishing section of $\nu_{\partial A}$ such that $\overline{\partial A}$ is in the complement of the tangent space of f , and define the twisting $\omega(A) \in \mathbb{Z}$ to be the obstruction to extending $\overline{\partial A}$ over A , i.e. $\omega(A)$ is the relative Euler number $\chi(\nu_A, \overline{\partial A})$ (cf. Remark 28 just above). Then A is said to be *framed* if $\omega(A) = 0$. Note that $\omega(A)$ is well-defined since the rotations (relative to A) of $\overline{\partial A}$ in $\nu_{\partial A} \cong S^1 \times D^2$ are determined by the 1-dimensional subspaces cut out by f , and $\omega(A)$ does not depend on a choice of orientation of A (as observed above for Whitney disks). Any such section $\overline{\partial A}$ will be referred to as an *accessory section* for A , and in this paper the adjective “parallel” applied to an accessory disk always means an extension over A of an accessory section.

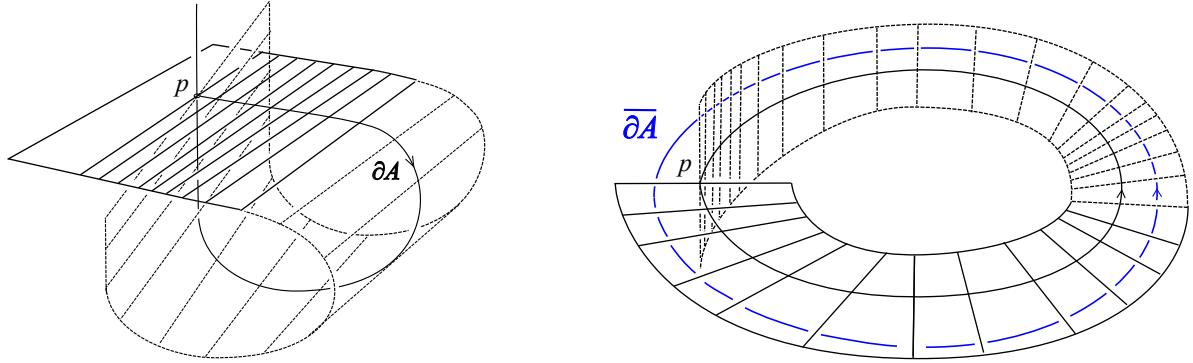


FIGURE 45. Left: Near the sheets of f along ∂A in X . Right: Inside an embedding of $\nu_{\partial A} \cong D^2 \times S^1$ into 3-space, an accessory section $\bar{\partial A}$ (in blue) in the complement of the tangent space of f . This embedding has $\bar{\partial A}$ corresponding to the 0-framing of $D^2 \times S^1 \subset \mathbb{R}^3$ (as can always be arranged), but the section determined by the canonical framing of ν_A may in general differ by $(\omega(A)$ -many) full twists relative to $\bar{\partial A}$.

8.7. Whitney moves guided by accessory disks. We discuss next how parallel copies of framed accessory disks can be used to guide Whitney moves on surfaces intersecting the two sheets of f near p , as in the constructions of accessory spheres in section 5.2.2 (Figure 13) and during Step 7 of the proof of Proposition 22 (section 7.15/Figure 34). See also Figure 46.

Before giving details, here is the main idea: Observe that any accessory section can be isotoped through nowhere-vanishing sections in $\nu_{\partial A}$ to be tangent to f along most of ∂A except along a small arc of ∂A near p where the section makes a “quarter-turn” through vectors normal to both sheets of f . This small arc can be pushed off of f slightly into A while preserving the twisting of the section, and “trimming” A along this pushed-in arc yields one of a family of parallel Whitney disks such as V in Figure 46.

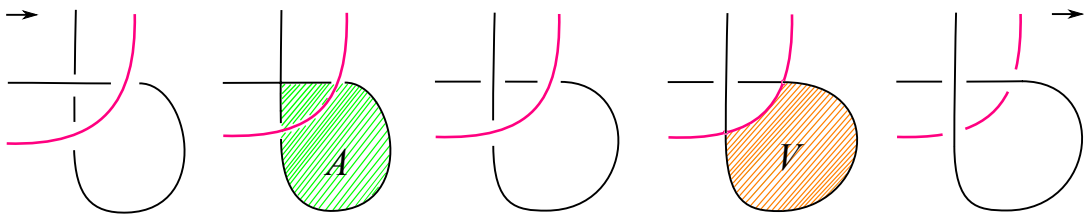


FIGURE 46. Near a framed embedded accessory disk A (green) on f (black), intersections between a surface sheet (red) and f are paired by a Whitney disk V formed from a (trimmed) parallel copy of A .

So let p be a self-intersection of f admitting a framed oriented immersed accessory disk A with embedded boundary ∂A . Thinking of ∂A as the image of an immersion of

an interval, $a : [0, 1] \rightarrow f(\Sigma) \subset X$ with $a(0) = p = a(1)$, let v_+ denote the unit tangent vector to f at p pointing positively along ∂A , and let v_- denote the unit tangent vector to the other sheet of f at p pointing back negatively along ∂A (See Figure 47). Denote the local sheets of f near p by f_{\pm} , where f_{\pm} contains v_{\pm} . Choose a tangent vector \bar{v}_+ to f_+ at p , such that \bar{v}_+ is orthogonal to v_+ , and extend \bar{v}_+ to a nowhere-vanishing section of the normal bundle of a in f . This section extending \bar{v}_+ defines an embedded arc $\bar{a} : [0, 1] \rightarrow f(\Sigma) \subset X$ with $\bar{a}(0) = \bar{v}_+$. We may assume that the terminal endpoint $\bar{a}(1)$ defines a tangent vector \bar{v}_- to f_- at p which is orthogonal to v_- (See Figure 47 and left side of Figure 48).

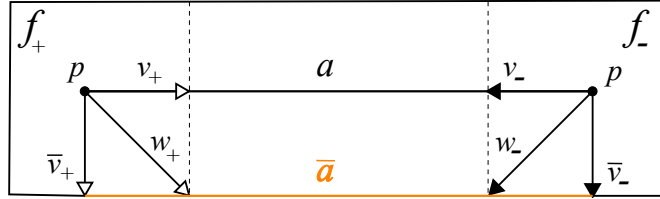


FIGURE 47. The preimage of a neighborhood of the accessory circle ∂A .

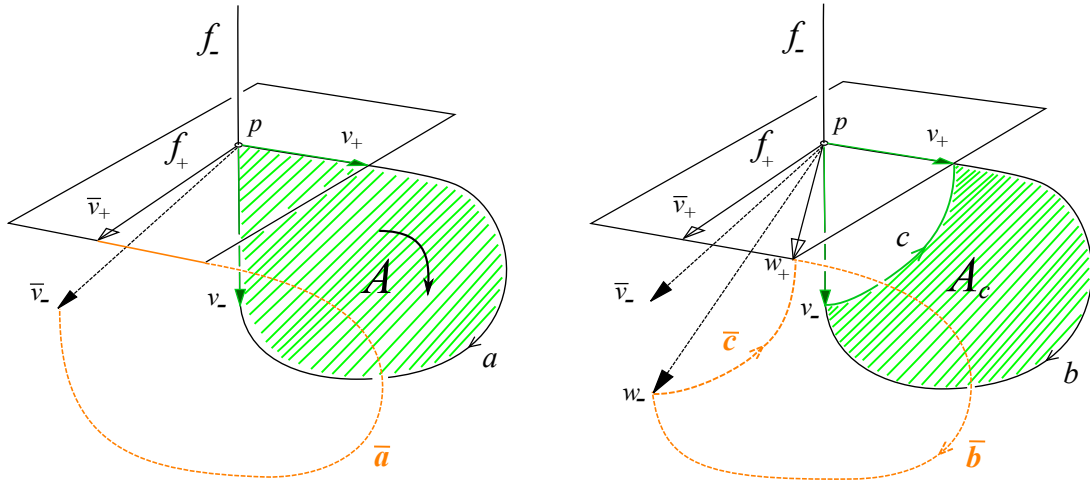


FIGURE 48. Left: The accessory disk A and the arc $\bar{a} \subset f$ parallel to $a = \partial A$ in f . Right: The trimmed accessory disk $A_c \subset A$ with boundary $b \cup c$, and the section $\bar{\partial A}_c = \bar{b} \cup \bar{c}$ of $\nu_{\partial A_c}$. Note that the dotted vectors \bar{v}_- and w_- point in the direction of an orthogonal ‘time’ coordinate.

Around p the vectors v_+ and \bar{v}_+ span an embedded square of f_+ , and similarly the vectors v_- and \bar{v}_- span an embedded square of f_- . By transversality, the vectors $v_+, \bar{v}_+, v_-, \bar{v}_-$ span a 4-dimensional cube of X around p , and it may be assumed that A intersects this cube in a square quadrant spanned by v_+ and v_- . Rotating v_- to v_+ traces out an embedded corner of A at p bounded by the union of (the segments) v_-

and v_+ together with the arc c traced out by the tips of the rotating vectors. Deleting from A all of this corner except for c yields a slightly smaller disk A_c whose boundary $\partial A_c = b \cup c$ is the union of c together with the arc $b \subset \partial A$ outside the corner (from the tip of v_+ to the tip of v_-). (See Figure 48).

Let $\nu_{\partial A_c}$ denote the restriction of the normal bundle ν_{A_c} of A_c in X to the boundary ∂A_c . Define a nowhere-vanishing section $\overline{\partial A_c}$ of $\nu_{\partial A_c}$ as follows: Over the arc $b \subset a$ take the vectors $\overline{b} \subset \overline{a}$. Specifically, \overline{b} starts at the tip of $w_+ := v_+ + \overline{v}_+$ (over the tip of v_+) and ends at the tip of $w_- := v_- + \overline{v}_-$ (over the tip of v_-). To define $\overline{\partial A_c}$ over the arc c of ∂A_c , note that rotating w_- to w_+ in the plane spanned by w_- and w_+ defines an arc \overline{c} (traced out by the tip of the rotating vector), which determines an arc of normal vectors to A_c over c . (To see that \overline{c} is normal to A_c , recall that A is contained in the quadrant spanned by v_+ and v_- in the cube around p , and this quadrant is disjoint from any non-trivial linear combination of w_- and w_+ .)

We claim that $\chi(\nu_{A_c}, \overline{\partial A_c}) = \omega(A)$, so in particular, $\overline{\partial A_c}$ extends to a nowhere-vanishing section over A_c if and only if A is framed. To see the claim, fix the endpoints of c , and let c_t denote a family of arcs determined by an isotopy of the interior of c across the corner of A and into the arc of ∂A passing through p , so $c_0 = c$ and $c_1 = v_- \cup v_+ \subset \partial A$. The union of the c_t with b forms a family of circles $c_t^\circ = c_t \cup b$ interpolating between $\partial A_c = c_0^\circ$ and $\partial A = c_1^\circ$, and these circles bound disks $A_{c_t} \subset A$ interpolating between $A_{c_0} = A_c$ and $A_{c_1} = A$. Observe that the (fixed) arc \overline{c} determines an arc of nowhere-vanishing normal vectors to A over each c_t for $0 \leq t \leq 1$. Over each c_t° define a section $\overline{\partial A_{c_t}}$ of the restriction of ν_A to $c_t^\circ = \partial A_{c_t}$ as follows: Over b (which is a common sub-arc of all the c_t°) take $\overline{\partial A_{c_t}} = \overline{b}$, and over c_t define $\overline{\partial A_{c_t}}$ to be the vectors determined by \overline{c} . Note first that although the section $\overline{\partial A_{c_1}}$ over $c_1^\circ = \partial A$ is tangent to f along the arc $b \subset \partial A$, this part of $\overline{\partial A_{c_1}}$ can be perturbed to be normal to f yielding an isotopic *accessory section* $\overline{\partial A} \subset \nu_{\partial A}$. So $\omega(A) = \chi(\nu_A, \overline{\partial A}) = \chi(\nu_A, \overline{\partial A_{c_1}})$.

On the other hand, from the isotopy $\overline{\partial A_{c_t}}$ of bundles with sections induced by the isotopy of arcs c_t we have:

$$\chi(\nu_{A_c}, \overline{\partial A_c}) = \chi(\nu_{A_{c_0}}, \overline{\partial A_{c_0}}) = \chi(\nu_{A_{c_1}}, \overline{\partial A_{c_1}}) = \chi(\nu_A, \overline{\partial A_{c_1}}),$$

so $\chi(\nu_{A_c}, \overline{\partial A_c}) = \omega(A)$.

Note that the interior of the arc \overline{c} is also disjoint from f , since f only intersects the span of w_+ and w_- when at least one coefficient of w_+ or w_- is zero. So if A is framed and has interior disjoint from f then parallel copies of A_c will also have interiors disjoint from f .

It follows from this discussion that if a surface sheet S intersects f near p in a pair of oppositely-signed points at the tips of w_+ and w_- , with S intersecting the normal disk bundle ν_A of A in the vectors corresponding to a section \overline{c} as in this model, then this intersection pair admits a Whitney disk which is a parallel copy of A_c and has the same twisting. This is exactly the case illustrated in Figure 46, and used in the

constructions of accessory spheres in section 5.2.2 (Figure 13) and during Step 7 of the proof of Proposition 22 (section 7.15/Figure 34).

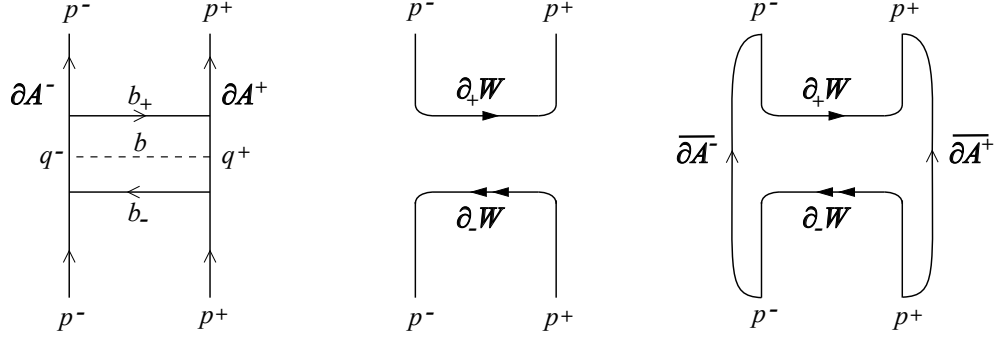


FIGURE 49. The view in the domain of f : Banding together ∂A^\pm along the dotted arc b (left) yields the boundary $\partial W = \partial_+ W \cup \partial_- W$ (center) of a Whitney disk W constructed by ‘half-tubing’ A^\pm together (Figure 50). Copies $\overline{A^\pm}$ of A^\pm (perturbed rel p^\pm) are still accessory disks for p^\pm .

8.8. Whitney disks from accessory disks. Here are some details on forming Whitney disks from pairs of accessory disks, as used in section 7.4 and during the double transfer move of Step 8 (section 7.16):

Let A^+ and A^- be accessory disks for a pair $\{p^+, p^-\}$ of oppositely-signed self-intersections of f such that $\partial A^+ \cap \partial A^- = \emptyset$. Choose an embedded arc b in f connecting a point $q^+ \in \partial A^+$ to a point $q^- \in \partial A^-$, with the interior of b disjoint from both ∂A^\pm . Banding together ∂A^\pm in f along b yields a Whitney circle for p^\pm which is the union of ∂A^\pm minus small arcs containing q^\pm together with arcs b_+ and b_- parallel to b (the preimage is shown in the left and center pictures of Figure 49). Denote this Whitney circle by ∂W since a Whitney disk W will be described shortly. Let z^\pm denote inward pointing tangent vectors to A^\pm at q^\pm . Choose a nowhere vanishing vector field z_t field over b such that for each $t \in [0, 1]$ z_t is normal to f , with $z_0 = z^-$ and $z_1 = z^+$. The arc of vectors z_t determines a half-tube H connecting A^- and A^+ , where arcs of H from b_- to b_+ are traced out by rotating a vector based at b from b_- to b_+ through the corresponding z_t (Figure 50). The Whitney disk W is formed by deleting small half-disks from A^\pm at q^\pm and connecting the resulting disks with H .

Observe that the twisting $\omega(W)$ is the sum of the twistings of A^+ and A^- : First note that since p^\pm have opposite signs, the quarter turns in the right side of Figure 45 fit together as in the right side of Figure 43. The vectors z_t extend by translation to nowhere-vanishing normal vectors over all of $H \subset W$ which are also in the complement of f . Choosing a Whitney section by extending the restriction to $b_\pm \subset \partial W$ over the rest of ∂W is the same as choosing accessory sections over ∂A^+ and ∂A^- . Since these sections already extend over H , the twisting $\omega(W)$ of W is equal to the sum $\omega(A^+) + \omega(A^-)$. (The choice of z_t (which can rotate around f) does not affect $\omega(W)$ because a rotation of

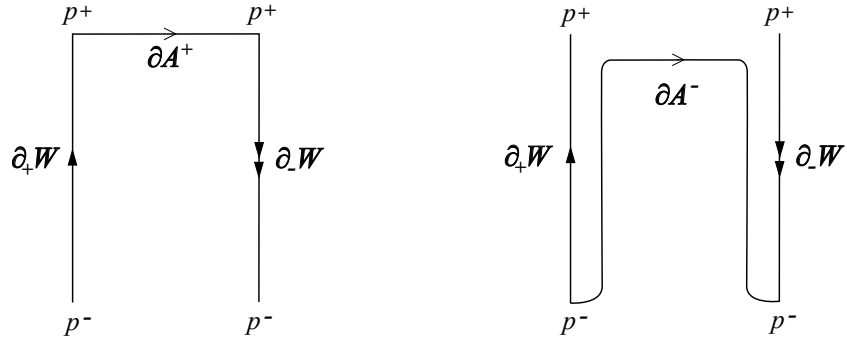


FIGURE 51. The view in the domain of f : Forming a negative accessory disk A^- (right) from parallels of the Whitney disk W and positive accessory disk A^+ (left).

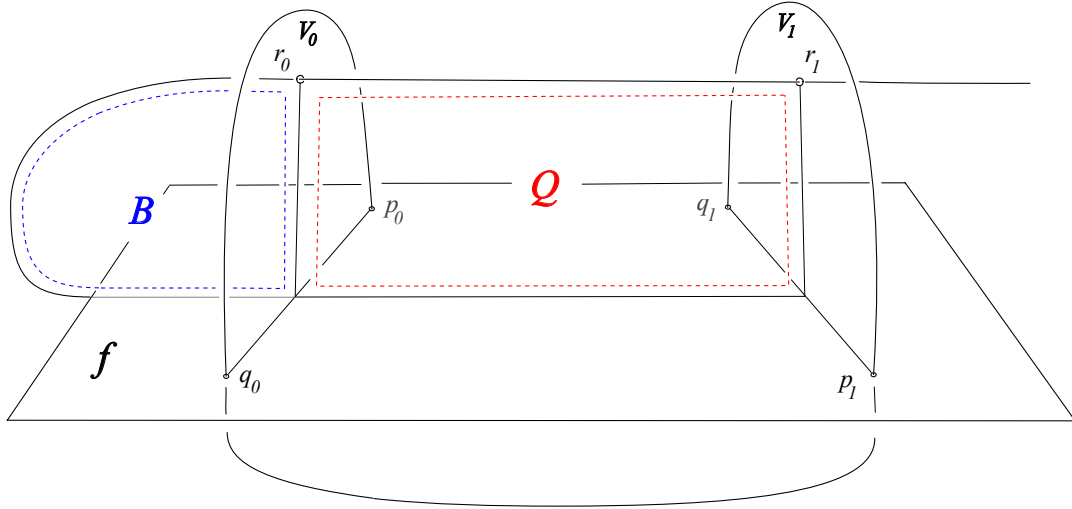
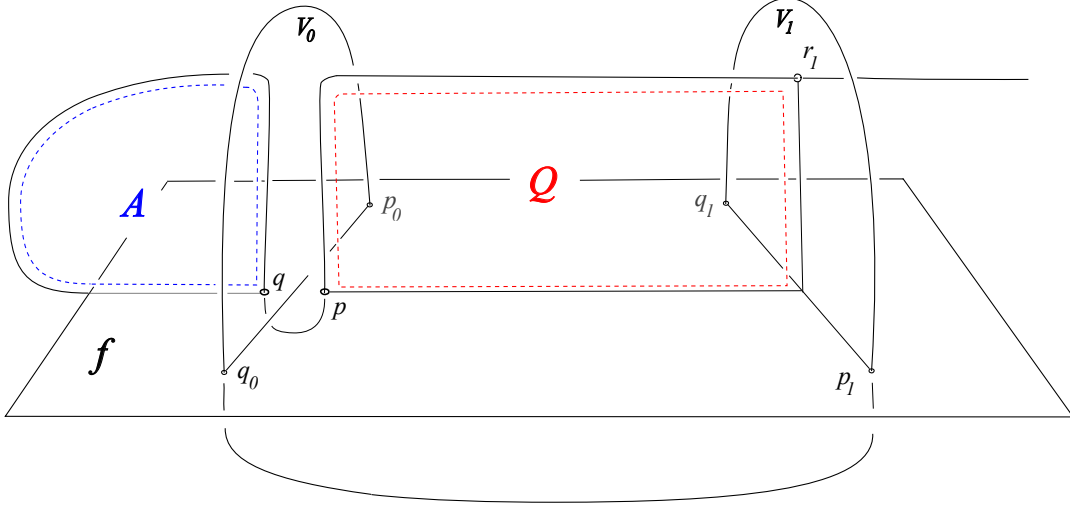
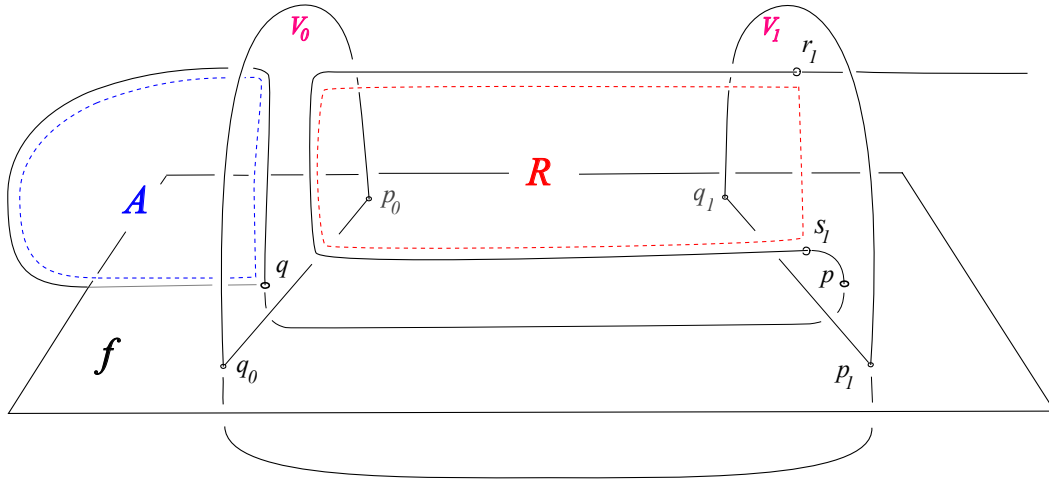


FIGURE 52. Before the transfer move.

8.10. **Transfer moves.** This subsection provides some more detail and background on the *transfer move* construction which “transfers” an intersection between f and the interior of one Whitney disk on f onto another Whitney disk, at the cost of creating new controlled intersections between Whitney disks and f . The origin of this construction appears to go back to [28], and it was generalized and used extensively in the development of an obstruction theory for Whitney towers in [10, 24, 25]. Here we focus on the setting for the transfer move in section 7.11 of the current paper (Step 5 of the proof of Proposition 22).

Figure 52 shows the configuration at Step 2 of the proof of Proposition 22 (section 7.8). The transfer move exchanges $r_0 \in V_0 \cap f$ for $s_1 \in V_1 \cap f$ by first performing a finger

FIGURE 53. After the first finger move on f along V_0 and across ∂V_0 .FIGURE 54. After the transfer move is completed by a pushing p along f across ∂V_1 , creating $s_1 \in V_1 \cap f$, with R pairing r_1, s_1 .

move along V_0 across ∂V_0 fig:transfer-move-1B, and then pushing one of the new self-intersections $p \in f \cap f$ across ∂V_1 (Figure 54). The finger move converts the bigon B from Figure 52 into an accessory disk A for the new intersection $q \in f \cap f$ in Figure 54, hence we refer to B as a *generalized accessory disk*. Similarly, the quadrilateral Q from Figure 52 gives rise to the Whitney disk R pairing $r_1, s_1 \in V_1 \cap f$ in Figure 54, hence we refer to Q as a *generalized Whitney disk*. From the local coordinates it is clear that A and R are framed, and this corresponds to B and Q being framed in the sense that normal sections over ∂B and ∂Q in the complement of the sheets containing ∂B and ∂Q extend

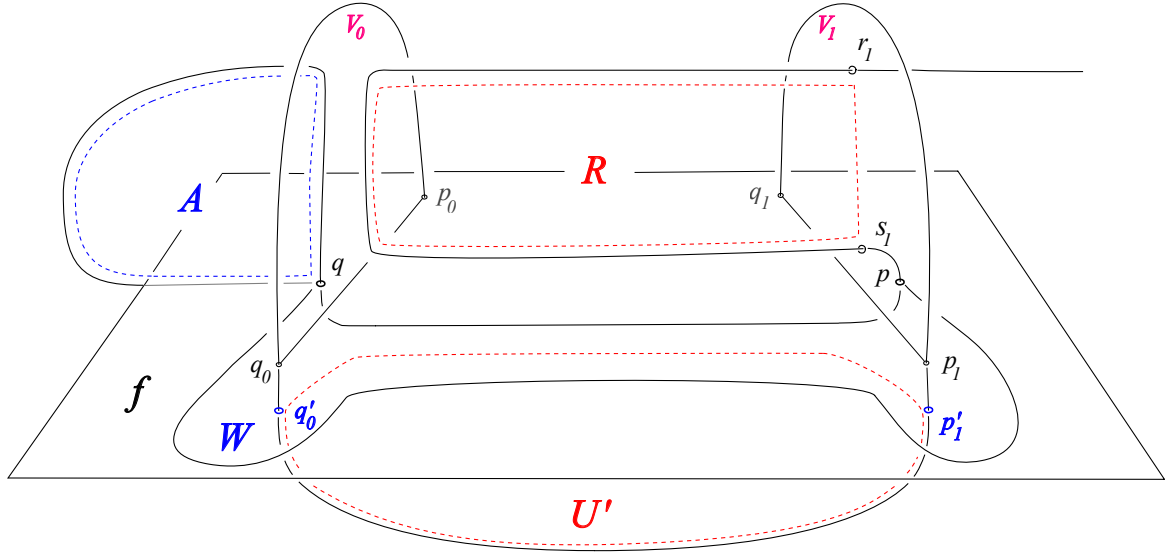


FIGURE 55. Whitney disks W and U' pair the newly created intersection pairs $p, q \in f \pitchfork f$ and $p'_1, q'_0 \in W \pitchfork f$, respectively.

over B and Q , as in the definition of framed Whitney disks (Remark 28) and accessory disks (section 8.6).

The constructions of Steps 3 and 4 of the proof of Proposition 22 (sections 7.9 and 7.10) create multiple disjoint parallel copies of B and Q extended by disjointly embedded disks, and the corresponding transfer moves can be carried out simultaneously yielding multiple disjoint parallel copies of A and R extended by embedded disks. During these Steps 3 and 4 the Whitney disks V_0 and V_1 are also tubed into framed immersed accessory spheres on f_2 , but this does not obstruct the transfer moves which are supported near arcs.

Figure 55 shows how after the transfer move the new intersections $p, q \in f \pitchfork f$ can be paired by a Whitney disk W which is supported near the the union of the arc from ∂V_0 which guided the second finger move along f together with sub-arcs of ∂V_0 and ∂V_1 . (In the figure, W appears to hang down underneath the horizontal plane of f .) And the pair of new intersections $p'_1, q'_0 \in W \pitchfork f$ can be paired by a Whitney disk U' formed from a parallel of the Whitney disk U from Lemma 24 of section 7.7. Multiple disjoint parallels of such framed embedded W can be constructed for multiple simultaneous transfer moves by nesting along ∂V_0 and ∂V_1 (compare Figures 25 and 40, but with V -parallels replaced by W -parallels). And the multiple pairs of intersections between f and these parallels of W can be paired by disjoint parallels of U' .

REFERENCES

- [1] **J Andrews, M L Curtis**, *Knotted 2-spheres in 4-space*, Annals of Math. 70, (1959) 565–571.
- [2] **E Artin**, *Zur Isotopie zweidimensionaler Flächen im \mathbb{R}^4* , Abh. Math. Sem. Univ. Hamburg 4 (1925), 174–177.

- [3] **B Audoux, J-B Meilhan, E Wagner**, *On codimension two embeddings up to link-homotopy*, preprint (2017) arXiv:1703.07999v2 [math.GT].
- [4] **A Bartels**, *Link homotopy in codimension 2*, Ph.D. Thesis, UC San Diego (1999).
- [5] **A Bartels, P Teichner**, *All two dimensional links are null homotopic*, *Geom. Topol.* Volume 3 (1999) 235–252.
- [6] **M Boege, G Hinojosa, A Verjovsky**, *Wild knots in higher dimensions as limit sets of Kleinian groups*, *Conformal geometry and dynamics*, AMS Volume 13 (2009) 197–216.
- [7] **J-C Cha, K Orr, M Powell**, *Whitney towers and abelian invariants of knots* preprint (2016) arXiv:1606.03608 [math.GT].
- [8] **T Cochran**, *Geometric invariants of link cobordism*. *Comment. Math. Helv.* 60 2 (1985) 291–311.
- [9] **J Conant, R Schneiderman, P Teichner**, *Higher-order intersections in low-dimensional topology*, *Proc. Natl. Acad. Sci. USA* vol. 108, no. 20, (2011) 8131–8138.
- [10] **J Conant, R Schneiderman, P Teichner**, *Whitney tower concordance of classical links*, *Geom. Topol.* 16 (2012) 1419–1479.
- [11] **J Conant, R Schneiderman, P Teichner**, *Cochran’s β^i -invariants via twisted Whitney towers*, *J Knot Theory Ramif* Vol. 26 No. 2 (2017).
- [12] **R Fenn, editor**, *Low dimensional topology*, London Math. Soc. LNS 95 (1985).
- [13] **R Fenn, D Rolfsen**, *Spheres may link in 4-space*, *J. London Math. Soc.* 34 (1986) 177–184.
- [14] **M Freedman, F Quinn**, *The topology of 4-manifolds*, Princeton Math. Series 39 Princeton, NJ, (1990).
- [15] **R Gompf, A Stipsicz** *4-Manifolds and Kirby Calculus*, AMS Providence, R.I. (1999).
- [16] **G T Jin**, Ph.D.Thesis, Brandeis University (1988).
- [17] **P Kirk**, *Link maps in the 4-sphere*, *Proc. Siegen Top. Symp.*, SLN 1350 Springer (1988) 31–43.
- [18] **U Koschorke**, *Link maps and the geometry of their invariants*, *Manuscripta Math.* 61 (1988) 383–415.
- [19] **G-S Li**, *An invariant of link homotopy in dimension four*. *Topology* 36 (1997) 881–897.
- [20] **A Lightfoot**, *The triviality of a certain invariant of link maps in the four-sphere*, preprint (2016).
- [21] **J Milnor**, *Link groups*, *Annals of Math.* 59 (1954) 177–195.
- [22] **J Milnor**, *Lectures on the h-Cobordism Theorem*, Princeton University press 1965.
- [23] **A Pilz**, *Verschlingungshomotopie von 2-Sphären im 4-dimensionalen Raum*, Diploma thesis, University of Seigen (1997).
- [24] **R Schneiderman, P Teichner**, *Higher order intersection numbers of 2-spheres in 4-manifolds*, *Alg. and Geom. Topology* 1 (2001) 1–29.
- [25] **R Schneiderman, P Teichner**, *Whitney towers and the Kontsevich integral*, *Proceedings of a conference in honor of Andrew Casson*, UT Austin 2003, *Geometry and Topology Monograph Series* Vol. 7 (2004), 101–134.
- [26] **S Smale**, *A classification of immersions of the 2-sphere*, *Trans. Amer. Math. Soc.* 90 No. 2 (1959) 281–290.
- [27] **P Teichner**, *Stratified Morse theory and link homotopy*, Habilitation in preparation, now a joint paper with Maciej Borodzik and Mark Powell.
- [28] **M Yamasaki**, *Whitney’s trick for three 2-dimensional homology classes of 4-manifolds*, *Proc. Amer. Math. Soc.* 75 (1979) 365–371.

LEHMAN COLLEGE, CITY UNIVERSITY OF NEW YORK
E-mail address: robert.schneiderman@lehman.cuny.edu

UNIVERSITY OF CALIFORNIA, BERKELEY AND MAX PLANCK INSTITUTE FOR MATHEMATICS, BONN
E-mail address: teichner@mac.com